



UNIVERSITY OF APPLIED SCIENCES KOBLENZ
DEPARTMENT OF ELECTRICAL ENGINEERING AND INFORMATION TECHNOLOGY



THE UNIVERSITY OF
WESTERN AUSTRALIA

SCHOOL OF ELECTRICAL, ELECTRONIC AND COMPUTER ENGINEERING

ELECTRONICS AND SENSOR DESIGN OF AN AUTONOMOUS UNDERWATER VEHICLE

Michael Drtil

A thesis submitted for the degree of
Diplom-Ingenieur Elektrotechnik (FH)

Supervisors:
Prof. Dipl.-Inf. Heinz Unkelbach
A/Prof. Dr. Thomas Bräunl

February 2006

Declaration

I hereby declare that this project was done by myself and that I have not used any resources beyond the given.

Michael Drtil

Perth, 24.02.2006

Abstract

Ongoing improvement in computer, sensor and battery technology allows constructing small and high efficient autonomous underwater vehicles. New technologies create possibilities, which were only a few years ago impossible. Underwater robotics represents a fast growing research area and promising industry as advanced technologies in various subsystems develop and potential application areas are explored.

Underwater vehicles acting completely autonomous have to work on numerous problems, which must be solved in real-time by the onboard computer itself. Recent research brought up many of solutions to improve autonomous behaviour, considering all the small details.

The outcome of this thesis is a small, high performance, easy to handle autonomous underwater vehicle, based on a former remote operated vehicle to keep costs low. However it is equipped with a huge sensor-suite and effective actuators for motion control. Carrying a powerful computer controller it is able to navigate and fulfil tasks autonomously. An inertial measurement system is implemented on the base of an accelerometer and a compass. An infrared distance measurement system helps to avoid hitting obstacles or walls. The software is adjusted to the dynamical behaviour of the vehicle in water.

Simplifications in the mathematical model concerning vehicle dynamics are due to the mechanical design including a low centre of mass and the low speed specification possible. Adjusted PID algorithms for each degree of freedom track the vehicle. Obstacles recognition is realized with a colour camera system, which allows processing downward or forward view. Most of the variables and set points can be easily changed in software for further investigation and research.

Acknowledgements

This project could not have been completed without the assistance of a number of particularly helpful people. I would like to thank my project supervisor's professor Heinz Unkelbach in Germany and associate professor Thomas Bräunl for giving me the opportunity to write my thesis at the Mobile Robotics Lab at the University of Western Australia.

My time at CIPPS, working on the USAL-AUV project has been a great opportunity. Everyone within the department and within the project team has been welcoming. This project has been a great systems engineering project to help utilize the knowledge I have acquired during my studies.

Further I want to thank Prof. Bollenbacher and Prof. Schultes for their assistance and support prior my visit by writing reports and references.

I had a lot of professional discussion and received a great number of practical tips from the staff of the General and Electronic Workshops, thank you very much for that.

I want to thank my parents for their invaluable support and encouragement during the past few months and for sending me special electronic parts from Germany.

Most of the results obtained for this thesis could not have been obtained so accurately without the help of fellow engineering students, who provided me with useful assistance. We had a good time in the lab.

I am deeply indebted to Tamara Dinneen, who spend hours to on my paper to edit this paper and to correct my English.

And last but not least I want to mention my housemates the friendly family Todhunter who hosted me on my stay here in Australia in their house and supported me with their friendship.

Table of Contents

ABSTRACT	V
ACKNOWLEDGEMENTS	VII
TABLE OF CONTENTS	IX
TABLE OF FIGURES	XV
ABBREVIATIONS	XVII
NAUTICAL TERMINOLOGY	XVII
LIST OF VARIABLES	XIX
1 INTRODUCTION	1
1.1 REMOTE OPERATED UNDERWATER VEHICLES	2
1.2 AUTONOMOUS UNDERWATER VEHICLES	2
1.3 UNDERWATER VEHICLE COMPETITIONS	3
1.4 BASIC DESIGNS OF AUVs	3
1.5 PROJECT MOTIVATION	6
1.6 THESIS OVERVIEW	7
2 BACKGROUND THEORY	8
2.1 FACTORS AFFECTING AN UNDERWATER VEHICLE	8
2.1.1 <i>Visibility</i>	8
2.1.2 <i>Gravity and Buoyancy</i>	9
2.1.3 <i>Stability</i>	10
2.1.4 <i>Hydrodynamic Damping</i>	11
2.1.5 <i>Hydrostatic Pressure</i>	12
2.1.6 <i>Environmental Forces</i>	12
2.2 THE AUV REFERENCE FRAMES	13
2.3 MOTION CONTROL	15
2.3.1 <i>Computed Torque Control</i>	15
2.3.2 <i>On/Off Hysteresis Tracking Control</i>	16
2.3.3 <i>PID Tracking Control</i>	16
2.4 NAVIGATION	19
2.4.1 <i>Dead Reckoning</i>	20
2.4.2 <i>Inertial Measurement System</i>	20
2.4.3 <i>Navigation and Position Error</i>	21
2.4.4 <i>Reduction of random noise using Kalman filter</i>	21
2.4.5 <i>Radio Navigation</i>	23
2.4.6 <i>Path Planning</i>	24
2.5 SUMMARY	24

3	AUV DESIGN	25
3.1	PRIOR CHANGES ON THE USAL	25
3.2	MECHANICAL DESIGN	26
3.2.1	<i>Bow Hull</i>	<i>27</i>
3.2.2	<i>Middle Part</i>	<i>28</i>
3.2.3	<i>Stern Hull.....</i>	<i>29</i>
3.2.4	<i>The Electronics Rack.....</i>	<i>30</i>
3.3	ELECTRONICS DESIGN	31
3.4	MAIN CONTROLLER.....	32
3.5	ENERGY CONTROL SYSTEM.....	34
3.5.1	<i>Battery</i>	<i>35</i>
3.5.2	<i>DC/DC step-down converter.....</i>	<i>36</i>
3.5.3	<i>Power Distribution Board.....</i>	<i>37</i>
3.5.4	<i>Decoupling.....</i>	<i>38</i>
3.5.5	<i>Power gauge</i>	<i>40</i>
3.5.6	<i>Battery recharger.....</i>	<i>41</i>
3.6	MOTOR DRIVER	42
3.6.1	<i>Dual Motor H-Bridge Driver</i>	<i>42</i>
3.6.2	<i>Bow Thruster Motor Driver.....</i>	<i>44</i>
3.7	ACTUATORS	46
3.7.1	<i>Stern Thruster.....</i>	<i>46</i>
3.7.2	<i>Heave Thruster.....</i>	<i>47</i>
3.7.3	<i>Main Rudder</i>	<i>48</i>
3.7.4	<i>Bow Thruster</i>	<i>48</i>
3.8	COMMUNICATION	50
3.8.1	<i>Different Ways of Underwater Communication.....</i>	<i>50</i>
3.8.2	<i>The USAL-AUV Bluetooth Communication System.....</i>	<i>51</i>
3.8.3	<i>The USAL-AUV Infrared Remote Control System</i>	<i>52</i>
3.9	REQUIREMENTS TO THE SENSOR SUITE	53
3.10	NAVIGATION SENSORS	54
3.10.1	<i>Ranging Sensors</i>	<i>54</i>
3.10.2	<i>Heading Sensors</i>	<i>57</i>
3.10.3	<i>Odometry Measurement.....</i>	<i>58</i>
3.10.4	<i>Depth Sensor System.....</i>	<i>60</i>
3.11	MISSION SENSORS.....	63
3.11.1	<i>Camera-System.....</i>	<i>63</i>
3.11.2	<i>Position of Camera System</i>	<i>64</i>
3.12	PROPRIOCEPTIVE SENSORS	65
3.12.1	<i>Water Detector</i>	<i>65</i>
3.12.2	<i>Eyebot Onboard Voltage Gauge.....</i>	<i>67</i>
3.13	ALTERNATIVE SENSORS	67
3.14	A/D CONVERTER	67
3.15	SUMMARY	68

4	TESTING AND SYSTEM IDENTIFICATION	69
4.1	ACTUATOR IDENTIFICATION	70
4.1.1	<i>Stern Thruster Identification</i>	70
4.1.2	<i>Heave Thruster Identification</i>	72
4.1.3	<i>Main Rudder Identification</i>	74
4.1.4	<i>Bow thruster Identification</i>	76
4.2	SENSOR SUITE IDENTIFICATION AND CALIBRATION	77
4.2.1	<i>PSD Sensor</i>	77
4.2.2	<i>Compass</i>	80
4.2.3	<i>Accelerometer</i>	82
4.2.4	<i>Depth Sensor</i>	84
4.2.5	<i>Battery Gauge</i>	87
4.2.6	<i>Colour Camera</i>	87
4.3	BODY IDENTIFICATION	88
4.4	ENVIRONMENT AND EQUIPMENT	90
4.5	SUMMARY	90
5	CONTROLLING AND NAVIGATION OF USAL	91
5.1	SIMPLIFICATIONS IN DYNAMICS	92
5.2	MOTION CONTROL	93
5.2.1	<i>On/Off Hysteresis Control</i>	93
5.2.2	<i>PID Tracking Control</i>	94
5.3	SENSOR DATA	95
5.4	CONTROLLER IMPLEMENTATION	96
5.4.1	<i>Control System Structure</i>	96
5.4.2	<i>Software Structure</i>	97
5.5	SUBSIM SIMULATOR	99
5.6	WALL FOLLOWING TASK	100
5.7	SUMMARY	100
6	CONCLUSION	101
6.1	CONTRIBUTIONS OF THE THESIS	101
6.2	DISCUSSIONS OF THE OUTCOMES	102
6.2.1	<i>Electronics System</i>	102
6.2.2	<i>Sensor Suite</i>	102
6.2.3	<i>Controller</i>	102
6.2.4	<i>Improvement on the mechanical design</i>	103
6.3	RECOMMENDATIONS AND FUTURE WORK	103
6.3.1	<i>Electronics System</i>	103
6.3.2	<i>Sensor Suite</i>	103
6.3.3	<i>Controller Software</i>	104
6.3.4	<i>Mechanical System</i>	104
6.4	FINAL WORD	105
	REFERENCES	106

APPENDIX	111
A TEST RESULTS	111
A.1 ACTUATOR IDENTIFICATION	111
A.1.1 Stern Thruster Identification	111
A.1.2 Heave Thruster Identification	113
A.1.3 Main Rudder Identification.....	114
A.1.4 Bow thruster Identification.....	114
A.2 SENSOR IDENTIFICATION	115
A.2.1 PSD sensors	115
A.2.2 Compass.....	117
A.2.3 Accelerometer	120
A.2.4 Pressure Sensor	123
A.2.4 Pressure Sensor	123
A.3 BODY MEASUREMENTS	126
B TECHNICAL DATA	127
B.1 MAIN CONTROLLER	127
B.2 ENERGY SYSTEM	128
B.2.1 Battery.....	128
B.2.2 Switching Voltage Regulator	128
B.2.3 Battery Gauge.....	129
B.2.4 Battery Charger.....	129
B.3 ACTUATORS	130
B.3.1 Stern Motor Thruster	130
B.3.2 Heave Motor Thruster	130
B.3.3 Main Rudder Servo	131
B.3.4 Bow thruster Pump.....	131
B.3.5 Camera Servo.....	131
B.4 SENSORS	132
B.4.1 PSD.....	132
B.4.2 Compass.....	132
B.4.3 Accelerometer	133
B.4.4 Pressure Sensor	133
B.4.5 Camera	133
B.5 COMMUNICATION DEVICE.....	134
C THE ORIGINAL ROV.....	135
C.1 VEHICLE	135
C.2 BODY HULL.....	135
C.3 UMBILICAL CABLE.....	136
C.4 POWER SUPPLY	136
C.5 CHARGER	136
C.6 CAMERA	137
C.7 CONTROL MODULE.....	137

D THE COMPETITION	138
D.1 RESTRICTIONS	138
D.2 MISSION TASKS.....	138
E USER INSTRUCTIONS	1
F ALTERNATIVE SOLUTIONS.....	158
G ALTERNATIVE SENSORS	161
<i>G.1 Ultrasonic Proximity Sensors.....</i>	<i>161</i>
<i>G.2 Rate Gyroscopes.....</i>	<i>162</i>
<i>G.3 Paddlewheel</i>	<i>163</i>
<i>G.4 Pressure Difference Measurement</i>	<i>164</i>
<i>G.5 Doppler Velocity Measurement.....</i>	<i>166</i>
H MODELLING OF AUVS.....	168
H.1 REFERENCE FRAME TRANSFORMATION.....	168
H.2 ATTITUDE REPRESENTATION IN EULER ANGLES	169
H.3 VEHICLE STATE REPRESENTATION	171
H.4 EQUIVALENT ANGLE-AXIS	174
H.5 TRANSFORMATION OF STATES POSITION STATE VECTOR	175
H.6 HYDRODYNAMIC FORCES AND MOMENTS	176
H.7 EXTERNAL FORCES AND MOMENTS.....	178
H.8 UNDERWATER DYNAMICS.....	179
H.9 MASS AND INERTIA MATRIX	181
I CONTENTS OF THE CD-ROM	182

Table of Figures

Figure 1.1: The Subjugator (University of Florida) [UoF, 2005]	4
Figure 1.2: The Orca VI (Massachusetts Institute of Technology) [MIT, 2005]	4
Figure 1.3: The Mako (The University of Western Australia) [UWA, 2005]	5
Figure 2.1: Light absorption in water [Chaplin, 2005]	9
Figure 2.2: The buoyancy effect	9
Figure 2.3: The stability effect a) unstable configuration b) stable configuration	10
Figure 2.4: Righting moment RM due to rolling or pitching of the vehicle	11
Figure 2.5: The AUV-coordinate system and DOFs.....	13
Figure 2.6: The two reference frames defined for modelling.....	14
Figure 2.7: Motion control	15
Figure 2.8: On/off hysteresis control	16
Figure 2.9: Response of a P and PID-controller [Winfact98, 2006]	17
Figure 2.10: Algorithm scheme of Kalman filter [Brown, 1997]	22
Figure 3.1: The USAL-AUV	26
Figure 3.2: The front hull without metal rack	27
Figure 3.3: The heave thruster unit.....	28
Figure 3.4: The stern hull.....	29
Figure 3.5: The electronics rack	30
Figure 3.6: Wiring scheme of the electronics system.....	31
Figure 3.7: The Eyebot controller	33
Figure 3.8: The scheme of the Eyebot controller [Braeuni et al, 2005].....	33
Figure 3.9: Circuit diagram of the energy control system.....	34
Figure 3.10: Circuit diagram of the DC/DC step-down converter	36
Figure 3.11: DC-DC step-down converter and battery gauge	37
Figure 3.12: Power distribution board	38
Figure 3.13: The layout of the power distribution circuitry should not contain ground loops	39
Figure 3.14: Measured noise of the brushed heave motor on 60 % load.....	39
Figure 3.15: Circuit diagram of the battery gauge.....	40
Figure 3.16: Operation mode of a H-Bridge a) Stop b) Forward Direction c) Reverse Direction	42
Figure 3.17: Circuit diagram of the dual H-bridge	43
Figure 3.18: The dual H-bridge attached to the stern-side of the heave thruster unit	44
Figure 3.19: Circuit diagram of the bow thruster motor driver	45
Figure 3.20: The bow thruster motor driver.....	45
Figure 3.21: The 3-winged propeller of the stern thruster	46
Figure 3.22: The heave thruster	47
Figure 3.23: The bow thruster system	49
Figure 3.24: The Bluetooth communication device	52
Figure 3.25: Triangulation with PSDs	55
Figure 3.26: Opened Sharp PSD 2Y0A02	56
Figure 3.27: Position and directions of the PSDs in the AUV	56
Figure 3.28: The V2XG Compass.....	57
Figure 3.29: The Sparkfun Accelerometer	59
Figure 3.30: From Acceleration to Distance.....	59

Figure 3.31: The pressure sensor attached on the amplifier board	61
Figure 3.32: The depth sensor system	61
Figure 3.33: Circuit Diagram of the Depth Sensor Amplifier Board [Sensortech, 2004].....	62
Figure 3.34: The camera module.....	64
Figure 3.35: The vision system.....	64
Figure 3.36: Circuit diagram of water detector.....	66
Figure 3.37: Water detector lines on bottom of hull	66
Figure 3.38: Circuit diagram of the one-pole filter	67
Figure 4.1: Stern thruster force direction and point of application.....	70
Figure 4.2: Stern thruster identification graph.....	71
Figure 4.3: Stern thruster force direction	72
Figure 4.4: Heave thruster identification	73
Figure 4.5: Heave propeller interaction.....	73
Figure 4.6: Main rudder force direction	74
Figure 4.7: Turning with a stern rudder.....	74
Figure 4.8: Main rudder identification graph	75
Figure 4.9: Bow thruster force direction	76
Figure 4.10: Front PSD triangulation problem	78
Figure 4.11: PSD calibration distance to output at various conditions	79
Figure 4.12: Thermal drift of compass	80
Figure 4.13: The tilt influence on the compass	81
Figure 4.14: Screen on accelerometer calibration process.....	82
Figure 4.15: Error caused by tilt.....	83
Figure 4.16: Calibration graph with syringe	85
Figure 4.17: Pool depth sensor calibration graph	86
Figure 4.18: Pool configuration.....	88
Figure 4.19: Velocity vs. Eyebot speed of the AUV	89
Figure 4.20: Calculating times using a video tape and time code.....	89
Figure 4.21: The load cell	90
Figure 5.1: Simulating the AUV using WinFact98.....	94
Figure 5.2: Control system structure.....	96
Figure 5.3: Three layer software structure	97
Figure 5.4: The Subsim simulator.....	99

Abbreviations

AC	Alternating Current
ADC	Analogue-to-Digital Converter
Ah	Amp-hour
ata	Atmospheric Pressure
AUV	Autonomous Underwater Vehicle
AUVSI	Association for Unmanned Vehicle Systems International
CMOS	Complimentary Metal-Oxide-Semiconductor
DC	Direct Current
DR	Dead Reckoning
EMI	Electromagnetic Interference
HDT	Hardware Description Table
INS	Inertial Measurement System
LCD	Liquid Crystal Display
MIT	Massachusetts Institute of Technology
DOF	Degrees of Freedom
PC	Personal Computer
PD	Proportional Derivative
PID	Proportional Integral Derivative
PSD	Position Sensitive Detector
PVC	Polyvinylchloride
PWM	Pulse Width Modulation
RAM	Random Access Memory
ROM	Read Only Memory
ROV	Remotely Operated Vehicle
UWA	University of Western Australia

Nautical Terminology

Bow	Front side of vehicle
Stern	Back side of vehicle
Starboard	Right side of vehicle
Portside	Left side of vehicle
Surge	Motion in the longitudinal or x direction
Sway	Motion in the lateral or y direction
Heave	Motion in the vertical or z direction
Forward	Towards the front
Aft	Towards the back

List of Variables

Symbol	Name / Description
x	x position
y	y position
z	z position
ϕ	roll
θ	pitch
ψ	yaw
W	weight
B	buoyant force
g	gravitational acceleration
RM	righting moment
m	mass
ρ	density of water
V	volume
c_D	drag coefficient
s	speed
$\{B\}$	body frame
$\{W\}$	world frame
R	rotation matrix
P_B	position state vector
x_B	position vector
VB	velocity state vector
u	surge
v	sway
w	heave
T_B	force/torque state vector
F_B	force vector
W_B	torque vector
M	Mass and inertia matrix
M_{RB}	rigid body mass matrix
M_A	added mass matrix
I_x	Mass moment of inertia coefficient (x-axis)
I_y	Mass moment of inertia coefficient (y-axis)
I_z	Mass moment of inertia coefficient (z-axis)
$C(V)$	Coriolis and centripetal matrix
$C_{RB}(V)$	rigid body Coriolis and centripetal matrix
$D(V)$	hydrodynamic damping matrix
G	gravitational and buoyancy vector
f_B	buoyant force vector
f_G	gravitational force vector
r_B	centre of buoyancy vector
r_G	centre of gravity vector
L	thrust mapping matrix
U	thrust vector

1 Introduction

Autonomous robots are robots, which can perform desired tasks in unstructured environments without continuous human guidance. Many kinds of robots are autonomous to some degree. Different robots can be autonomous in different ways. A high degree of autonomy is particularly desirable in fields such as space and sub-sea exploration, where communication delays and interruptions are unavoidable.

Some modern factory robots are "autonomous" within the strict confines of their direct environment. Perhaps not every degree of freedom exists in their surrounding environment but the work place of the factory robot is challenging and can often be unpredictable.

The exact orientation and position of the next object of work and in the more advanced factories even the type of object and the required task must be determined. This can vary unpredictably at least from the robot's point of view. From the start, factory robots have not been subject to continuous human guidance or necessarily any human guidance at all. One important area of robotics research is to enable the robot to cope with its environment whether this is on land, underwater, in the air, underground or in space. A fully autonomous robot in the real world has the ability to:

- Gain information about their environment
- Work for a longer time period without human intervention.
- Travel from point A to point B, without human navigation assistance.
- Avoid situations that are harmful to people, property or itself.
- Repair itself without outside assistance.

A robot may also be able to learn autonomously which includes the ability to:

- Learn or gain new capabilities without outside assistance.
- Adjust strategies based on the surroundings.
- Adapt to surroundings without outside assistance.

1.1 Remote operated Underwater Vehicles

These days are a lot of submersible remote operated vehicles (ROV) are used frequently. They tend to be highly specialized for their specific task. Some are designed for scanning wide swaths of the ocean floor while others are designed for photography and recovery. A number of deep-sea animals and plants have been discovered or studied in their natural environment only through the use of ROVs.

Submersible ROVs have been used to locate many shipwrecks, including that of the RMS Titanic, the Bismarck, USS Yorktown, and SS Central America. In some cases, such as the SS Central America and airline crashes such as Alaska Airlines Flight 261. ROVs have been used to recover material from the sea floor and bring it to the surface. They have been used to study the behaviour and micro distribution of krill under the ice of Antarctica. Underwater robots can help us better understand marine and other environmental issues, protect the ocean resources of the earth from pollution, and efficiently utilize them for human welfare. However, extensive use of manned submersibles and ROVs are currently limited to a few applications because of very high operational costs.

1.2 Autonomous Underwater Vehicles

Autonomous underwater vehicles tend to be very similar to the ROVs. However these vehicles are usually battery powered and carry its own computer. This onboard computer is the requirement for their autonomous behaviour. They gain information from their sensors for navigation and mission tasks. In military applications, AUVs are also known as Unmanned Undersea Vehicles (UUVs). They can operate in water as deep as 6000 meters and with recent advances in battery technology, these robotic submarines can travel tens of kilometres.

Primarily oceanographic tools, AUVs carry sensors to navigate autonomously and map features of the ocean. Typical sensors include compasses, depth sensors, side-scan and other sonar's, magnetometers, thermistors and conductivity probes.

Underwater robots require adequate guidance and control to perform useful tasks. Visual information is important to these tasks and visual servo control is one method by which guidance can be obtained. A connectionist learning approach can replace complex models and control schemes to coordinate and control thrusters.

The demand for advanced underwater robot technologies is growing and will eventually lead to fully autonomous, specialized, reliable underwater robotic vehicles.

1.3 Underwater Vehicle Competitions

There are only a small number of underwater vehicle competitions available. The most popular is the annual competition of the Association for Unmanned Vehicle Systems International (AUVSI). The AUVSI is the world's largest non-profit organization devoted exclusively to advancing the unmanned systems community. With members from government organizations, industry and academia it is committed to fostering, developing, and promoting unmanned systems and related technologies. [AUVISI, 2005] By providing opportunities for information exchange, networking and business development, AUVSI forums are the best resource for simply learning about unmanned systems or for staying abreast of the latest program and technology updates. The University of Western Australia is also presenting a competition for real and simulated AUVs. The tasks are at this stage more elementary and described in the appendix.

1.4 Basic Designs of AUVs

The area of AUVs is being researched by a number of universities and research centres around the world. Currently a wide variety of AUVs are being developed with the aim to further utilize the expansive underwater environment.

A few of the AUVs designs currently in use are described below, including aspects relating to the control methodologies implemented in the AUVs.

The "Subjugator" is an AUV being developed at the University of Florida. Five thrusters provide motion. A Pentium embedded single board performs its vision system and Atmel AVR micro controllers manage sensors and actuators. These micro-controllers make higher-level decisions and control analogue and timing related interfaces. This AUV won the 2005 AUVISI competition.



Figure 1.1: The Subjugator (University of Florida) [UoF, 2005]

"Orca VI" has been designed and built at the Massachusetts Institute of Technology. This AUV navigates with the help of four marine thrusters. It is equipped with a huge sensor suite including a six axes inertial measurement system, cameras and sonar's and a compass. Recent work performed on the AUV has been on the stereovision system and on a simulation program.

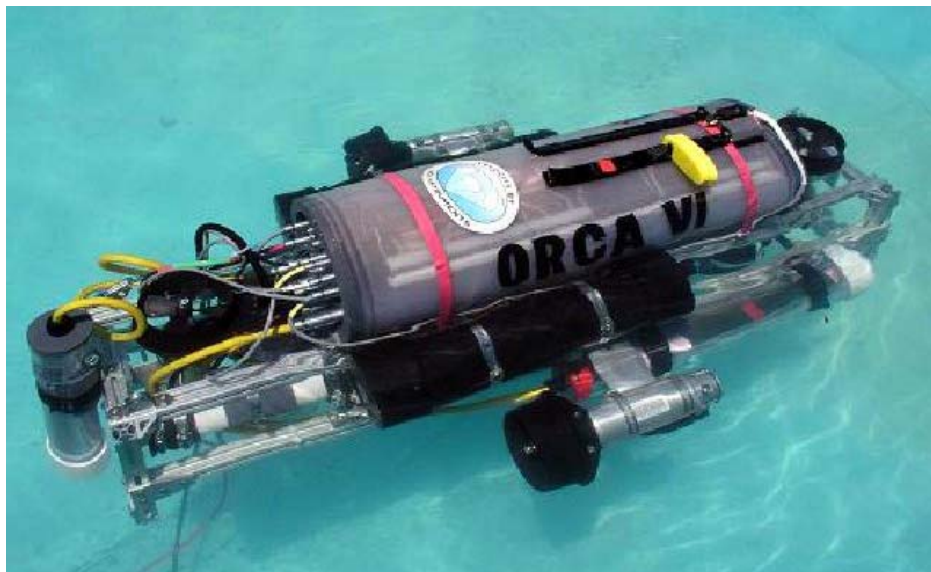


Figure 1.2: The Orca VI (Massachusetts Institute of Technology) [MIT, 2005]

The “Mako” is the first AUV of the University of Western Australia developed in 2004 at the Mobile Robotics Lab of CIPPS. It has a strongly symmetric design with two vertical thrusters for heave motion and two thrusters attached on the sides for surge and yaw motion. Recent research on the AUV deals with motion control and the sensor suite.

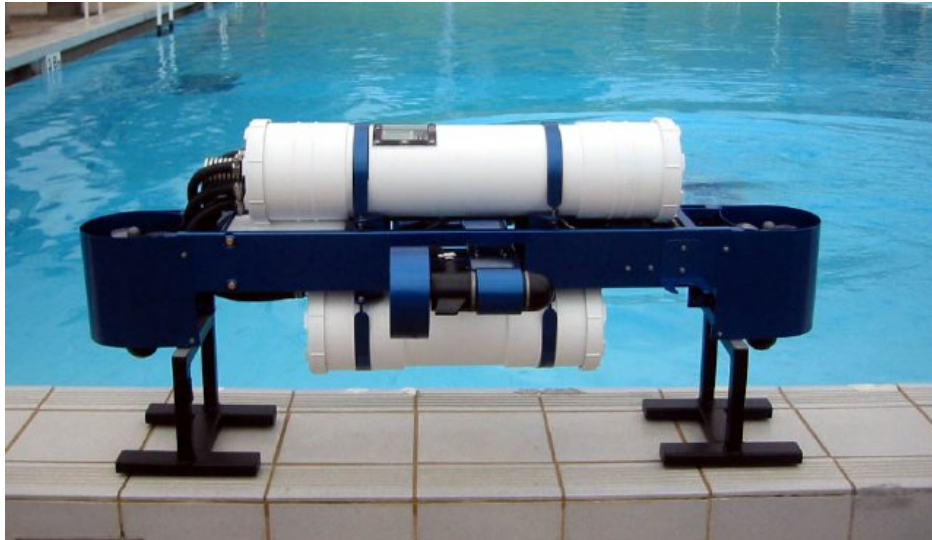


Figure 1.3: The Mako (The University of Western Australia) [UWA, 2005]

1.5 Project Motivation

The outcome of this project should be a small, highly transportable and high performance AUV, constructed to participate in AUV competitions and to provide groundwork for future research. For purposes of economy, it is based on a former ROV, which was given to the university in gratuitous. Following modifications, navigation and map building from the inclusion of the sensor suite, as well as motion control with the help of actuators controlled by onboard controller make the vehicle able to perform mission tasks autonomously.

The yellow USAL-AUV is the second AUV constructed in this lab. The first one is far larger and heavier, which makes transportation to competitions expensive.

The objectives of this thesis were:

Design of the electronic system, which provides:

- Motion control
- Energy control and recharge
- Communication
- Easy and reliable design
- All controller values soft coded for easy modifications
- Failsafe connectors

Choose, build up and calibrate the sensor suite including:

- Navigation sensors: for sensing the motion of the vehicle
- Mission sensors: for sensing the operating environment
- Proprioceptive sensors for vehicle diagnostics.

Implement a controller system for controlling, tracking and navigation of the AUV.

1.6 Thesis Overview

This thesis documents the process by which the electronics and sensor suite for USAL-AUV have been derived. A short description for each of the chapters follows.

Chapter 2 – Background Theory

This chapter contains background theory that has been required during the course of the project. There were four main sections to the theory. It starts with a spotlight on factors affecting an underwater vehicle followed by some issues on states of underwater vehicles. It continues with different ways of providing and controlling motion. A general overview of navigation purposes including noise filtering using a Kalman filter for exact positioning in the last section completes the background theory.

Chapter 3 AUV Design

Design of the underwater vehicle depends on the specific tasks it has to pass. The requirements of these tasks decide the mechanical shape, the active controlled degrees of freedom, the onboard computer system, the sensor suite and the energy source. This chapter gives a survey of the design, the restrictions and the hardware used to complete the whole system. It also describes the process by which the final set of sensors, which will make up part of the navigation system, was arrived at.

Chapter 4 – System identification and testing

A mechanical model and system-identification are necessary to establish control algorithms for manoeuvring and navigation. The sensors had to be fitted on their optimal location and have to be adjusted and calibrated. Several tests and measurements described in this chapter helped investigating the AUV.

Chapter 5 – Control of USAL AUV

In this chapter, theory and system identification meet each other. Once modelling has been undertaken, a control system can then be designed for the underwater vehicle. Control systems are required to provide signals to the actuators in order to achieve the desired positions and velocities for the vehicle. Controlling underwater vehicles is different from controlling other vehicles due to the nature of underwater dynamics. Control device is an Eyebot-embedded computer system with attuned PID algorithms.

2 Background Theory

This chapter contains background theory that has been required during the course of the project. The first section deals with factors affecting an underwater vehicle. The second section spotlights mathematical background of modelling underwater vehicles, section three presents basic knowledge about motion control and section four navigation systems.

2.1 Factors Affecting an Underwater Vehicle

Venturing offshore into water comes together with a myriad of changes in surroundings and design directives. The robot has to be watertight, actuator and sensor requirement has to be changed and adjusted for the underwater world. Due to the nature of underwater dynamics a large number of external mostly non-linear properties affect the submarine when it is in or under water.

2.1.1 Visibility

The visibility under water is affected by different factors. White light such as sunlight consists of all colours mixed together. As white light travels through water, the water absorbs colours one by one: first red, followed by orange and yellow. Since each colour makes up a part of the total light, less light remains as depth increases and the water absorbs each colour. This makes deeper water darker and less colourful. Red, orange or yellow objects often appear to be brownish, grey or black. To see more vivid colours on deeper water it is necessary to carry a light [Padi, 2004].

Another factor decreasing visibility is the amount of particles in the water. A large number of fine particles, maybe dispersed from the ground by the thrusters could set visibility down to nearly zero meters. Figure 2.1 shows the absorption rate of water for different light waves. Especially infrared light is well absorbed, which becomes later a problem when designing the sensor suite.

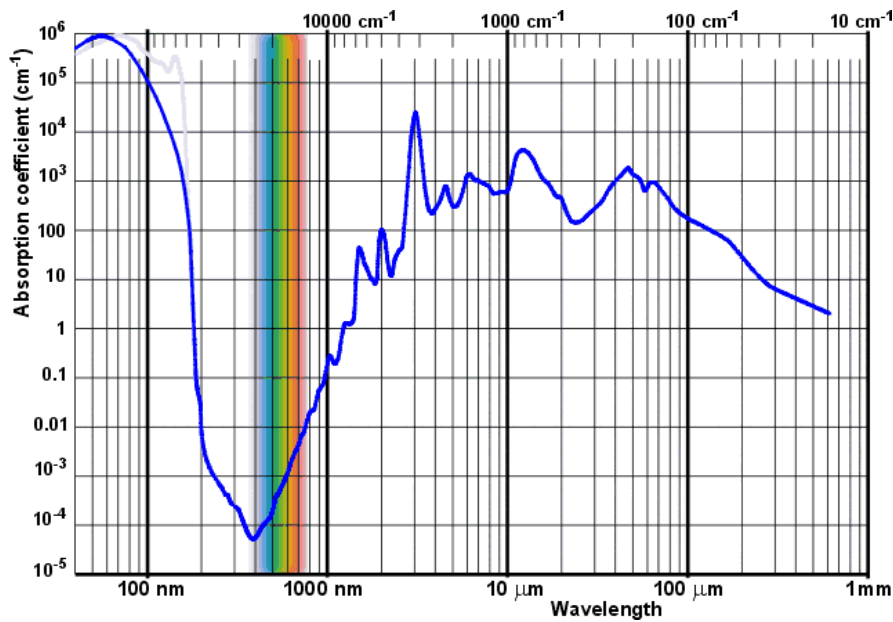


Figure 2.1: Light absorption in water [Chaplin, 2005]

2.1.2 Gravity and Buoyancy

A solid body submerged in a fluid will have upward buoyant force acting on it equivalent to the weight of displaced fluid, enabling it to float or at least to appear to become lighter. If the buoyancy exceeds the weight, then the object floats; if the weight exceeds the buoyancy, the object sinks. If the buoyancy equals the weight, the body has neutral buoyancy and may remain at its level. Discovery of the principle of buoyancy, which is a result of the hydrostatic pressure in the fluid, is attributed to Archimedes.

[Wikipedia buoyancy, 2005]

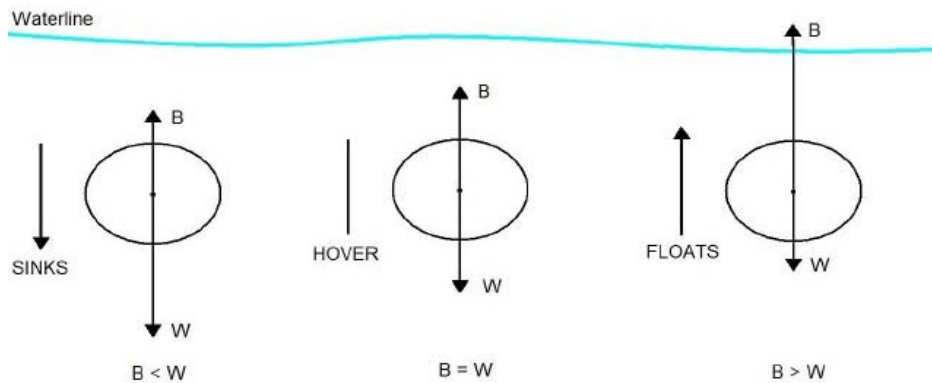


Figure 2.2: The buoyancy effect

2.1.3 Stability

A floating object is stable if it tends to restore itself to a balanced position after a small displacement. For example, floating objects will generally have vertical stability, as if the object is pushed down slightly, this will create a greater buoyant force. This force, unbalanced against the weight force will push the object back up. Rotational stability is of great importance to floating vessels. Given a small angular displacement, the vessel may return to its original position (stable), moving away from its original position (unstable), or remain where it is (neutral). Rotational stability depends on the relative lines of action of forces on an object. The upward buoyant force C_B on an object acts through the centre of buoyancy, being the centric of the displaced volume of fluid. The weight force C_M on the object acts through its centre of gravity. An object will be stable if an angular displacement moves the line of action of these forces to set up a 'righting moment'. [Wikipedia stability, 2005]

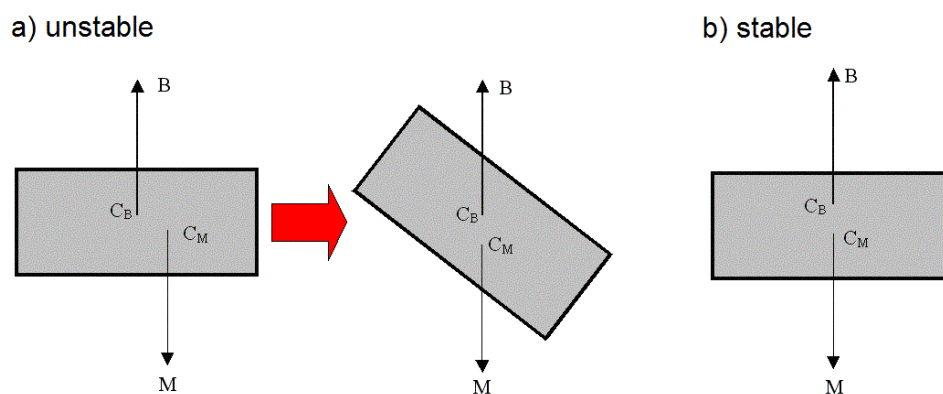


Figure 2.3: The stability effect a) unstable configuration b) stable configuration

If C_M and C_B have the same position the vehicle will retain stability. The result of this is a rightening movement RM, when the vehicle rolls or does a pitch movement (shown on Figure 2.4). This moment RM can be written as:

$$RM = \frac{1}{2} d(B + W) \sin \lambda ,$$

where

B, W are forces of the vehicle and
d distance between centres of mass and buoyancy.

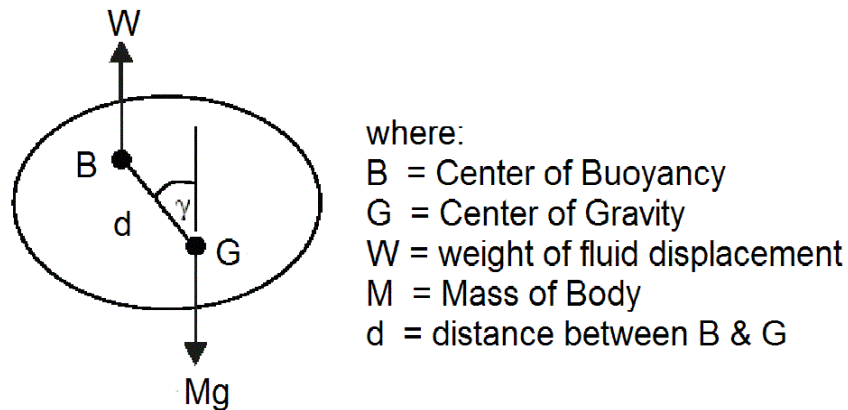


Figure 2.4: Righting moment RM due to rolling or pitching of the vehicle

2.1.4 Hydrodynamic Damping

Drag is a mechanical force, generated by the interaction and contact of a solid body with a fluid (liquid or gas). The drag equation gives the drag experienced by an object moving through a fluid:

$$D = \frac{1}{2} \rho v^2 A C_d$$

where

D is the force of drag,

ρ is the density of the fluid*,

v is the velocity of the object relative to the fluid,

A is the reference area, and

C_d is the drag coefficient (a dimensionless constant, e.g. 0.25 to 0.45 for a car).

*Note that for the Earth's atmosphere, the density can be found using the barometric formula. In the case of fluid at 15 °C and standard atmospheric pressure.

Drag is a force and is consequently a vector quantity having both a magnitude and a direction. Drag acts in a direction that is opposite to the motion of the submarine. This effect can be without doubt modelled with added mass. Added mass is quite a significant effect and is related to the mass and inertial values of the vehicle.

2.1.5 Hydrostatic Pressure

The force acting on the object in the water depending on the depth is the sheer weight of the fluid above, up to the water's surface - such as from a water tower. The resulting hydrostatic pressure is isotropic: the pressure acts in all directions equally, according to Pascal's law:

$$p = \rho gh ,$$

where

p is the water pressure

ρ the water density

g the gravity force

h the water depth

The pressure increases linear with the water depth.

Depth	Pressure	Volume of Air
0	1 bar	1.00 L
5	1.5 bar	0.75 L
10	2 bar	0.50 L
15	2,5 bar	0.31 L

Table 2.1: Water Pressure on various depths [Padi, 2004]

2.1.6 Environmental Forces

Waves and wind on the surface, currents and turbulences underwater affecting the stability and motion of the AUV have to be considered. Other factors as extreme high or low temperature or extreme sunshine can affect the computer or interfere with sensor recognition. Changes in temperature can also cause condensing water in the hermetic closed inside of the AUV, potentially resulting in electronic damage.

2.2 The AUV reference frames

Small unmanned marine vehicles suitable for use in both naval and commercial operations have unique mission requirements and dynamic response characteristics. In particular, they are required to be highly manoeuvrable and very responsive as they operate in obstacle avoidance and object recognition and localization scenarios. The need, therefore, arises to maintain an accurate path in keeping to confined spaces and shallow waters under the influence of steady and time varying external forces.

A frame of reference is the perspective from which a system is observed. Analogous to flying vehicles, an AUV has six DOF, three spatial coordinates x , y , z and three attitude defining Euler angles yaw ψ pitch θ and roll ϕ . Figure 2.5 shows the AUV-coordinate System and its DOFs.

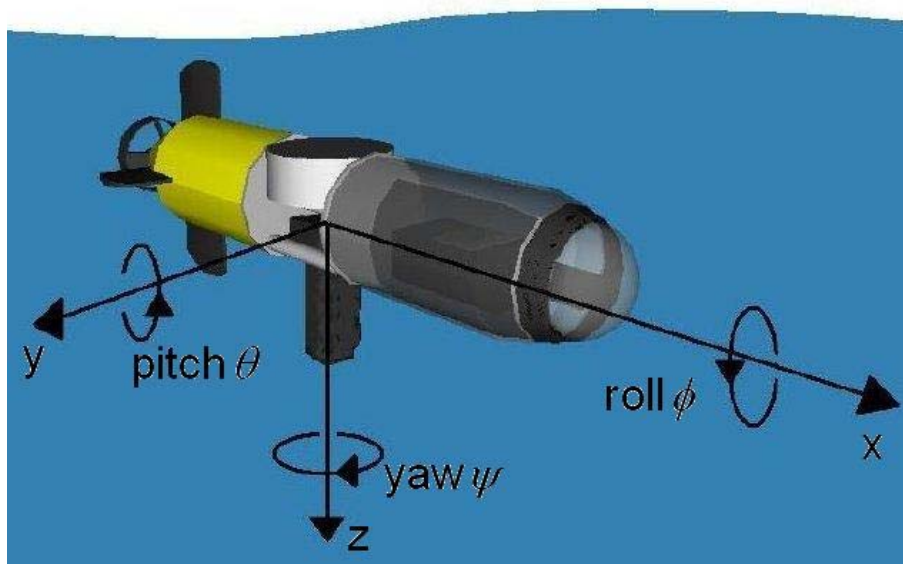


Figure 2.5: The AUV-coordinate system and DOFs

The x-axis points along to forward direction, the y-axis to starboard and the z-axis - because of positive declaration - downwards. Most AUVs are designed to control as many DOFs as possible active with actuators.

In modelling AUVs it is necessary to deal with two reference frames. The first reference frame is the world reference frame $\{W\}$, which is a global fixed frame attached to the real world. This frame is useful to track where the vehicle is, how it is orientated and how the vehicle moves. The body frame is the AUV reference frame $\{B\}$, which is a local frame attached to the AUV. This frame is defined as an instantaneous reference frame at any time t . Thus the frame $\{B\}$ moves relative to frame $\{W\}$ along with the AUV.

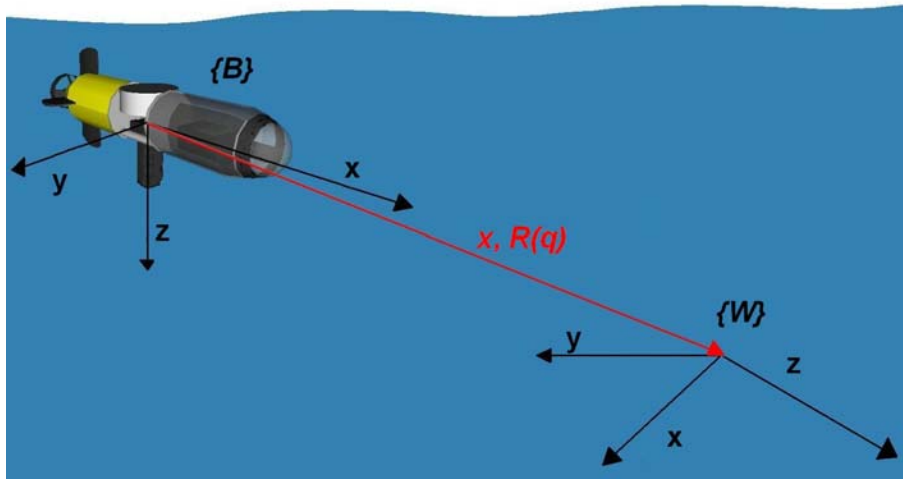


Figure 2.6: The two reference frames defined for modelling

For further information concerning reference frames, attitude representation in Euler Angles vehicle state representation and transformation between states please refer the appendix section I.

2.3 Motion Control

Motion control is an essential part of several control applications. Controlling AUVs is a very challenging problem due to the fact that they operate underwater. In underwater conditions, hydrodynamics are the major sources of non-linearity in the system dynamics. A large number of controllers have been investigated for AUV motion control.

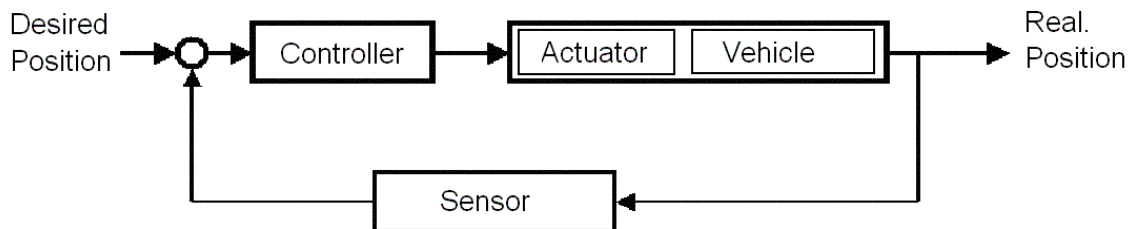


Figure 2.7: Motion control

The three main control methods in common use are Fuzzy Logic, Neural Networks and hybrid Neural-Fuzzy systems. These algorithms allow the controller to adapt to the changing environment seen in dynamic waters such as found in oceanic conditions. In systems limited to static water or pool use, especially in competition AUVs, PID-controllers are broadly used.

A control loop consists of three parts:

- Measurement by a sensor attached to the process
- Decision in a controller unit
- Action through an output device ("actuator") such as a motor driver

2.3.1 Computed Torque Control

In controlling robotic manipulations a computed torque scheme is often used. [Craig, 1989] Computed torque control usually works well when the system dynamics are known fairly accurately. It is a feedback linearisation of non-linear systems.

The purpose is to make non-linear systems behave like linear systems so that the well-established knowledge in linear control theory can have applied in the designing controller. The feedback-signal cancels the effects of gravity, friction, the manipulator inertia tensor, and Coriolis and centrifugal forces. Use of the Lagrange-Euler dynamic model will implement this cancellation.

2.3.2 On/Off Hysteresis Tracking Control

The simplest way of controlling is an on/off control with a hysteresis. A good example for a controller like this is the iron. Switched on the temperature goes up to the desired temperature then the switch (normally realized with a bimetal) switches the heater off. Due to heat transfer to air and clothes temperature drops down to a specific point where the switch reactivates the heater.

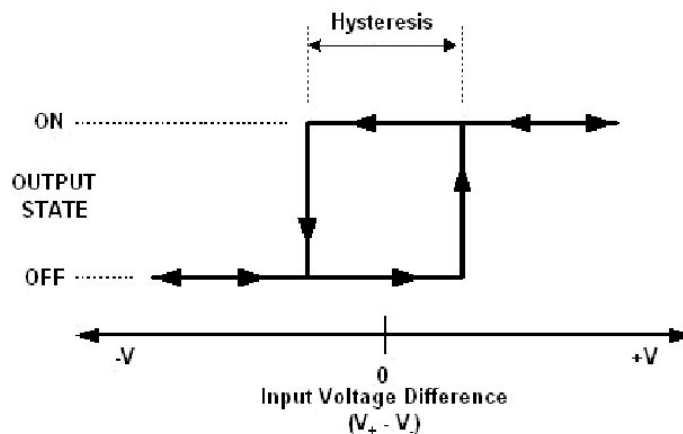


Figure 2.8: On/off hysteresis control

2.3.3 PID Tracking Control

A PID controller is the most common used controller to control any measurable variable which can be affected by manipulating some other process variable such as temperature, pressure, flow rate, chemical composition, force, speed, or other variables. Development of PID control originated from the observation that a proportional-only control can only eliminate the error between set point and process variable at one particular set point. At any other setting, there would be an offset between the set point and the true process value.

The derivative term reflects the ability to observe the rate of change of the process variable and again adjust the set point in anticipation of the final value.

A Proportional Integral Derivative (PID) Controller is a closed loop feedback controller used to control an output to a desired value. The following explanation has been adapted from [Wikipedia PID, 2005]:

The controller works by creating an error signal, $\varepsilon(t)$ from the difference between the desired output $R(t)$ and the measured output $\hat{Y}(t)$ which is expressed as:

$$\varepsilon(t) = R(t) - \hat{Y}(t) \quad (2.1)$$

A PID controller then generates a control signal for the plant to be controlled according to

$$u(t) = K_p \varepsilon(t) + K_I \int_0^t \varepsilon(t) dt + K_D \frac{d\varepsilon(t)}{dt} \quad (2.2)$$

Where K_p , K_I and K_D are the constant proportional, integral and derivative gains respectively.

Suitable numerical values can either be calculated from a mathematical plant model or experimentally determined. The response from a typical P and a PID-controller with desired value of 1 simulated in WinFact98 is shown in Figure 2.9.

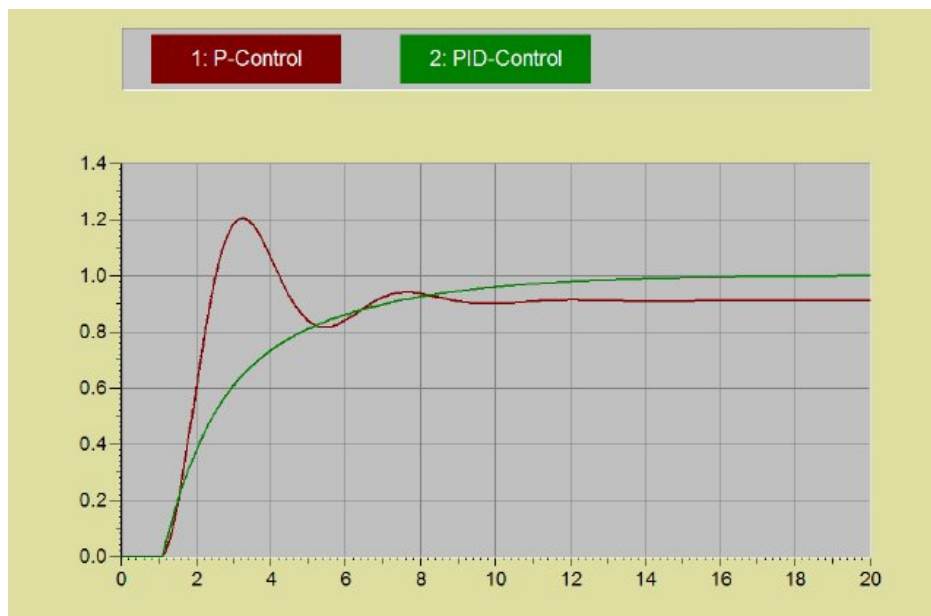


Figure 2.9: Response of a P and PID-controller [Winfact98, 2006]

Output from the controller exhibits four major measurable characteristics, rise time, overshoot, settling time and steady-state error. Rise time defines the time taken for the controller to first reach its desired value, which it may then overshoot reaching a peak value (overshoot) before returning toward the desired value. This can be seen in the figure above. Settling time is the time the system takes to 'settle' on the desired value, just over 1 second in Figure 2.9. It is possible for the controller to be incapable of settling on the desired value, settling elsewhere. The difference between the desired value and the value the controller eventually settles on is referred to as steady-state error. These four parameters are influenced by the PID controller gains K_p , K_I and K_D , Table 2.2 summarises the effect of modifying these constants.

Gain Constant	Rise Time	Overshoot	Settling Time	Steady State Error
K_p	Decrease	Increase	Small Change	Decrease
K_I	Decrease	Increase	Increase	Eliminate
K_D	Small Change	Decrease	Decrease	Small Change

Table 2.2: PID Gain Constants Modifying Effects [Wikipedia PID, 2005]

"Tuning" a control loop is the process of adjustment of its control parameters to the optimum values for the desired control response. The optimum behaviour on a process change or set point change varies depending on the application. Some processes must not allow an overshoot of the process variable from the set point. Other processes must minimize the energy expended in reaching a new set point. Generally stability of response is required and the process must not oscillate for any combination of process conditions and set points. Tuning of loops is made more complicated by the response time of the process; it may take minutes or hours for a set point change to produce a stable effect. Some processes have a degree of non-linearity and so parameters that work well at full-load conditions do not work when the process is starting up from no-load.

2.4 Navigation

Movement between two points is typically considered a navigation problem, separate to the control problem. Depending on the work location and desired tasks there are several designs suitable. Today, most AUVs work in conjunction with surface vessels for navigational purposes, although ultra-low-power, long-range variants such as underwater gliders are becoming capable of operating unattended for days or weeks, periodically relaying data by satellite to shore, before returning to be picked up.

When a surface reference such as a support ship is available, ultra-short baseline (USBL) positioning is used to calculate the location of the sub-sea vehicle relative to the known (GPS) position of the surface craft by means of acoustic range and bearing measurements. For the longer range types, the AUV itself will surface and take its own GPS fix. In between position fixes and for precise manoeuvring, an inertial navigation system onboard the AUV measures the acceleration of the vehicle and velocity technology is used to measure rate of travel. These observations are filtered to determine a final navigation solution.

Positioning technologies can broadly be divided into two main streams: relative positioning and absolute positioning. Absolute position means that the currently calculated position does not depend on the previous positions. An example of an absolute positioning system is the Global Positioning System (GPS). The advantage of this system is that there is no accumulation of drift error. However, GPS has the signal blockage problem in the outdoor environment. Also, it cannot be used indoors and has relatively low output rate. For a relative positioning system, the dead-reckoning method is employed to find the position. [Abbot, 1999; Barshan, 1993]

2.4.1 Dead Reckoning

Dead reckoning is the process of estimating a global position of a vehicle by advancing a known position using course, speed, time and distance to be travelled. That is figuring out where you momentarily are or where you will be at a certain time if you hold the speed, time and course you plan to travel.

Dead reckoning is a method of navigation used in ships, aircraft, trucks, cars, construction sites engines and more recently, mobile robots. Essentially it is used to estimate an object's position based on the distance it travelled in its current direction from its previous position.

A navigation system using this method uses the vehicles last known position (fix), then plots the vehicles expected position for a given fix interval (elapsed time from one fix to the next) according to the compass course it is steering, the speed, and allowance for currents. In modern navigation, this plotted position is compared to a fix, taken at the time for which the DR was plotted, to determine set and drift (the combined external forces which act upon a ship causing it to deviate from its intended course).

2.4.2 Inertial Measurement System

One of the commonly used relative positioning systems is the inertial navigation system (INS). Dead reckoning positioning with gyros and accelerometers is called inertial navigation. The gyro measures the angular rate and the accelerometer senses the accelerations. Integration of angular velocity with time yields angle data. Distance data can be obtained by double integration of acceleration with time. INS is a self-contained device, which requires no external electromagnetic signals. Thus, INS does not have the signal coverage problem found in GPS. Moreover, the data output rate of INS could be much faster than GPS. However, the disadvantage of INS is the bias drift problem. These errors would be accumulated and the accuracy deteriorates with time due to integration. Methods such as the Kalman filter are employed to reduce errors due to the random bias drift. [Barshan, 1995]

2.4.3 Navigation and Position Error

The navigation and positioning accuracy required in an AUV will be determined by the mission requirements. Positional accuracy is any error made by an AUV determining geographic position. Navigation accuracy is the precision with which the AUV can guide itself from one geographical point to another.

A very basic navigational error model for AUV navigation uses the following terms:

$$\text{Total Error}(1\sigma) = \sqrt{\varepsilon_p^2 + (D \sin \varphi_o)^2 + (D \sin \varphi_{DI})^2 + (D \delta V_o)^2 + (D \delta V_A)^2}$$

where

ε_p = initial vehicle position error

δV_A = along-track velocity error

φ_o = initial heading error

δV_o = cross-track velocity error

φ_{DI} = sensor heading misalignment

The values for these terms are combined to give a root-sum-square estimate (1σ) of vehicle position error as a function of distance travelled (D). All of these error contributions are independent of vehicle speed and higher order terms such as heading drift rate are not included.

It should be stressed that this is a worst-case scenario as it assumes the vehicle is on a constant heading throughout the mission. In many operations, the vehicle changes or reverses heading frequently, and in these cases, other error models are used to account for cancellation of navigational errors. [Loebis et al, 2003]

2.4.4 Reduction of random noise using Kalman filter

A Kalman filter is a commonly used method for random noise reduction and data fusion for positioning applications. In this method, statistical characteristics of a measurement model is used to recursively estimate the required data. Kalman filtering is basically a statistical method that combines knowledge of the statistical nature of system errors with knowledge of system dynamics, as represented by a state-space model, to provide an estimate of the state of a system. [Mostov, 2005] Any number of unknowns can be included in the states. In a navigation system, we are usually concerned with position and velocity. The state estimate is obtained using a weighting function called the Kalman gain, which is optimised to produce a minimum error variance [Kaplan, 1996].

A Kalman filter can be used to blend measurements from multiple sensors and provide both an estimate of the current state of a system and a prediction of the future state of the system. The algorithm scheme of a Kalman filter is shown in Figure. 2.10. [Brown, 1997]

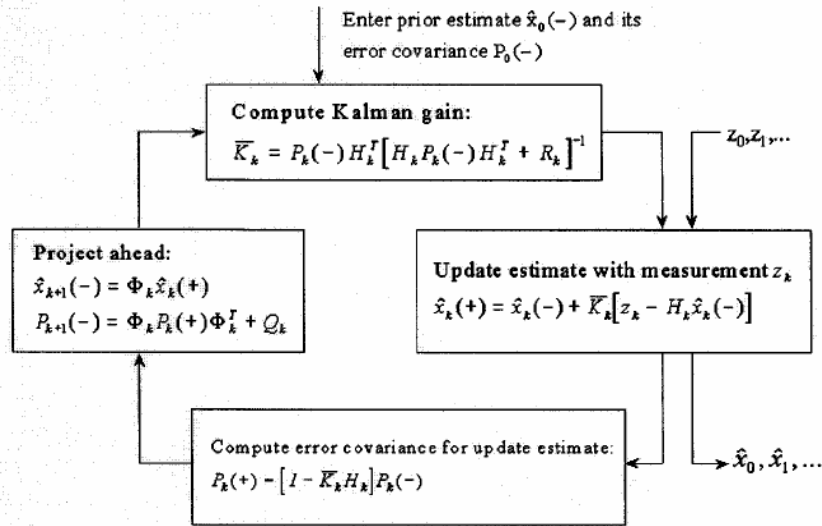


Figure 2.10: Algorithm scheme of Kalman filter [Brown, 1997]

where

x_k is the system state,

z_k is the measurement,

w_k is the plant noise with its covariance Q_k ,

v_k is the measurement noise with its covariance R_k ,

"(-)" indicates the a priori values of the variables

(before the information in the measurement is used),

and "(+)" indicates the a post-priori values of the variables.

\bar{K} is the Kalman gain, Φ_k is the transition matrix at time t_k , P_k is the error covariance matrix, H_k and is the measurement matrix, whereas

$$\phi_k = \begin{bmatrix} 1 & \Delta t & \Delta t^2/2 \\ 0 & 1 & \Delta t \\ 0 & 0 & 1 \end{bmatrix}, \quad Q_k = \begin{bmatrix} \frac{W}{20} \Delta t^5 & \frac{W}{8} \Delta t^4 & \frac{W}{6} \Delta t^3 \\ \frac{W}{8} \Delta t^4 & \frac{W}{3} \Delta t^3 & \frac{W}{2} \Delta t^2 \\ \frac{W}{6} \Delta t^3 & \frac{W}{2} \Delta t^2 & W \Delta t \end{bmatrix}.$$

2.4.5 Radio Navigation

Radio navigation is the application of radio frequencies to determining a position on the Earth. Like radiolocation, it is a type of radio-determination.

The first system of radio navigation was the radio direction finder, or RDF. By tuning in a radio station and then using a directional antenna to find the direction to the broadcasting antenna, radio sources replaced the stars and planets of celestial navigation with a system that could be used in all weather and times of day. Taking two such measurements and plotting the directions on a map will result in an intersection, your current location.

LORAN (LONg RANge Navigation) is a terrestrial navigation system using low frequency radio transmitters that use the time interval between radio signals received from two or more stations to determine the position of a ship or aircraft. The current version of LORAN in common use is LORAN-C, which operates in the low frequency 90 to 110 kHz band. The navigational method provided by LORAN is based on the principle of the time difference between the receipt of signals from a pair of radio transmitters. A given constant time difference between the signals from the two stations can be represented by a hyperbolic line of position (LOP). If the position of the two synchronized stations are known, then the position of the receiver can be determined as being somewhere on a particular hyperbolic curve where the time difference between the received signals is constant. [Xiaoping et al, 2000]

The GPS system is made up of a satellite constellation of at least 24 satellites in an intermediate circular orbit (ICO), in 6 orbital planes. Ground stations around the world monitor the flight paths of the GPS satellites, synchronizing the satellites' onboard atomic clocks, and uploading data for transmission by the satellites.

A GPS receiver compares time signal transmissions from four or more satellites to calculate the precise time and its current position (latitude, longitude, elevation), using trilateration. The receiver computes the distance to each of the four satellites from the difference between local time and the time the satellite signals were sent (this distance is called a pseudo-range). It then decodes the satellites' locations from their radio signals and an internal database.

2.4.6 Path Planning

At the heart of the execution level there exists the functions of navigation, guidance, and control. The guidance and control functions are linked to the higher software intelligence levels through path planning. The path planner takes information from charted obstacles and friendly or hostile environments and generates a smooth path for the vehicle to follow. A certain level of feedback exists in this operation through the use of sonar's in order to replan a path when uncharted objects are encountered or when the mission requirements have changed. Based on the desired vehicle position and orientation pairs at certain points, several classes of smooth paths containing sets of straight-line segments and circular arcs or cubic splines can be obtained. The fundamental breakdown of the motion control functions between guidance and control relies on the notion that an autopilot is responsible for stabilizing the motion dynamics of the vehicle in terms of its speed, heading, and depth. The guidance law combines commands the motion controller for the path and position to be followed and other attitude requirements. [Valavanis et al, 1997]

This separation of guidance and motion control functions is not without its problems. However, for accurate path keeping the dynamics of the guidance law must be as fast as possible. This sets a lower bound for the motion controller reaction time. Ocean vehicles suffer from a number of dynamic lags in their motion response and actuator sizing, and these lags set an upper bound for their reaction time.

2.5 Summary

This chapter presents an outline of the theories behind controlling vehicles underwater. The USAL-AUV INS has a sensor suite that contains a number of sensors that measure a few of the state variables. It also contains a dynamic model of the USAL-AUV system and thus, given the values for the thrusters inputs, the resulting system reaction can be calculated. All of this information, i.e. the sensor readings, thrusters inputs and dynamic model calculations need to be collated to give an output of USAL-AUVs state. The problem of more state variables than sensors to measure them also has to be addressed. The use of a Kalman filter overcomes all of these problems. The Kalman filter uses knowledge of the current values of some of the state variables (obtained from sensor readings) and the dynamic model of the system to give an estimate of all of the state variables.

3 AUV Design

This chapter spotlights the design of the AUV. It starts with the changes done on the shape of the initial ROV by a former student followed by necessary modifications to this construction. The developed electronic system with its different components facing the challenge of fulfilling all requirements the within the restrictions is described as well as the selection of sensors and their locations in the vehicle. Technical data and features are presented.

3.1 Prior changes on the USAL

The original torpedo shaped ROV “C’Cat” distributed by Sherwood Overseas Ltd. was divided in the middle to fit a heave thruster unit between bow and stern hull for active controlling z-movement. The former design was strongly positively buoyant and realized the movement in z-direction via two rudder blades, which were attached on the back and whose effectiveness was strongly coupled to a movement in x-direction.

Due to the added thruster the AUV gets one more active controlled degree of freedom and should now be able to dive without movement in x-direction. This design had no more need for the vertical rudder blades on the back so they were demounted. Due to the high weight of the heave motor the AUV becomes centre and bottom stable. This bottom stable design implements the idea that pitch and rolling need not to be active controlled or considered. For this reason the AUV is under actuated.

Movement in sway (y-direction) is not needed and not possible. However for the desired tasks and the small world of a pool the AUV was still hardly manoeuvrable. Turning yaw was only possible in combination with in x-movement. A bow thruster system was integrated to add the ability to turn on the spot.

3.2 Mechanical Design

The USAL-AUV torpedo shaped hull consists mainly of three parts, put together with four screws on each side of the heave thruster, constructed from polycarbonate-based plastic with excellent impact strength, dimensional stability and mechanical performance. Further additives ensure chemical resistance and protection from ultra-violet light degradation.

The shape is fairly symmetrical. The centre-of-mass lies in the bottom and in the lateral middle. Its dimensions are 865 mm lengths with a diameter of 150 mm. Its weight is 14.08 kg. Due to the water displacement of 13.76 litres it has a small buoyancy body attached on the bow-hull to keep it slightly positive buoyant. The maximum depth is rated to 15 meters. Figure 3.1 shows the whole AUV.



Figure 3.1: The USAL-AUV

The requisites of the mechanical design are:

- Provide water proof hull
- Light construction, easy to transport
- Space for all onboard systems
- Windows for sensors and displays
- A highly symmetrical shape for simplifications in modelling and controlling
- Connectors through the hull for recharging and sensors
- Easy access to the electronics for maintenance

3.2.1 Bow Hull

The bow hull with a length of 320 mm consists of transparent acrylic plastic. A non-transparent plastic ring located at the nozzles of the bow thruster system establishes pressure stability. The bow part contents computer, power distribution, battery, several sensors and the camera-vision-system all mounted on a metal rack, which can be taken out for maintenance purposes. Due to the transparent hull material it is possible to check the controller and the electronics. This transparency is also required for the camera and the PSD-sensors. The camera is located in the top end where the front hemispherical viewing dome is moulded in clear polycarbonate. A transparent cover, called the contact lens, provide additional protection. A metal nose on the top was integrated to establish a recharging system.



Figure 3.2: The front hull without metal rack

The two fore noses are for vehicle protection and improved stability and are designed to be a snap fit. In the event of a collision the fore noses will protect the hull and may dislodge.

3.2.2 Middle Part

The mid-part is a heavy 165 mm long metal construction. It is mainly dominated by the heave-thruster, which has a diameter of 130mm, fitted between two metal plates. On bow-side it is equipped with a depth-sensor and on the stern side with the motor-drivers, which use the metal-body as heat sink. Power cables on backboard and signal cables on starboard tubes are connecting the bow electronics with the stern-hull. Two O-rings on each side guarantee watertight closure. A connection through the metal plate was necessary for the depth sensor. The heave thruster is based on a small former outboard motor. A ring around the propeller reduces rotation movement (yaw) of the AUV and amplifies thrust.



Figure 3.3: The heave thruster unit

3.2.3 Stern Hull

The yellow stern hull contains the stern thruster, mechanics and the servo for the main rudder. This part of the AUV has a length of 380mm. The stern-thruster is sitting in the end and has 100mm three wing propeller. To reduce propeller walk (the term for a propeller's tendency to rotate a boat as well as accelerating it forwards or backwards) and to amplify the thrust, a plastic ring is mounted around the propeller. Two 10 mm x 8 mm rudder blades are attached on the back to steer in lateral direction. These can be turned out to 35 degree in both directions. O-rings on the shaft prevent from water leakage. To compensate less weight in this hull and to improve stability thought balanced mass a massive lead-weight is integrated on the bottom. There is also the possibility to attach more lead-weight in a special bottom rack outside for fine trimming of balance.



Figure 3.4: The stern hull

3.2.4 The Electronics Rack

For easy maintenance all electronic circuits located in the bow hull are mounted on a detachable metal rack. This construction, which is hold by guide tracks in the bow hull, secures right positioning of all the sensors including PSDs, compass and camera. Maintenance becomes very uncomplicated.

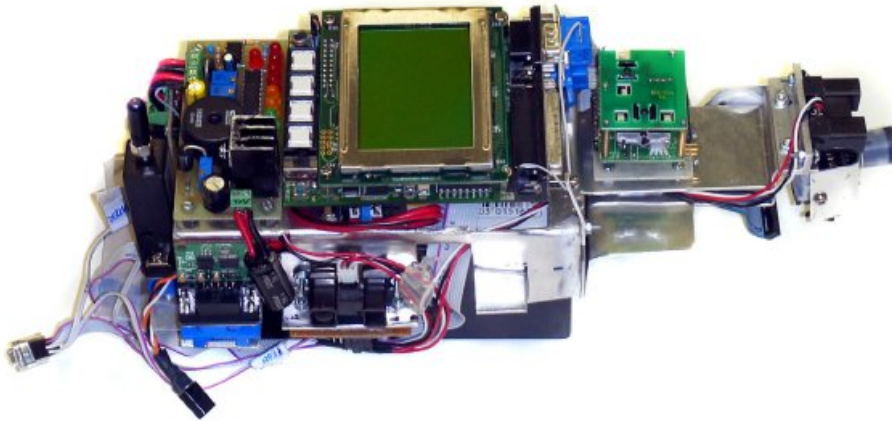


Figure 3.5: The electronics rack

3.3 Electronics Design

Designing the electronics system was one of the main issues of this thesis. The electronics design archived for the AUV should provide:

- Motion control
- Water leakage detection
- Energy control and recharge possibility
- Communication
- Easy and reliable design
- All controller values soft coded for easy modifications

The system has to deal with heavy current devices, which produce a lot of electromagnetic noise on the one side and sensitive devices like computer or sensors on the other side. To prevent problems several systems are shielded and filters has been necessary to protect them. Due to the simple mechanical design all systems have to be very compact and the cable tree has to support easy connecting and disconnecting for maintenance purposes.

A scheme of the wiring is given in Figure 3.6. All sensors are directly attached to the controller, which supplies them except the depth-sensor with power. This sensor and the motor-driver are directly connected to the energy controller. The whole system is powered by one battery, which can be recharged without opening the hull.

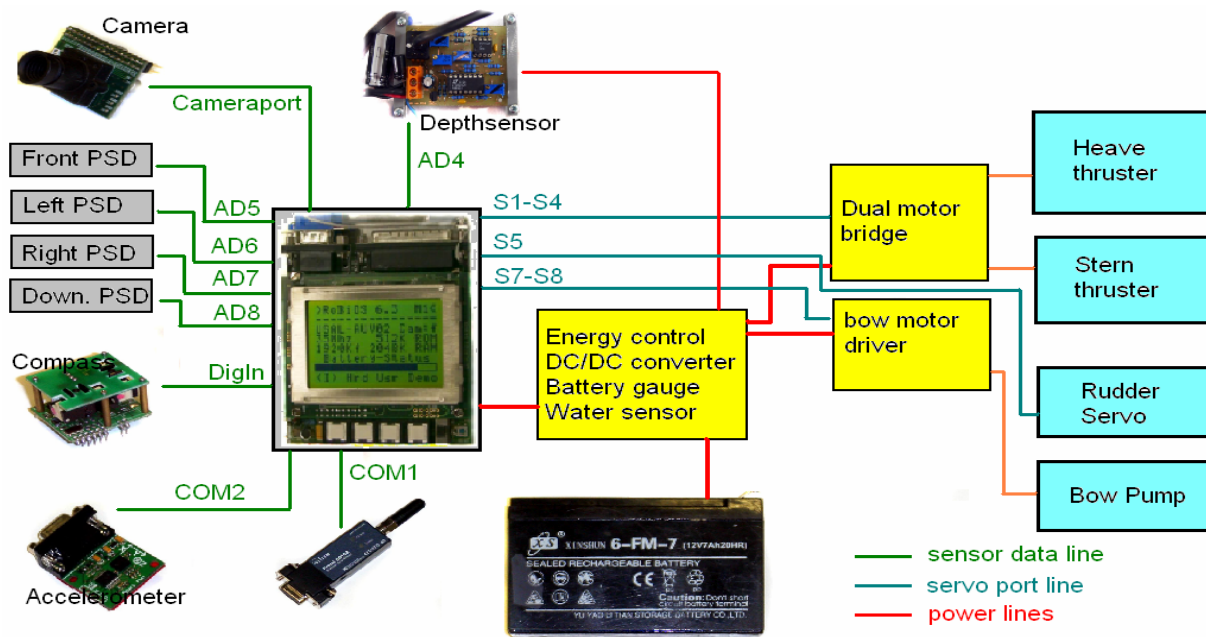


Figure 3.6: Wiring scheme of the electronics system

3.4 Main Controller

An embedded computer system called “Eyebot” is used as main controller. It consists of a powerful 32-Bit micro-controller board with a graphics display and a digital colour camera interface. This controller, specially designed for robotics applications comes with a huge variety of interfaces and an optimised operation system. This platform allows writing powerful robot control programs without a big and heavy computer system. [Braeunl et al, 2005]

Its main features are:

- Ideal basis for programming of real time image processing
- Integrated digital colour camera interface
- Large graphics display (LCD)
- Low power consumption
- Small dimensions
- Can be easily extended with actuators and sensors
- A huge variety of onboard communication ports
- Onboard 8-channel ADC
- Programmed from IBM-PC or Unix workstation
- Relative insensitive against electromagnetic noise.

Figure 3.7 shows the Eyebot from the top view, which is mainly dominated by the graphical display. Under the thus are 4 keys for basic functions.



Figure 3.7: The Eyebot controller

An overview of the system scheme is displayed on Figure 3.8.

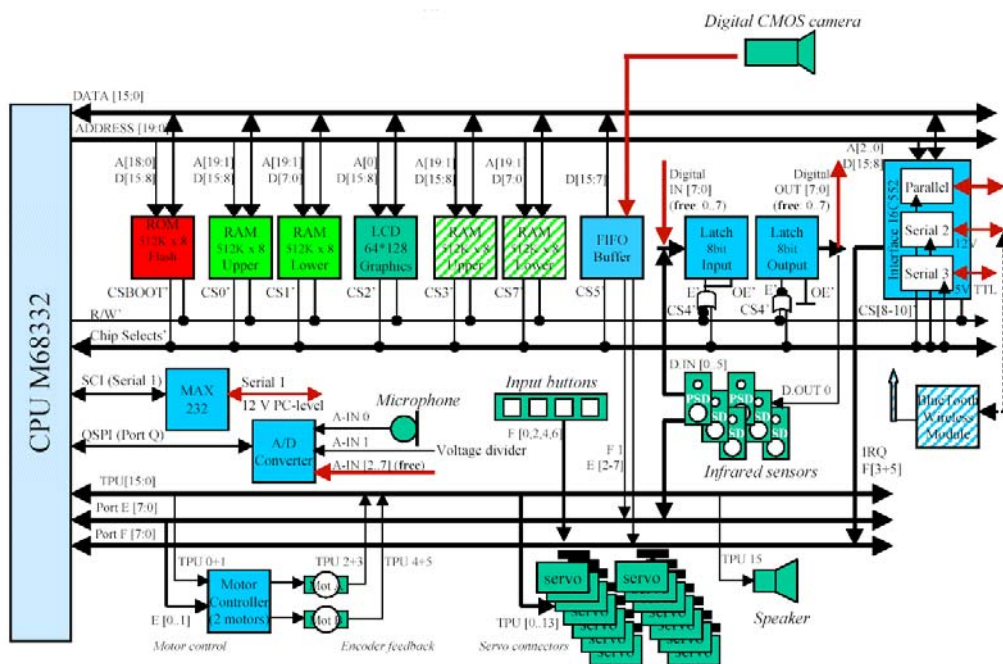


Figure 3.8: The scheme of the Eyebot controller [Braeunl et al, 2005]

3.5 Energy Control System

A mobile robot system requires a power system that can meet several goals simultaneously. The power source must store enough energy sufficient to allow the robot to perform a useful amount of work. To ensure proper operation of the onboard electronic circuits, power must be provided at a constant voltage. Noise and power glitches produced by one circuit component must not be allowed to interfere with any other component.

The energy control system manages the onboard energy resources and provides basic functions and two supply voltages. Therefore it consists of several parts. Figure 3.9 exhibits the circuit diagram and the several parts of the system.

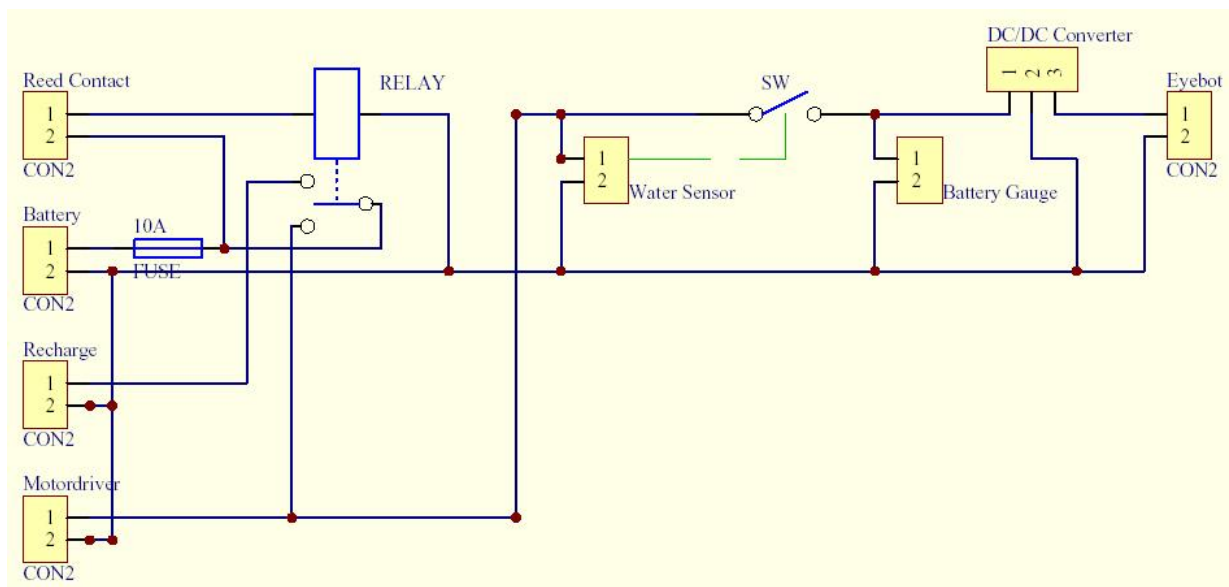


Figure 3.9: Circuit diagram of the energy control system

3.5.1 Battery

To carry out its mission the vehicle must also carry sufficient energy and provide sufficient power to operate the various elements of the payload. Batteries are by far the most common solution employed by mobile robots for the problem of energy storage. A battery converts chemical energy into electrical energy on demand.

An ideal battery would have high energy density and maintain a constant voltage during discharge. It should also withstand temperature extremes, exhibit an unlimited shelf life, be rechargeable and sell for a low unit cost. Unfortunately, no single battery technology exhibits all these characteristics.

In the selection of batteries, the lead-acid type remains popular but by no means dominates the market. The nickel-cadmium and the more expensive silver-zinc batteries are frequently used and the lithium primary based batteries are becoming more popular. An advantage of the lead-acid and NiCad batteries is their low internal resistance. Due to this issue voltage drops only little when drawing high current, which makes them perfect for this application. Due to the high desired current, it was not possible to fit standard lithium batteries.

The characteristics for lead-acid and NiCad Batteries are quite similar. Energy density of lead-acid batteries is 40 Whr/kg and the internal resistance 0.006 ohms. NiCad batteries have a density of 38 Whr/kg and an internal resistance of 0.009 ohms. [Holland, 2004]

Price, availability, maintenance issues and charger options pointed to the lead-acid type. The USAL-AUV uses a powerful 12V lead-acid battery block with a capacity of 7 ah. This is the largest, which fits into the vehicle.

It allows running the AUV an average of 70 minutes, depending on the usage of the actuators.

Runtime

Without using actuators:	16 hrs
Average:	1.10 hrs
Full usage of actuators:	0.40 hrs

3.5.2 DC/DC step-down converter

The DC/DC converter is recognized as a high effectively switched step-down regulator to perform 6.5 Volts for the controller, the servos, the sensors (except the depth sensor) and the camera. It can supply up to 3 amps current.

A standard linear voltage regulator was not suitable due to the average need of high current and the affecting heat dissipation, a waste of limited energy.

Electronic switch-mode DC/DC converters are available to convert one DC voltage level to another. These circuits, very similar to a switched-mode power supply, generally perform the conversion by applying a DC voltage across an inductor or transformer for a period of time (usually in the 100 kHz to 5 MHz range) this causes current to flow through it and store energy magnetically, then switching this voltage off and causing the stored energy to be transferred to the voltage output in a controlled manner. By adjusting the ratio of on/off time, the output voltage can be regulated even as the current demand changes. This conversion method is more power efficient (often 80% to 95%) than linear voltage conversion, which must dissipate unwanted power. This efficiency is beneficial as it increases the running time of battery-operated devices. A drawback to switching converters is the electronic noise they generate at high frequencies, which must be filtered. The step-down converter is also known as buck converter.

The chip used in this circuit is produced by National Semiconductors and comes along with a simulation program. Using this program allows setting and simulation of the best parameters and components for the current application. It also gives an idea of heat dissipation and the necessary kind of heat sink. [National, 2005]

Figure 4.6 shows the circuit diagram of the DC/DC converter and Figure 4.7 a picture of the DC/DC converter located on the PCB together with the battery gauge.

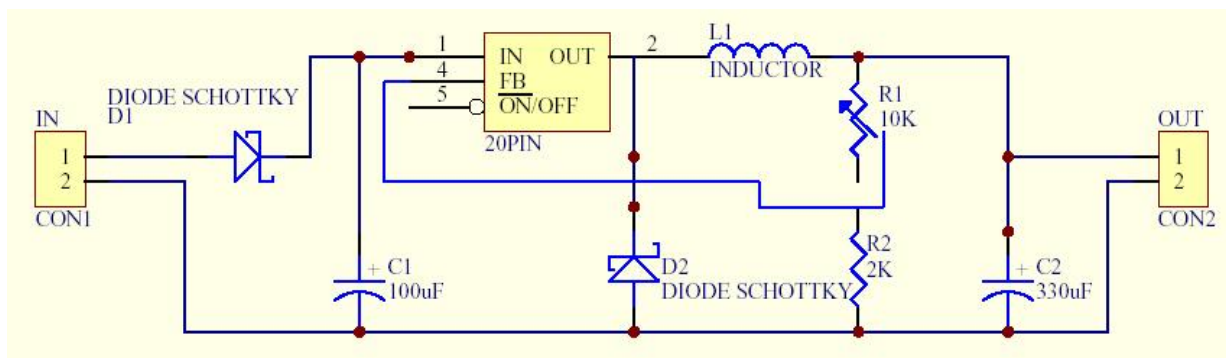


Figure 3.10: Circuit diagram of the DC/DC step-down converter



Figure 3.11: DC-DC step-down converter and battery gauge

3.5.3 Power Distribution Board

The power distribution board manages the 12 Volts bank. It also provides the possibility to switch the AUV on, off and to set it to recharge-mode. For this procedure it has a reed switch and a metal nose on the top of the bow-hull. The AUV can be simply recharged without the need to open the hull by attaching the external recharge-device to this point and to the massive heave thruster unit.

A magnet is required to switch between the different modes. The reed-switch is located on the bottom side of the bow-hull to prevent the user from switching the AUV to recharge mode when located in the water, which would connect the battery to the metal nose. Figure 3.9 shows the circuit diagram of the power distribution with blocks of the integrated water detector, battery gauge and DC/DC converter, which are described separately. The reed-contact switches without an attached magnet the main-battery relay to the consumer electronics (AUV on), otherwise it connects to the recharging contacts (AUV off/recharge mode). Figure 3.12 shows a picture of the PCB. It consists of only a few parts mainly dominated by the battery and “water-sensor”-relays.

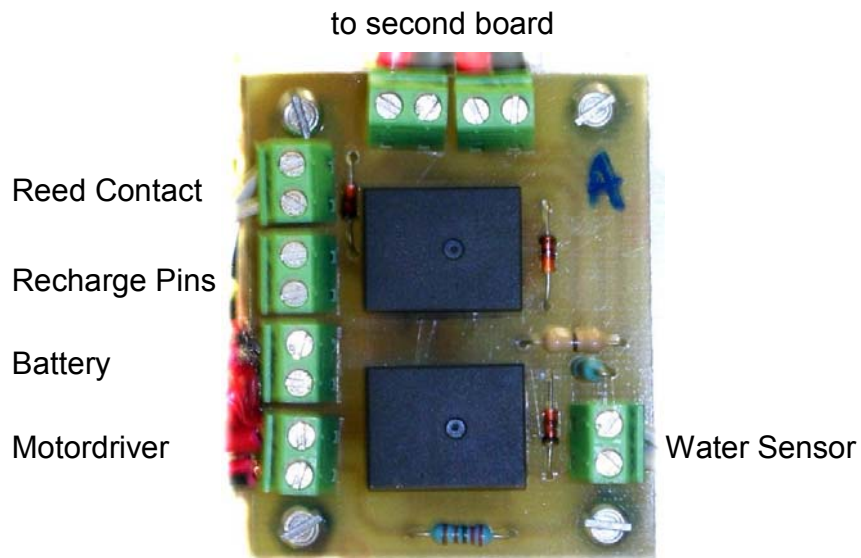


Figure 3.12: Power distribution board

3.5.4 Decoupling

Power supplies can become very noisy. For instance, when digital chips change state, they place a very brief demand for large amounts of current on the power supply. Similarly, each time the brush of a motor slides past a section of the commutator a voltage spike is generated, which can find its way into the power supply circuitry. All these noise sources challenge the proper operation of the AUV. To fight the transient drain posed by state changes in digital chips are often small capacitors connected.

The threat posed by stray magnetic fields can be countered by using what is called a single-point ground. Power distribution wires or printed circuits boards traces must be laid out in such a way that no ground loops are formed, as shown below in Figure 3.13.

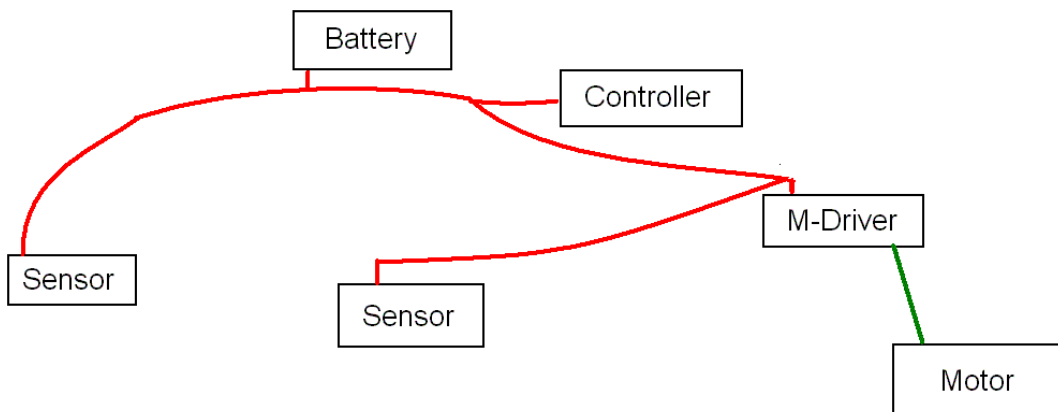


Figure 3.13: The layout of the power distribution circuitry should not contain ground loops

It is good practice to separate motor and logic components. This also prevents any voltage drop in the distribution wires caused by the high current demand of the motors. Hence the motor drivers and motors are located in the back hull, provided with its own connection to the battery. Filters stop noise coming from the stern to the bow unit. The computer and sensors are located in the front hull, most of them in grounded housings. Figure 3.14 shows an example of electric noise generated through the heave-motor on 60% load measured in the power cable of the motor-driver with an oscilloscope.

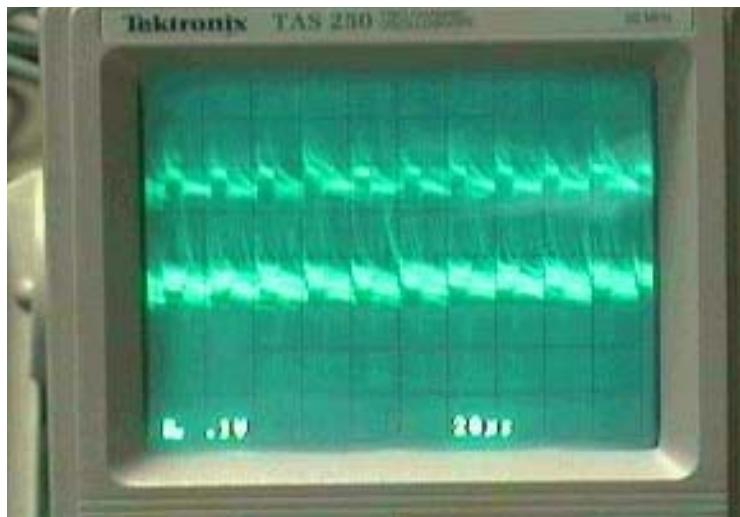


Figure 3.14: Measured noise of the brushed heave motor on 60 % load

3.5.5 Power gauge

A power gauge shows a line of 10 round 5mm LEDs the status of the battery. It consists of four green, two yellow and four red LEDs. The last two LEDs start blinking as signal when power down to a critical level.

The upper end is adjusted to 13 Volt and goes down in 0.5 Volt steps. This circuit is based on a LM3914 chip manufactured by National Semiconductors. This monolithic integrated circuit senses analogue voltage levels and drives up to 10 LEDs, providing a linear analogue display with only few external components necessary. Figure 3.15 shows the circuit diagram of the battery gauge.

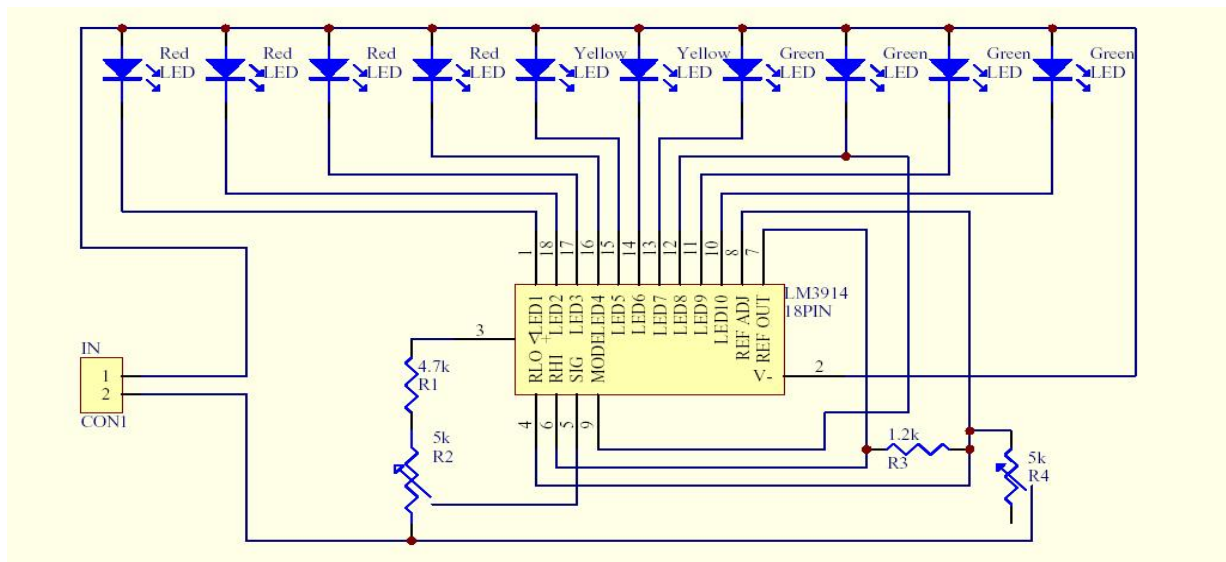


Figure 3.15: Circuit diagram of the battery gauge

3.5.6 Battery recharger

The battery charger delivers constant 0.75 Amp charging current to raises battery terminal voltage to approximately 80% recharged during bulk charge mode, charging current will then drop gradually. It then automatically switches to a float charge mode. During float charge mode, the output voltage of the battery charger is 13.2 VDC, which is well below the gassing voltage of a lead acid battery. This keeps the battery topped up, while minimizing any detrimental effects to do gassing. The battery charger is able to perform these complex switching functions because its electronic circuitry is controlled by an on board microprocessor. It uses a 3-Step Constant Current Charging Program:

Step 1) Qualification:

Qualification check to ensures safety by verifying battery status prior to charging.

Step 2) Bulk charge:

Constant current at 0.75 Amps to raises battery voltage to be approximately 80% recharged. Current drop then gradually until voltage reaches 14.4 VDC. When the battery voltage reaches 14.4 VDC, will transit to Step 3, Float Charge.

Step 3) Float charge:

Maintain fully charged battery at 13.2VDC float voltage. If an external load is applied to the battery while the charger is in Step 3, Float Charge, and if the battery voltage drops below a range between 12.0 to 12.5 VDC, then the charge cycle will restart.

3.6 Motor Driver

The Eyebot controller is not able to deliver high current so it can not drive the motors directly. A powerful motor driver is necessary to supply the motors with energy. An introduction on PWM Theory can be found in the appendix.

3.6.1 Dual Motor H-Bridge Driver

The main motor-driver unit consists of two classic H-bridges on a single board. In an H-bridge, four switching components are used to alternately connect each of the motor terminals to either the positive or negative supply rails. By adjusting the duty cycle of the various switches, the average voltage applied to the motor terminals may be adjusted from full positive to full negative, permitting smooth control from full forward to full reverse.

Figure 3.16 shows the basic states of a H-bridge where

- a) Stop, all switches are open
- b) Forward, one switch to VCC and one switch on the other side of the H to Ground
- c) Reverse, otherwise than Forward

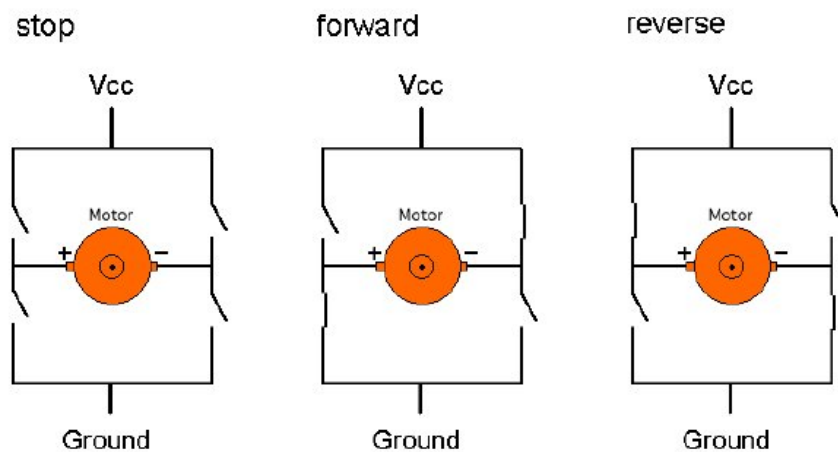


Figure 3.16: Operation mode of a H-Bridge a) Stop b) Forward Direction c) Reverse Direction

The USAL AUV dual H-bridge is realized with 8 12 Amp MOSFETs. Logic circuits prevent from wrong switching and reduce wiring. That means there are only two wires necessary: One for the PWM (enable) signal and one for direction change of each bridge. These are directly connected to the PWM-outputs of the Eyebot. A poly-switch acts as a fuse to prevent the MOSFETs from over-current. Figure 3.17 gives an overview over the realization of the bridge.

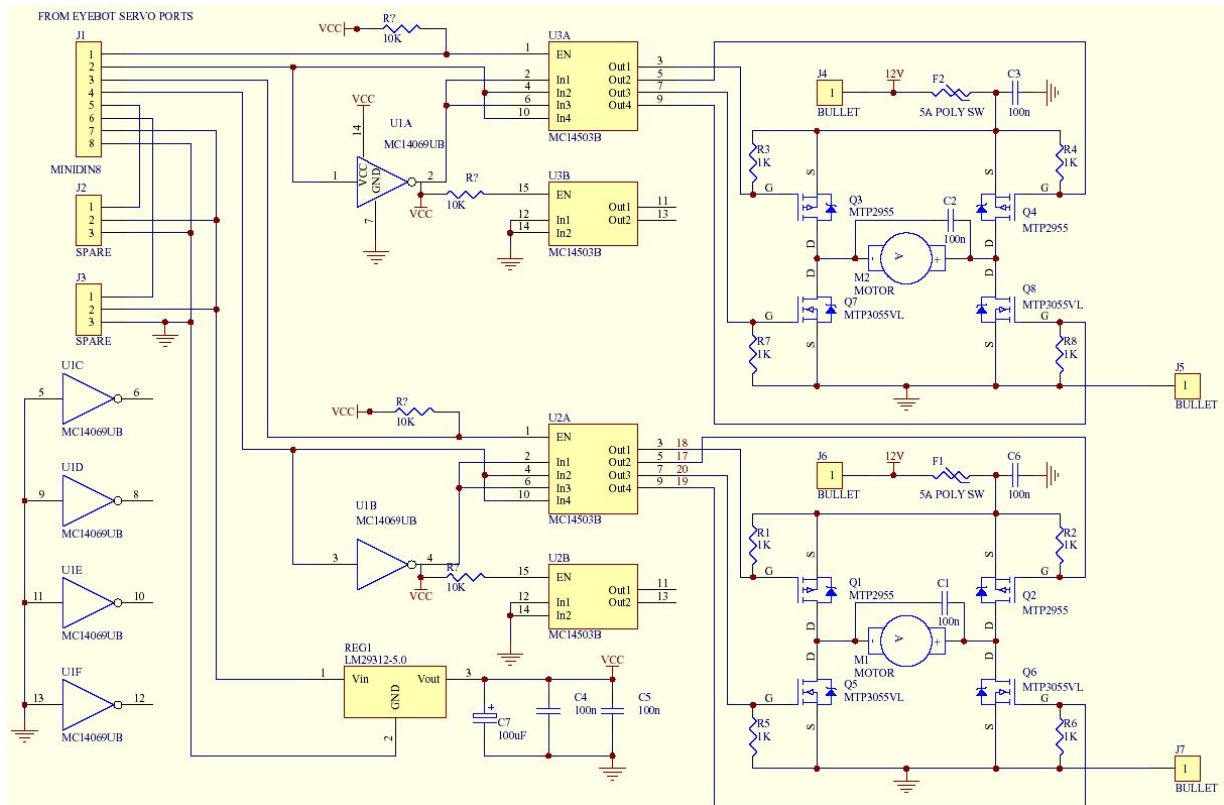


Figure 3.17: Circuit diagram of the dual H-bridge

The dual H-bridge uses the metal of the heavy thruster unit as heat sink. Figure 3.18 shows the circuit board attached on the stern side of the thruster unit.

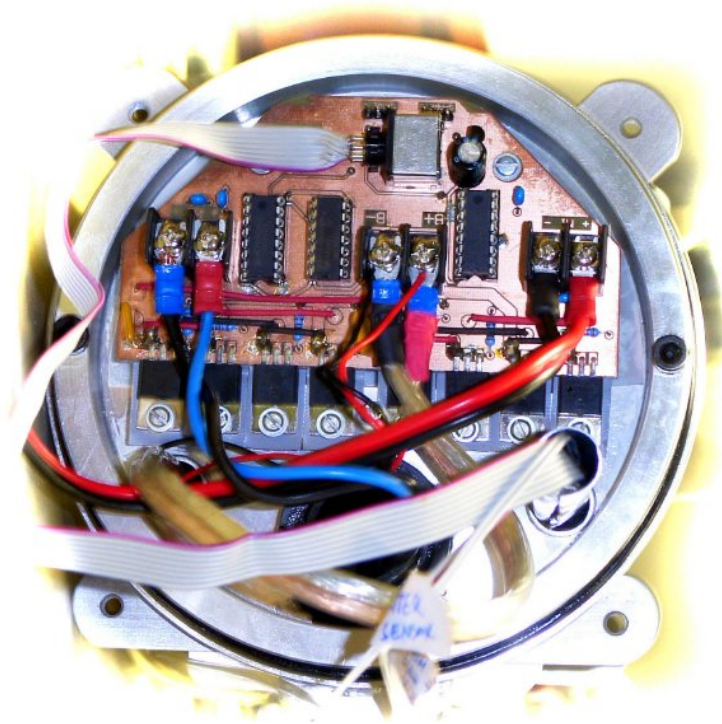


Figure 3.18: The dual H-bridge attached to the stern-side of the heave thruster unit

Pull-up resistors are used in the design of the electronic logic circuits at inputs to logic systems so that a definite logic level is asserted if an external device is disconnected or disrupted. Electromagnetic interfering problems between input cables made these necessary.

3.6.2 Bow Thruster Motor Driver

Due to the fact that it is not necessary to control the speed of the bow thruster motor, this driver consist only of two small relays, two transistors to drive the relays, a 10k resistors in each PWM line to keep current low, two flyback diodes and a poly-switch fuse. It allows to switch the pump on and to reverse the pump direction. It is directly connected to the PWM output of the Eyebot, although not supporting speed control. The pump is stopped when both channel have the same state. Figure 3.19 shows the circuit diagram and Figure 3.20 a picture of the unit.

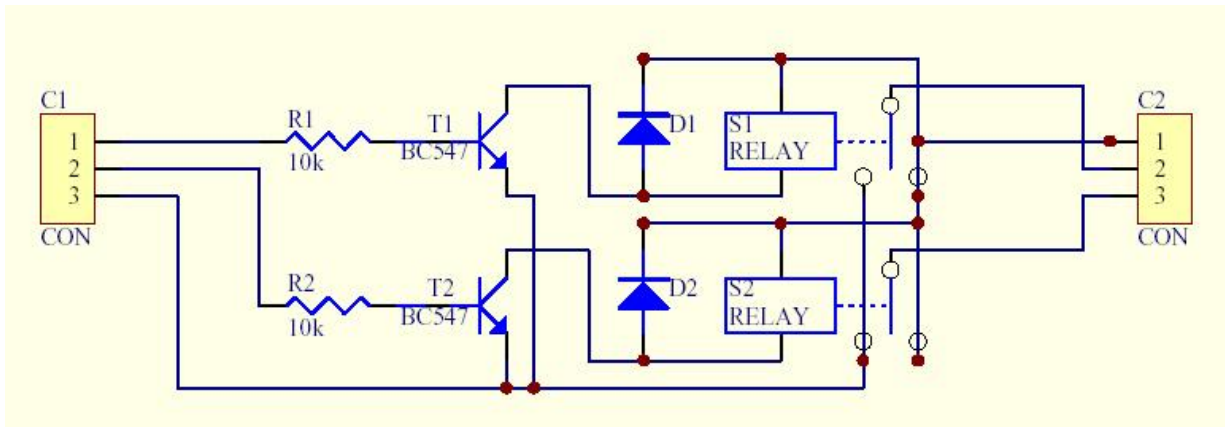


Figure 3.19: Circuit diagram of the bow thruster motor driver

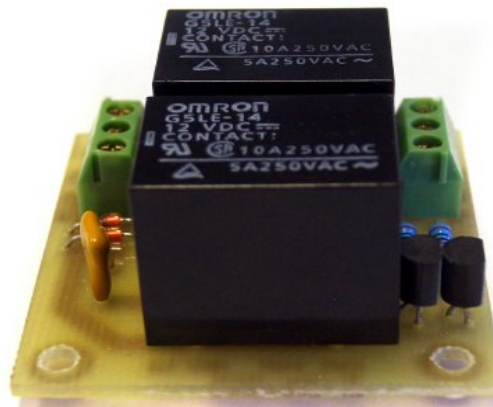


Figure 3.20: The bow thruster motor driver

3.7 Actuators

The AUV is equipped with different actuators to perform navigation and movement in and under water. The thrusters enable yaw, heave, and surge manoeuvres. Hence, it is under-actuated and not able to perform direct sway (lateral) motion. Pitch and roll movements are negligible, due to the bottom stable design, which prevent the AUV from doing these movements.

3.7.1 Stern Thruster

The stern motor thruster is still the original system 12 Volt brushed motor. Its interference is suppressed with two capacitors from the wires to its metal housing. The generated torque is transferred with the help of a magnetic coupling through the hull to the shaft of the 3 winged 100mm diameter stern-propeller.

Maximum load current is 4,8 amp and the maximum thrust is measured with 4.12 N forward and 3.66 N backward. The stern thruster is supplied by channel 1 of the dual motor driver board. Figure 3.21 shows the 3-winged propeller of the stern thruster with the ring around.



Figure 3.21: The 3-winged propeller of the stern thruster

3.7.2 Heave Thruster

The heave motor thruster is originally from an outboard motor unit. The advantage of this unit is that it is originally watertight. However, on the downside it has a very high moving resistance. This is due to the o-rings on the motor shaft, and as a consequence requires a high start up current and up to 8 amps when running.

Maximum thrust is measured with 5.30 N downward and 1.08 N upward. Buoyancy force of the AUV is 3.34 N. The heave thruster is attached to channel 2 of the dual motor driver board. Due to the original area of application it was not interference suppressed, which become necessary when working with the sensitive computers. The motor drives a 3 winged 130 mm diameter propeller. The propeller is primary designed for forward movement; so measured backward thrust is lower. Nevertheless its not required due to the positive buoyant behaviour of the AUV. Figure 3.22 shows a picture of the heave thruster.

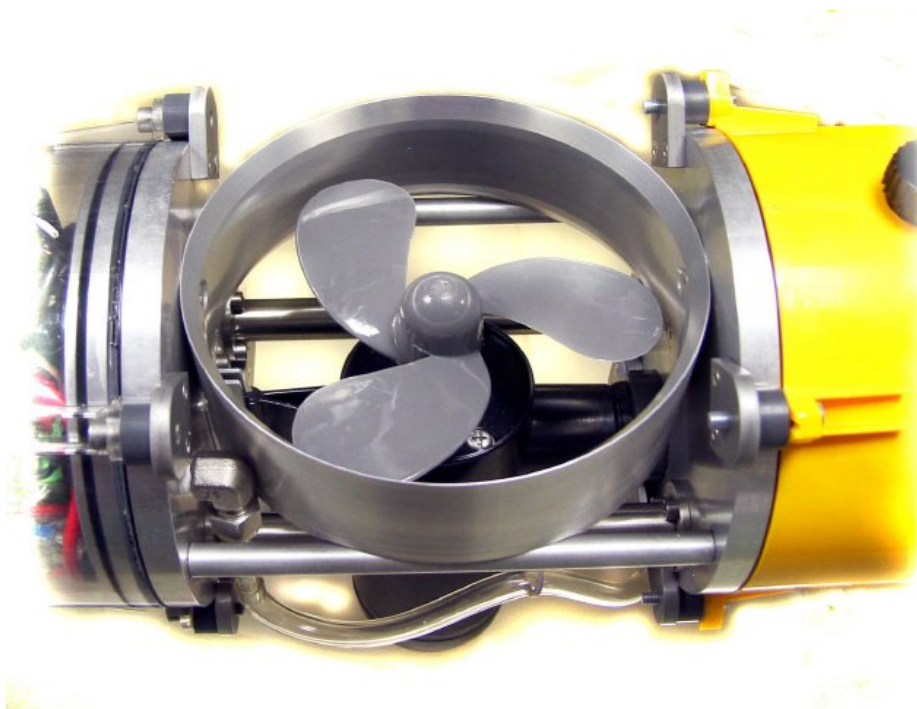


Figure 3.22: The heave thruster

3.7.3 Main Rudder

The main rudder system consists of two paddles attached to the stern hull. Due to the o-rings in the hull the rudder-mechanics needs a high power servo to move. This rudder is due to its design strongly coupled to a forward or backward moving of the AUV and is due to this only effective when the AUV is moving. The flow produces a force on the turned paddle. Due to this the boat move first with the stern-part in the wrong directing when turning and starts then moving in the desired direction. This has some affects to simple tasks like wall following. When following the wall on the left side, a turn to the right side could affect touching the wall with the bow end. Figure 3.21 above shows the two rudder blades attached close to the stern thruster.

3.7.4 Bow Thruster

The bow thruster system is an independent active system and can also turn the vehicle when it is not moving forward or backward. Its forces are located in the bow part of the AUV. Activating it generates a force in the bow that turns the vehicle in circle with the back paddle in the centre of this rotation.

Usually, a bow thruster is just a tunnel below the waterline through the bow. An impeller in the tunnel can create thrust to both ways, which makes the vehicle turn. The worst problem was running out of space when designing this rudder. There are different concepts possible to establish a force. The initial idea was to set up an external impeller-system on the front of the AUV. However an impeller system in the AUV was not possible due to limitations of space. So, I designed a pump system, which consists of two nozzles, each side one, a water pump and a motor driver for this pump. The pump propels water from the left side to the right side and vice versa. The outcome of this is a negative pressure on the one side and a positive pressure on the other side. This affects a force, which turns the vehicle. Figure 3.23 shows the nose and the pump of the bow thruster system.

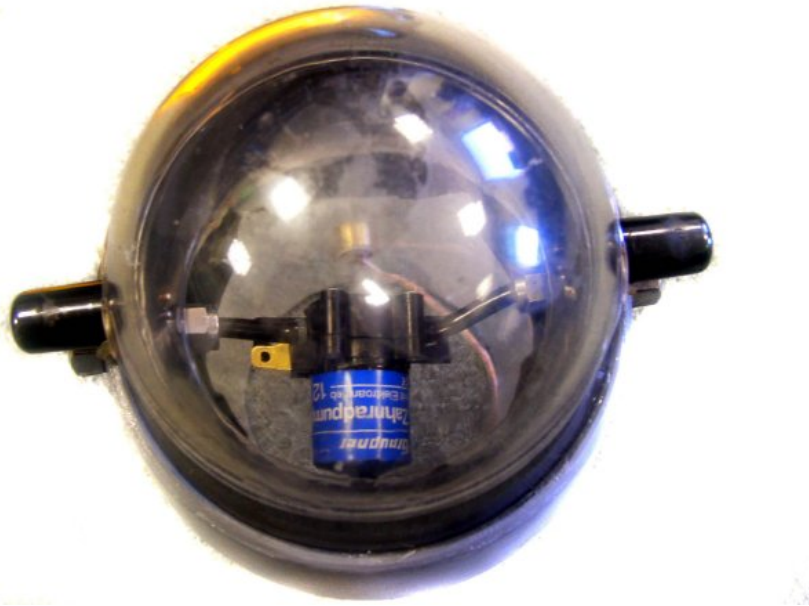


Figure 3.23: The bow thruster system

3.8 Communication

Even though an AUV is capable of fully autonomous operation, a well-designed system provides the operator with communications links to the vehicle whenever possible. At a minimum, a link is needed to start the mission after the AUV has been launched. This contact confirms that all systems are ready and allows the operator to command the start with knowledge that the AUV is fully functional. During the mission it is often possible for the support ship to maintain contact to allow for occasional vehicle health checks. Contact also allows the support ship sufficient data transmission to confirm that the payload is logging worthwhile information.

3.8.1 Different Ways of Underwater Communication

Electromagnetic radiation such as normal radio communication cannot travel through thick conductors such as salt water, so communication with submarines when they are submerged is a difficult technological task, requiring specific techniques and devices. In many cases, the obvious solution is to surface and raise an antenna above the water surface to use standard technology. Several technologies have been developed and deployed [Nasa, 2005]:

Sound travels far and fast in water, and underwater loudspeakers and hydrophones can cover quite a distance. Acoustic Telemetry ISE's experience has been that 150 bps should provide sufficient bandwidth to monitor the vehicle periodically, and to send it high-level commands. The amount of data that may be required to oversee the quality of the survey record depends on the nature of the survey equipment used.

Very low frequency radio waves (3–30 kHz) can penetrate seawater down to a depth of roughly 20 meters. Hence a submarine staying at shallow depth can use these frequencies.

Extremely low frequency electromagnetic waves in the ELF frequency range can travel through the oceans and reach submarines anywhere. However, building an ELF transmitter is a formidable challenge, as they have to work at incredibly long wavelengths. Two facts should be noted: First, the communication link is obviously one-way. No submarine could have its own ELF transmitter on board, due to the sheer size of such a device. Secondly, on such low frequency, information can be transmitted only very slowly, on the order of a few characters per minute.

3.8.2 The USAL-AUV Bluetooth Communication System

The USAL-AUV Communication System provides:

- Initialising the System
- Upload of Programs to the Eyebot
- Download of Data from the Eyebot
- Sending Commands for Testing
- Receiving Information for Testing

Bluetooth is best described as a low cost, low power, short-range radio technology developed as a cable replacement to connect mobile phones, headsets, portable computers and PDAs.

Bluetooth operates in the 2.4GHz Industrial Scientific and Medical (ISM) band using Frequency Hopping Spread Spectrum (FHSS) signalling to minimize interference from devices sharing the band including wireless networking (802.11b/g), cordless telephones and microwaves.

Specifically microwaves selecting this band are strongly absorbed by water. Thus prevents Bluetooth communication with USAL-AUV whilst underwater.

In order to prevent connections from unauthorized devices, a process called pairing is used. When one Bluetooth device connects to another for the first time, a passkey is exchanged between them and used for all further communications. This process is remembered by both devices, allowing previously paired devices to connect in future without the need to re-pair. Many devices now require password for successful pairing.

The USAL AUV uses a serial to Bluetooth-stick, connected to serial port two to communicate with the host computer when surfaced. The Intinium Promi-SD™ 102 Bluetooth system is developed for long range, easy-to-install low-cost wireless serial communications. Provided is point-to-point wireless connection without standard RS232 cables.

It is a class 2 device with an output power of 2.5mW (4dBm) provided with variable baud rate up to 115200 baud, with automatic detection of hardware flow control and DTR/DSR for loop-back & full transfer. Figure 3.24 shows a picture of the Bluetooth communication device.



Figure 3.24: The Bluetooth communication device

A waterproof housing with a cable was available for testing purposes, which could be localized close to the submerged AUV so that communication becomes possible whilst the AUV is underwater.

3.8.3 The USAL-AUV Infrared Remote Control System

The USAL-AUV is also equipped with an infrared sensor. For demonstration or testing purposes it is possible to control the AUV with an infrared remote control such as Nokia VCN 620. This is a one-way control system with limited range. Remote control unit and AUV have to be in a visible contact. Depending on the waves on the surface, diving deeper than 0.4 meters interrupts this connection.

Feedback is only possible by looking on the display or by regarding the behaviour of the AUV.

3.9 Requirements to the sensor suite

There are a huge variety of different sensors in different accuracies and prices available. But because of the specialization on the topics small, cheap and underwater suitable the range becomes very small.

Just as there are many different types of robotics and autonomous vehicles, there are a variety of different ways in which these vehicles can sense their surrounding environment. [Everett. 1995]

This is particularly true of the underwater environment. Many surface autonomous vehicles use light as a way of sensing. However, in the sub-sea environment, light becomes attenuated over shorter distances meaning that vision becomes more difficult and RF communication and GPS (global positioning system) become impossible. Therefore, an alternative or adjusted means of sensing in the water environment is required. The sensory system is one of the major limitations in developing vehicle autonomy. The vehicle's sensors can be divided into three groups:

- (1) Navigation sensors: for sensing the motion of the vehicle
- (2) Mission sensors: for sensing the operating environment
- (3) Proprioceptive sensors: for vehicle diagnostics.

This chapter spotlights several sensors and several techniques to sense state and surrounding of the AUV. It presents reasons why different sensors found not their way into the sensor suite. Important sensor considerations and requirements are:

- Size and weight should be kept to a minimum.
- Supply voltage of less than 12 Volts.
- Low power requirements.
- Digital output ideal but not necessary as Analogue to Digital converters available.
- Sampling rate greater than 20Hz ideal.
- Output voltage swing should be sufficient over possible range of readings.

Different tasks require different sensors. In the case of USAL-AUV limited space and limited calculation-power have to be considered. The navigation and positioning accuracy required will be determined by the mission requirements.

The most important issue for the sensory system is that the data needs to be updated at a fast enough rate to enable the AUV a continuous view of the environment. It becomes very difficult to steer the AUV when the data-intervals are relatively long. If the data rate is insufficient, then the AUV may be blind at crucial times.

3.10 Navigation Sensors

The set of navigation sensors is described in the following section. These sensors are primarily used for navigation purposes. From their information gains the vehicle its surroundings and movements in its world. There are different sensors for different states of the vehicle and to sense various values.

3.10.1 Ranging Sensors

Sensors that measure the actual distance to a target with no direct physical contact can be referred to as non-contact ranging sensors. Non-contact ranging sensors can be broadly classified as either active (radiating some form of energy in the field of regard) or passive (relying on the energy emitted by the various objects in the scene under surveillance). The commonly used terms radar (radio direction and ranging), sonar (sound navigation and ranging), and lidar (light direction and ranging) refer to active methodologies that can be based on any of several ranging techniques.

The PSD is very often used in land-operated vehicles. However, it is known that the propagating distance of infrared light is much shorter in water than in air. This is because the photon absorption of infrared light is considerably stronger in water than in air. A wave absorption diagram is given in chapter 2.1.1, Figure 2.1.

PSDs are purely analogue devices and rely on a current generated in a photodiode dividing in one or two resistive layers. This simple design gives the advantages of stability and reliability. The electronics needed for signal processing of the analogue output is quite simple and can be implemented at low cost.

PSDs will measure the position of the centre of gravity of a light spot. That's about the only thing it can do, but it does it within nanoseconds with nanometers resolution. Accuracy of about 0.1% is achievable and the dynamic light-range is over several decades. Using stored reference points as a look up table can enhance this accuracy of the PSD several decades. Usually the optical components used along with the sensor will add distortion, which can be implemented into the look-up table and thus minimized. As the PSD provides the position-sensing information through the diodes' photo response, the device can be treated as a normal large area photodiode using standard method for signal processing such as for example using modulated light to avoid interference from stray light. A PSD can be manufactured to have any shape. Some odd examples are the helix, circular and spherical PSDs used for 2-D and 3-D angular measurements. For some applications (like for example surface inspection equipment) arrays of PSDs have been designed. [Buzinski et al, 1992]

PSDs are widely used in displacement sensors systems using triangulation. Such a system can be made at a low cost using rather simple electronics. The downside is that the condition of the surface being measured can cause considerable variations in measurement values. Also the texture of the surface may distort the shape of the light spot used for measurements. This will shift the centre of gravity of the light spot thus fooling the PSD.

Another problem is that dark surfaces, for example black rubber, have low reflectivity and a normal PSD may, unlike a CCD, encounter a low signal. To remedy this a new family of sensitivity-enhanced PSDs has been developed. These devices are position-sensing phototransistors in contrast to the standard PSD, which is based upon a photodiode. The phototransistor PSD shows an enhanced light sensitivity currently giving at least five times more photocurrent for the same light input. Light sensitivity is expected to increase further, in the near future, as the fabrication processes are perfected. The principle of measuring distance with triangulation is shown in Figure 3.25. A picture of the Sharp PSD 2Y0A02 without housing and lenses is displayed in Figure 3.26. On the right side is the IR-LED on the other the sensor-strip. The positions and directions of the PSDs used in USAL AUV are shown in Figure 3.27.

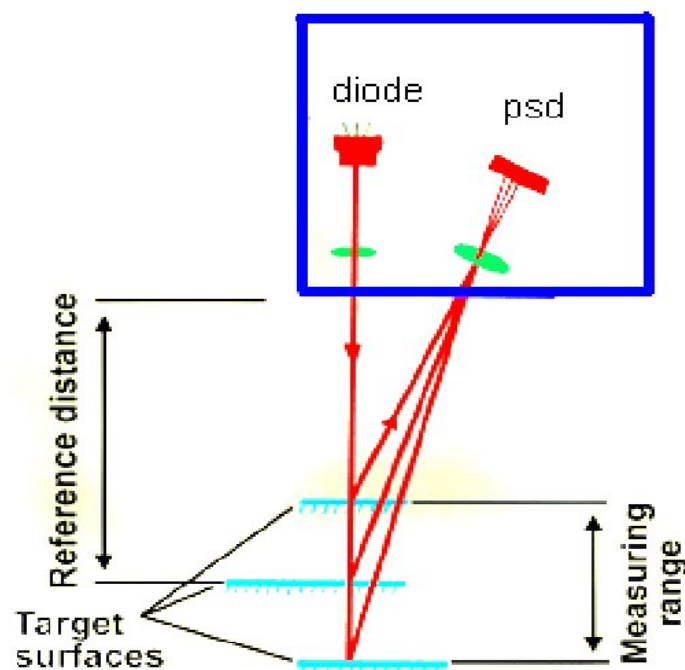


Figure 3.25: Triangulation with PSDs

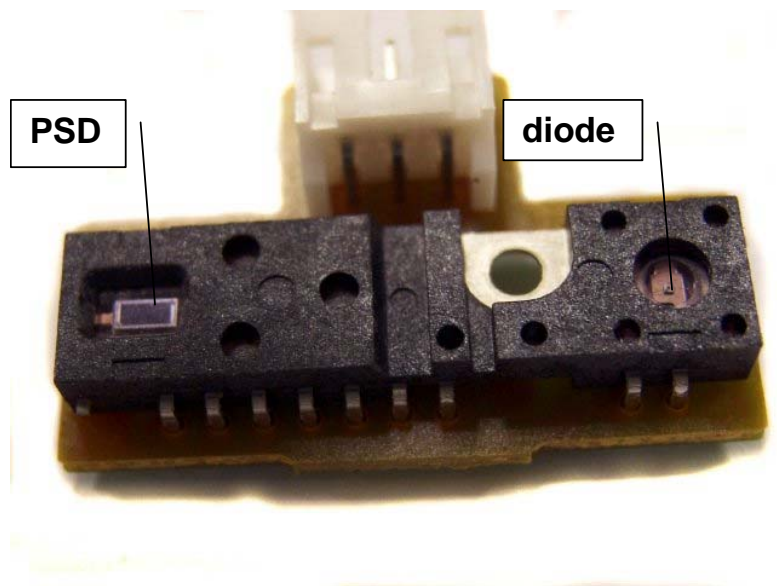


Figure 3.26: Opened Sharp PSD 2Y0A02

Figure 5.04 gives an overview of PSD-sensor locations and directions in the AUV.

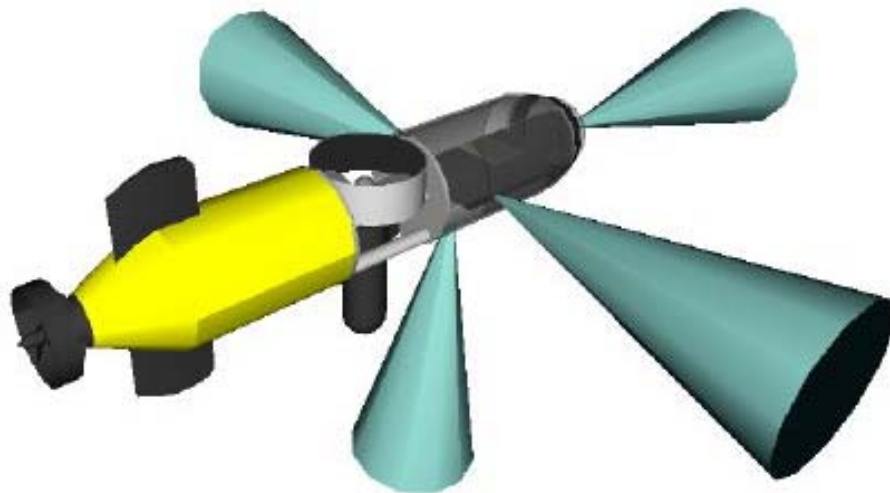


Figure 3.27: Position and directions of the PSDs in the AUV

3.10.2 Heading Sensors

Measurement heading is often used to hold or to set a course. Vehicle heading is the most significant of the navigation parameters (x, y and z) in terms of its influence on accumulated dead reckoning errors. For this reason, sensors, which provide a measure of absolute heading or relative angular velocity, are extremely important in solving the real world navigation needs of an autonomous platform. The most commonly known sensor of this type is probably the magnetic compass.

The average strength of the earth's magnetic field is 0.5 gauss, and can be represented as a dipole that fluctuates both in time and space, situated roughly 440 kilometres off centre and inclined 11° to the planet's axis of rotation [Fraden, 1993]. This difference in location between true north and magnetic north is known as declination, and varies with both time and geographical location. Corrective values are routinely provided in the form of declination tables printed directly on the maps or charts for any given locale.

A low-cost Vector 2XG digital magnetic compass module was chosen to provide yaw or heading control. The small module delivers high accuracy at low power, interfacing with the Eyebot controller via digital input port. The Vector 2XG is a 2-axis magnetometer that measures the magnetic field in a single plane. This plane is the plane created by its two sensors, which are perpendicular to each other on the board. To calculate heading accurately, a compass must measure the Earth's field in the plane, which is level.

"Level" means the plane parallel to the surface of a glass of water - even though the glass tilts, the water's surface will remain "level". If the V2XG is not level, the calculated heading will have errors related to the tilt of the board from level. The V2XG has a self-levelling construction for a tilt level up to 15 degree. Figure 3.28 shows the compass and this self-levelling construction.

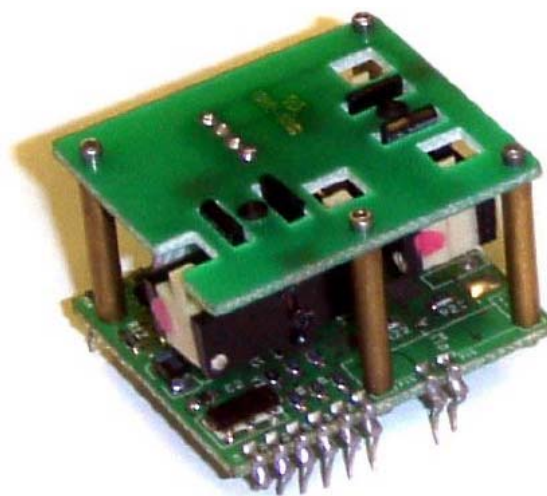


Figure 3.28: The V2XG Compass

3.10.3 Odometry Measurement

This sensor measures the curvilinear distance a vehicle travels. Odometer or velocity measurement is very important for dead reckoning.

An accelerometer is an electromechanical device that measures acceleration forces. These forces may be static such as constant force of gravity pulling at your feet, or dynamic - caused by moving or vibrating the accelerometer. The accelerometer measures the linear acceleration of the robot along (two) three mutually orthogonal axes on the robot frame. The measured value naturally incorporates the gravity vector needing to be compensated.

Compared to an odometer, a three-axis accelerometer can sense three-dimensional movements, while the former can only sense single-axis movements. Also, the data rate of an accelerometer can be much higher than that of an odometer. Moreover, an accelerometer is a self-contained device, while an odometer must be fixed to the shaft of some wheels, which could be inconvenient in some cases. A solid-state accelerometer also has the advantages of being small sized, having low cost, and being self-contained. Thus, this kind of accelerometer can be a viable solution as a short-duration distance-measuring device for a mobile robot or platform.

The SerAccel v5 is a 3-axis accelerometer up to +/-6g with a simple serial interface. The latest SerAccel development has many new improvements including variable baud rate, a factory reset command and a complete triple axis measurement system based on the newly released MMA7260Q sensor from Freescale.

Power is gained from RS232 port so no external power supply is needed. The onboard PIC (16LF88) runs at 10MHz and outputs three different types of outputs including calculated, binary, and raw outputs. The SerAccel v5 has software configurable settings to select between 4 sensing ranges (+/- 1.5, 2, 4, and 6g), as well as a software selectable measurement frequency (0-590Hz).

The SerAccel outputs real-time accelerations from 9600 to 57600bps using visible ASCII characters. The SerAccel is compatible with any RS232 Com-port in conjunction with any terminal program (HyperTerminal, VB Programs, or anything else that can read the com-port). [Sparkfun, 2005]

Using this module was an easy and cheap to integrate solution with the benefit being free from environmental manipulation. (e.g. driftage that causes from water flow)

Figure 3.29 shows a picture of the Sparkfun Accelerometer Unit. Figure 3.30 shows how to get speed and distance by integrating over time.



Figure 3.29: The Sparkfun Accelerometer

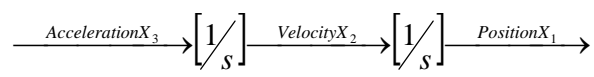


Figure 3.30: From Acceleration to Distance

3.10.4 Depth Sensor System

It is essential for an AUV to measure the depth of its body. Travelling too deep can cause water leakage and destroy the AUV.

Due to hydrostatic pressure in water, the depth can be determined by measuring the outside water pressure. The depth sensor system is based on a Sensym SX15AD2 pressure sensor. These sensors are specifically designed to be used with non-corrosive and non-ionic media, such as air and dry gases. The absolute device has an internal vacuum reference and an output voltage proportional to absolute pressure. Main advantages of this sensor are [Sensortek, 2004]:

- Low power
- Low noise
- Low pressure
- High Resolution

The pressure sensor is connected via a plastic tube through the metal hull of the AUV to the outside. There another plastic hose ends up facing down in the rack holder. A major advantage of the position of the pressure sensing point is its resistance to turbulences created by the moving AUV or the acting Heave Thruster. Depth sensing works by the following steps:

1. Water goes in the downward facing tube and compresses the air in it. Due to the air between water and sensor the sensor itself has no contact to the water.
2. The sensors signal is amplified and filtered by an electronic circuit. This circuit is shielded and has an electronic filter in the power supply line to protect it from electro-magnetically interferences.
3. V_O of the amplifier circuit is converted by the AD converter to a 10 Bit reading.
4. With the help of an onboard calibration table this reading could be translated to the actual depth.

Figure 3.31 shows the pressure sensor itself, attached on the amplifier board; Figure 3.32 spotlights the whole system.

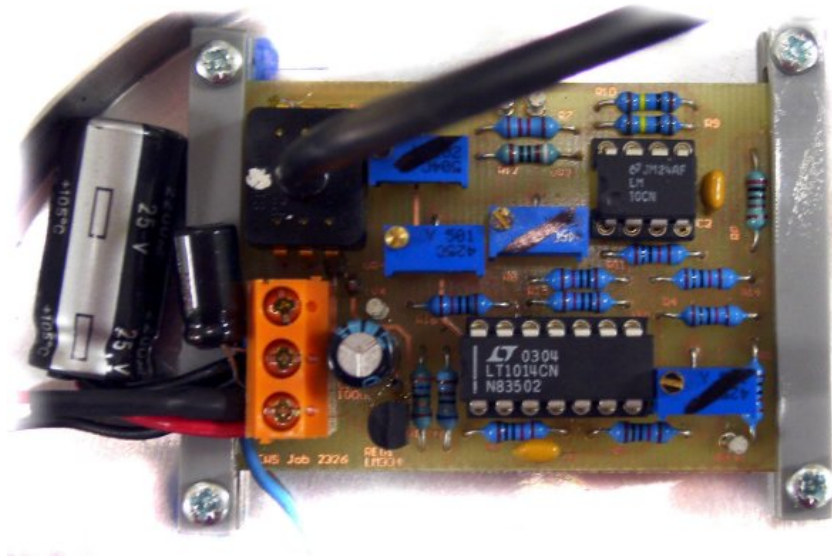


Figure 3.31: The pressure sensor attached on the amplifier board



Figure 3.32: The depth sensor system

The circuit in Figure 3.33 was chosen to both temperature-compensate and to amplify the 110mV span of the SX15GD2 pressure transducer to a 0-4.9V linear output capable of being directly interfaced with the EyeBot controller. This circuit is adapted from the SenSym SX-series datasheet [Sensortek, 2004].

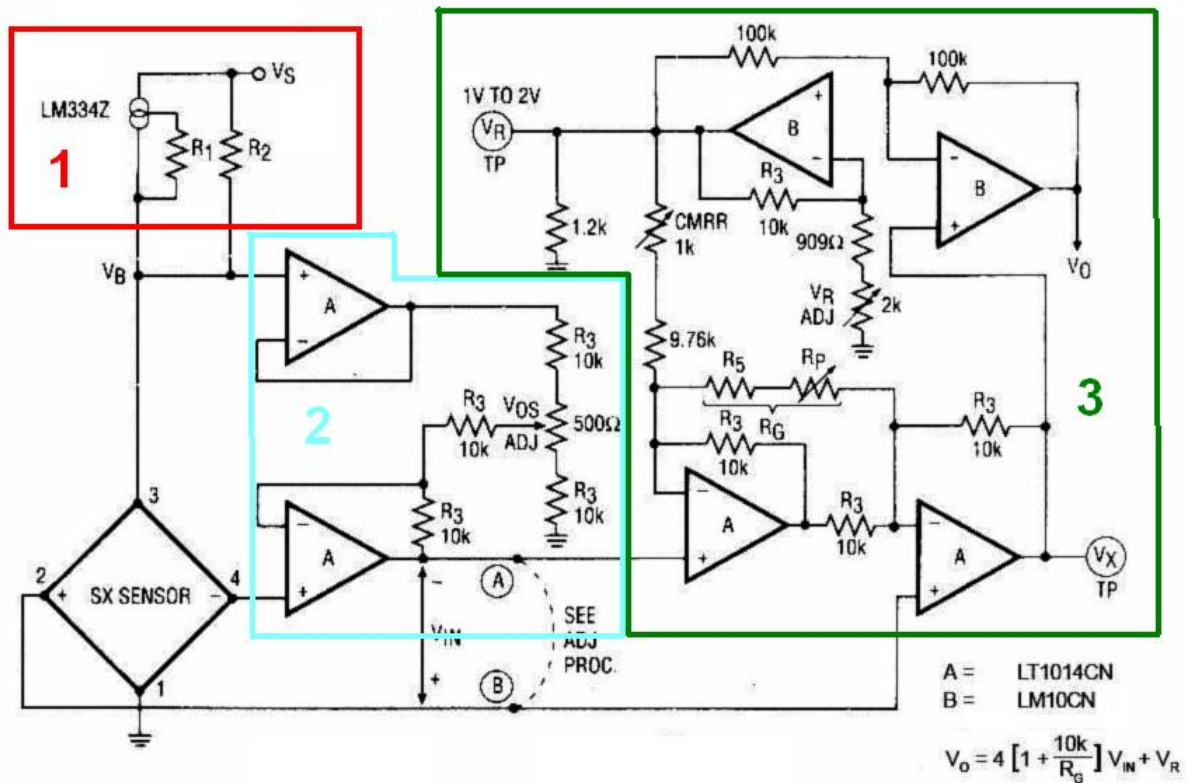


Figure 3.33: Circuit Diagram of the Depth Sensor Amplifier Board [Sensortechinics, 2004].

In Figure 3.33 the region labelled 1 is responsible for providing constant current excitation and temperature compensation for the pressure transducer. Selecting appropriate values for R_1 and R_2 sets the LM334 current source. ($V_s=12V$) Referring the calibration procedure detailed in the SenSym sx-series datasheet [Sensortechinics, 2004] values for R_1 and R_2 were found to be 36.5Ω and $7.15k\Omega$ respectively. The closest match 1% metal-film resistors were found to be 39Ω and $6.8k\Omega$.

The region labelled 2 is responsible for providing offset compensation for the zero-point voltage, V_{offset} . For the operational amplifiers (OP amps) in this region, LT1014 precision amplifiers as recommended in the application notes were chosen for temperature stability and overall linearity.

The region labelled 3 provides common-mode-rejection and the final stage of amplification in order to scale the signal to the desired output span of 0-4.9V. The resistors R_5 and R_p determine the output range of the circuit. For a 0-4.9V output, R_5 was chosen as $1.82k\Omega$ and R_p as a $5k\Omega$ potentiometer for fine adjustment. These values were determined from table 3 given in the SenSym SX-series datasheet. This span corresponds to the range of the EyeBot's 10-bit analogue to digital converter. [Sensortechinics, 2004].

3.11 Mission Sensors

The additional mission sensor suite is limited to an optical colour camera vision system. Tasks like obstacles recognizing or pipeline following become very easy using a camera and a suitable algorithmic code.

The only sensor on the small AUV that is capable of detection obstacles in the environment is its vision-sensors. Recently, vision based AUV navigation had much attention. However, due to undesirable optical behaviour underwater [Kayan, 2004], there were many occasions where problems were encountered. For example the cable is not visible enough for the vision processor to track the cable. In addition, the environment itself makes the cable invisible with time, due to the growth of underwater plants, etc. Due to the light absorbed by water, [Balasuriya et al, 1997] distant ranges will appear to be darker than the close ranges and highly directional active light sources make regions in the image to appear darker and brighter. This will result in a non-uniform lighting condition in the underwater image, which is undesirable for most of the available computer vision algorithms.

An improved system was examined 2002 Kondo and Ura [Kondo and Ura, 2002]. They added three laser pointers to the vision system and works with a space-encoding method.

3.11.1 Camera-System

The Vision System uses a small CMOS-colour camera with a native resolution of 640x480. Due to the camera interface on the Eyebot, no special frame grabber is required. When recognising obstacles, it must lower its resolution due to the calculation power of the Eyebot-controller down to 60*80 Pixels. The OV7620 is a highly integrated high resolution (640x480) Interlaced / Progressive Scan CMOS digital colour video camera chip. The digital video port supports 60Hz YCrCb 4:2:2. 16Bit / 8 Bit format, ZV Port output format, RGB raw data 16Bit/8Bit output format and CCIR601/CCIR656 format. The built-in SCCB (Serial Camera Control Bus) interface provides an easy way of controlling the built-in camera functions. [Omnivision, 2000]



Figure 3.34: The camera module

3.11.2 Position of Camera System

The Camera is has its position in the front end of the AUV. It is attached to a servo that allows it to change its position, facing forward or downward.



Figure 3.35: The vision system

3.12 Proprioceptive Sensors

A proprioceptive sensor is any sensor used to measure the internal state of the vehicle. Monitoring these sorts of sensors ensure smooth functioning of the AUV. These Sensors are hard coded and not connected to the Eyebot to guarantee continued operation even when the controller has a malfunction.

3.12.1 Water Detector

Due to the incompatibility of water and electronics a water detector was integrated to prevent damage on electronics when a leakage occurs.

It has a sensor in form of two blank wires mounted close to each other on the bottom of bow and stern hull (Figure 3.37). When the resistance between these wires drops due to water connecting them an electronic circuit switches off all electronics connected with the AUV.

The AUV then comes up to the surface automatically because of its positive buoyant design. Water detection is signalled through a red LED.

As seen on Figure 3.36 the circuit works with a LM311 comparator, which can be assigned to the group of operation-amplifiers. This comparator switches on smallest voltage differences on its inputs the open collector output to ground. In this case the output is connected to a relay, which is able to cut the electronics from the power supply. Input (–) of the comparator is attached to the voltage divider R2/R5, which has voltage of 6 volt. Input (+) is connected over R1/R3 to Vcc. R1 is connected to one of the blank wires as well. In normal situation the connection R1/R3 to R4 is open. Voltage on Input (+) is more than 6 volts, so the output is not active. When water connects the R1/R3 to R4, the voltage on Input (+) drops and the comparator activates the relay. The 1M Ω resistor in the back-trace of the comparator serves to dampen the whole circuit.

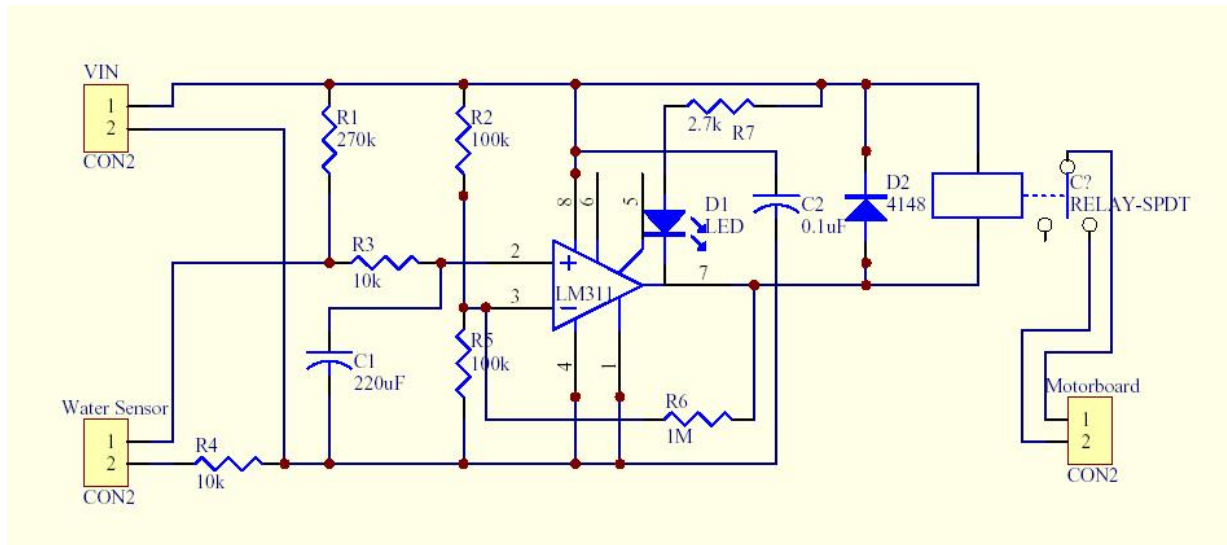


Figure 3.36: Circuit diagram of water detector

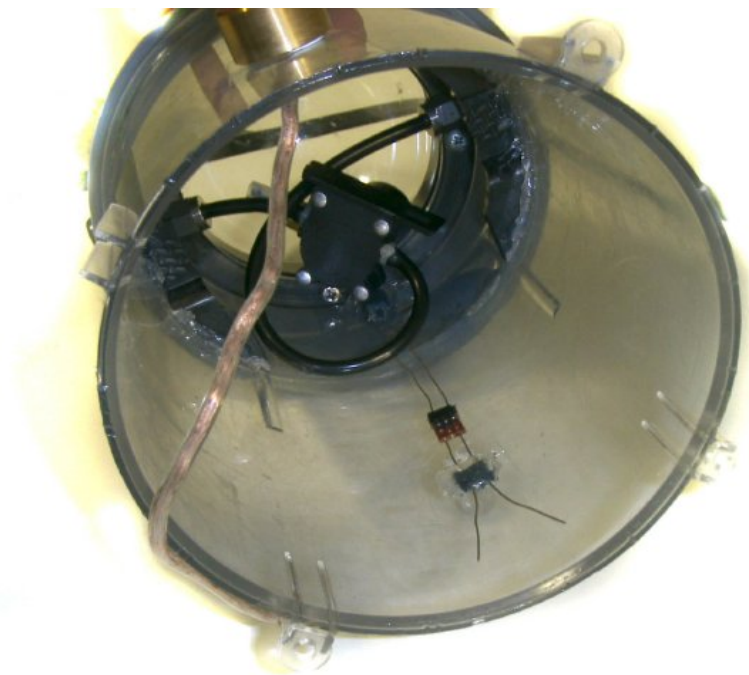


Figure 3.37: Water detector lines on bottom of hull

3.12.2 Eyebot Onboard Voltage Gauge

The Eyebot is applied with an onboard voltage gauge, which is shown in the root menu. Due to the regulated 6.5 Volts supply, this gauge will never drop and does not show the actual battery voltage. The real battery voltage will never drop the 9 Volt mark.

The power-board of the AUV is provided with a LED-Dot bar gauge, which shows the actual voltage level of the battery. It is not connected to the Eyebot.

3.13 Alternative Sensors

Alternative sensors such as ultrasonic proximity sensors (sonar) for ranging, rate gyroscopes for angle change measurement, paddlewheel, pressure difference and Doppler velocity measurement for odometry information, bottom distance measurement for depth can be found in the appendix section E.

3.14 A/D Converter

The PSDs and the depth-sensor provide voltage as a measurement unit. This voltage has to be converted into a digital form to be readable for the microprocessor system. The Eyebot has an onboard 8 channel 10 Bit analogue to digital converter. It can sense from 0 up to 4.5 Volts and divided into 1024 steps. For higher voltage a voltage divider becomes necessary. Two channels are already used onboard for the Eyebot battery-gauge and for the Eyebot microphone.

This voltage measurement system generates a significant amount of electro-magnetical noise. A one-pole depth-pass consisting of a resistor and a capacitor as shown on Figure 3.38 was required to filter the noise.

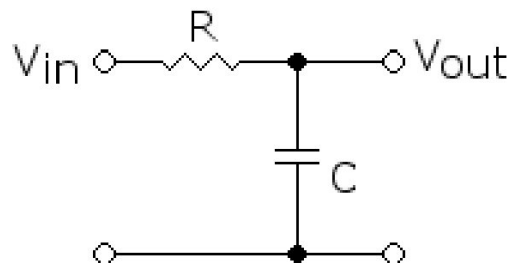


Figure 3.38: Circuit diagram of the one-pole filter

A low-pass filter is a filter that passes low frequencies well, but attenuates (or reduces) frequencies higher than the cut-off frequency. The first-order filter used here will reduce the signal strength by half (about -6 dB) every time the frequency doubles.

The simple electronics circuit that will serve as a low-pass filter consists of a resistor in series with a load, and a capacitor in parallel with the load. The capacitor exhibits reactance, and blocks low-frequency signals, causing them to go through the load instead. At higher frequencies the reactance drops, and the capacitor effectively functions as a short circuit. The break frequency, also termed the turnover frequency or cut-off frequency (in hertz), is determined by the choice of resistance and capacitance:

$$f_c = \frac{1}{RC2\pi} \quad (3.1)$$

The filter was realized with a 0.33 μ F and a 10 k Ω Resistor in each channel. A cut frequency f_c of 480Hz is the result.

3.15 Summary

This chapter gives an overview over the various parts of the mechanical, electronics and sensor design. Due to the orientation on the former AUV there was no complicated designing process and no significant changes, so it is still a torpedo shaped vehicle, providing all requisites. Designing electronics for an AUV is inhibited by many restrictions comes along with a lot of restrictions and rules. Sensitive circuits have to work with strongly disturbing circuits such a motor drivers. It is essential that the system be secure and act failsafe. Access for maintenance and setup was also necessary. Most of the circuits used are adapted from standard applications, an important restriction was limited energy and so efficiency was the most important factor. A large variety of sensors have been introduced in this chapter. A choice of the most suitable sensors for the application found its way into the sensor suite. Copious restrictions must be considered particularly concerning space and power to find suitable sensors, however simplifications in vehicle dynamics implements simplifications in the sensor suite as well. Due to the bottom heavy design an INS can be realized with the three axes accelerometer and the compass, which renders the rate gyrometer unnecessary. Range sensors realized with PSDs is not the first choice for underwater vehicle, but applicable in the pool area where the water is clear and where long-range measurement is not required.

4 Testing and System Identification

The first aim in any navigation system development is to identify a model of the system to be controlled. Currently work is being done on conducting some test trials to get input/output data for model identification and validation.

System Identification of a dynamical system generally consists of the following four steps.

1. Data acquisition
2. Characterization
3. Identification
4. Verification

To ensure that the system implementation is working as expected, a number of experiments have been performed. These experiments aim to ensure that, as the different sensor readings enter the system, the controller reacts by producing appropriate outputs to the thrusters. Controlling software was written to get the sensor outputs and to control the actuators. The original code can be found on the CD-ROM. The experiments and measurements are described together with the results in the following section.

4.1 Actuator Identification

The AUV is equipped with several actuators. For proper control it is necessary to know how much force the actuators can deliver or deliver at a certain value. Further on it is important to know how the generated force acts on the vehicle and its reaction. Coupled forces or their effects, which comes along by generating force have to be identified. Environmental issues affecting the force have to be addressed.

4.1.1 Stern Thruster Identification

The stern thruster generates surge. This actuator delivers forward (and backward) movement. A three-winged propeller generates the thrust. Figure 4.1 shows the force-direction and point of application of the stern-thruster, which is located at the stern of the AUV. The main direction of the acting force is in x-direction. The thruster location becomes necessary when turning the vehicle, which is described later.

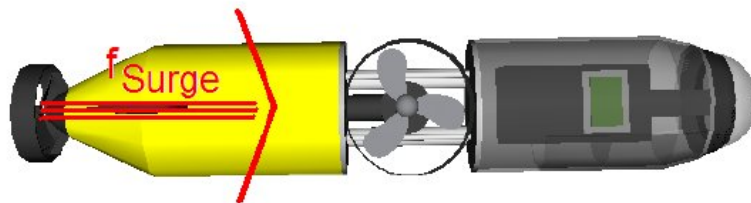


Figure 4.1: Stern thruster force direction and point of application

The next figure shows the generated thrust dependent on the motor control value. To get these thrust values a test was achieved where the AUV was attached on a string located in the middle of the pool. This position was chosen to minimize interference with other effects and to guarantee free water flow. The string was attached on the poolside to a load cell. This load cell comes with a calibrated display unit. The AUV was set to the different speed values and the readings on the load cell display noted. The resulting graph is shown of Figure 4.2. It was recognised that the propeller moved slightly out of water on high motor values at surface manoeuvres.

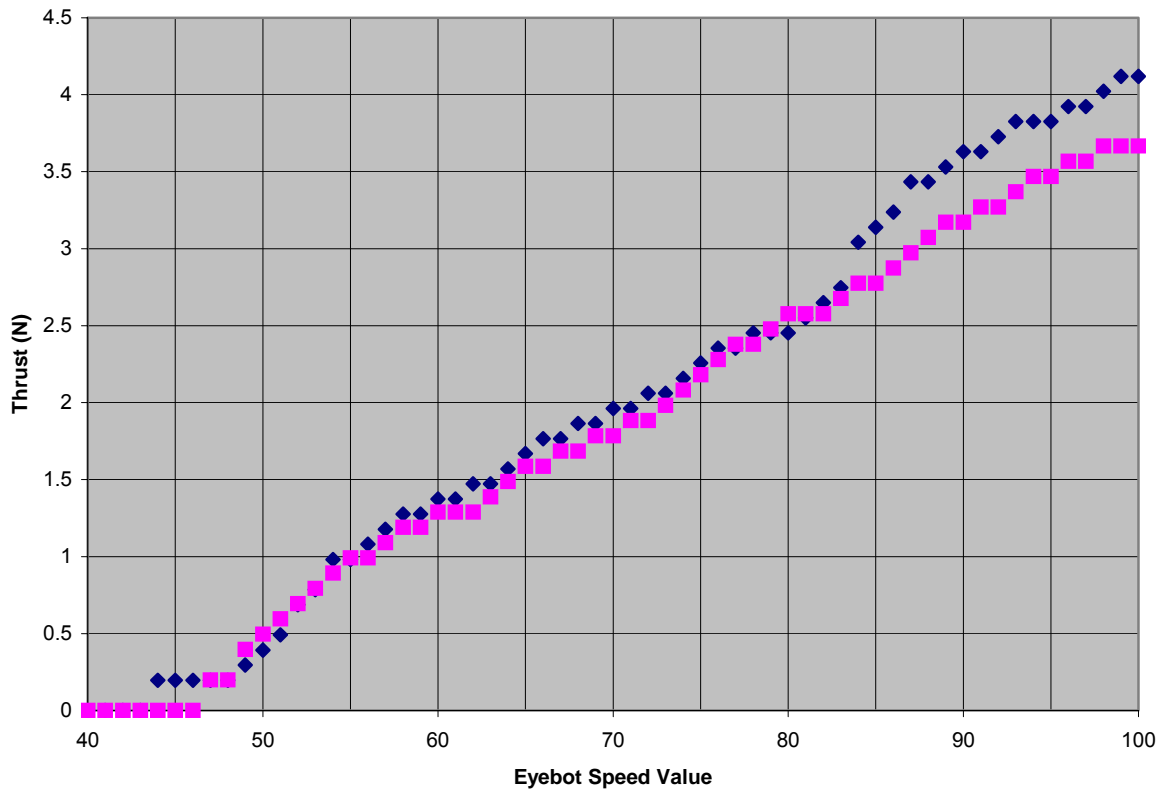


Figure 4.2: Stern thruster identification graph

For this case the weight in the rack was raised to guarantee that the propeller remains completely in water.

A right-handed propeller (which rotates clockwise when in forward gear) will tend to push the stern of the vehicle to starboard. When in reverse gear, the effect will be much greater and opposite. A right-handed propeller will now push the aft of the boat to port. This effect on boats is called working wheel error or propeller walk.

Due to the ring around the propeller and due to the big rudder blades there was no effect measurable or observable.

4.1.2 Heave Thruster Identification

The Heave Thruster provides movement in z-direction. It is mainly used for diving or hovering at one depth. Figure 4.3 shows the force diagram. The former system is mainly optimised for movement on forward direction, so the thruster is build into the AUV facing downward. To get force measurements, the load cell was connected with a string over reel to the AUV.

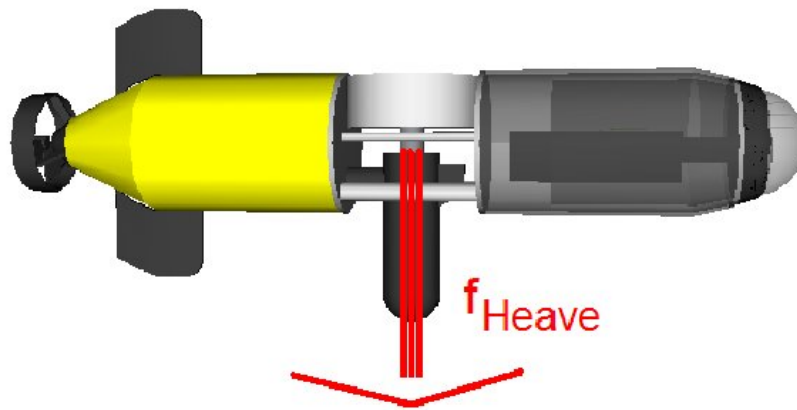


Figure 4.3: Stern thruster force direction

Figure 4.4 shows the thruster generates more thrust in downward direction than in upward direction. Upward direction is nearly not necessary, due to the positive buoyant behaviour of the AUV. This characteristic comes from its original area of application where the main focus of design was on forward movement.

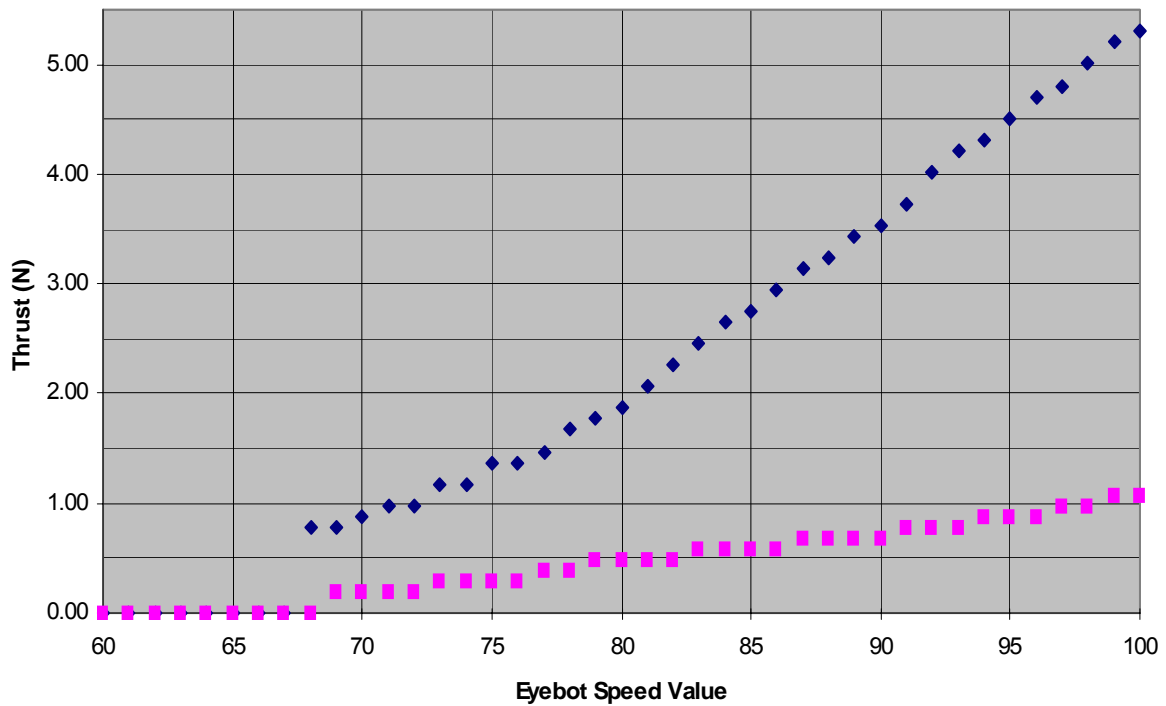


Figure 4.4: Heave thruster identification

Due to its construction the heave propeller creates a turning forces acting on the AUV. This force turns the AUV clockwise when diving or hovering. Measuring this force was difficult, so the turning rate on several speed values was observed and noticed.

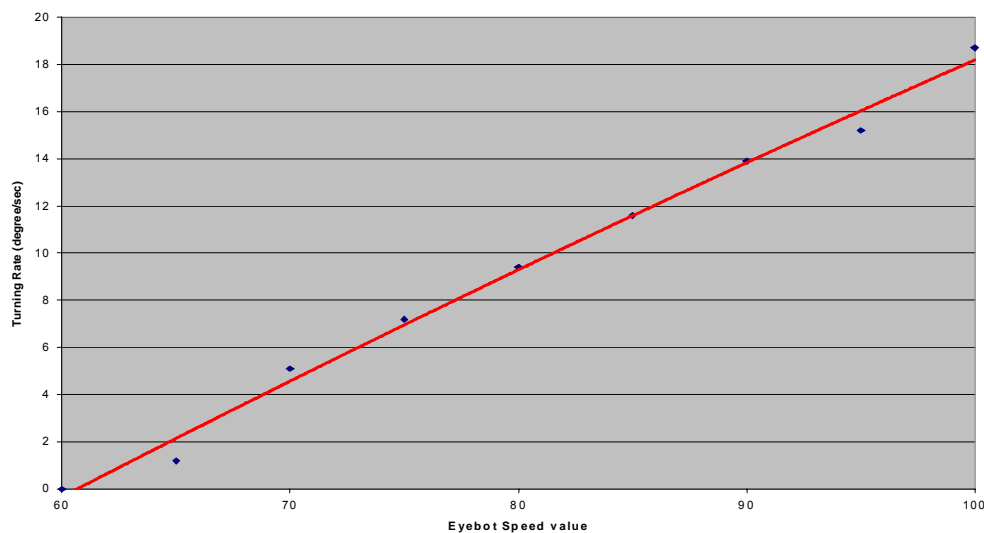


Figure 4.5: Heave propeller interaction

4.1.3 Main Rudder Identification

The main rudders force and yaw-rate is strongly coupled with movement in x-direction. The force of the main rudder acts at the stern of the AUV. This is in some situations problematic, because it moves when turning with the stern into the wrong side until it starts to move. Figure 4.6 shows the rudder force diagram.

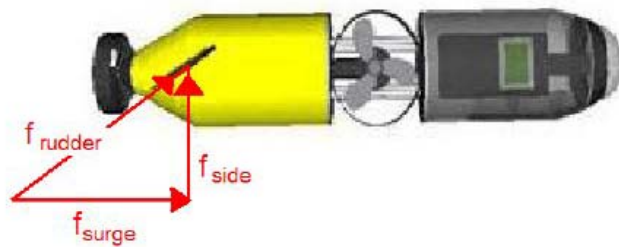


Figure 4.6: Main rudder force direction

Figure 4.7 spotlights the problem with a back mounted rudder blade on tasks like wall following and turning on edges. Because of the point of force in the stern, the AUV starts moving into the “wrong” direction before it starts moving into the desired direction.

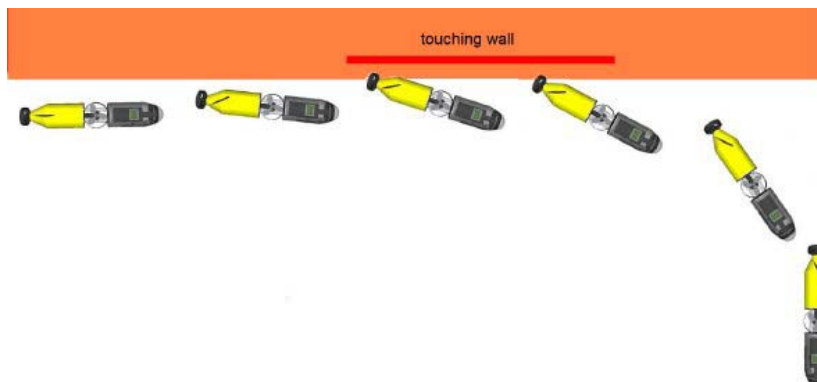


Figure 4.7: Turning with a stern rudder

The force of the yaw rudder can be calculated from its dimensions and the actual angle of the paddles. But the turning diameter or turning rate is also dependent of the vehicles shape. To get an idea of the force and the effect of the main rudder, a test was performed, which shows the turning rate at different angles of the rudder blades (Figure 4.8). With the help of a video camera the turning behaviour was recorded at different rudder angles. Marker on the side of the pool and the camera time code helped to acquire the values.

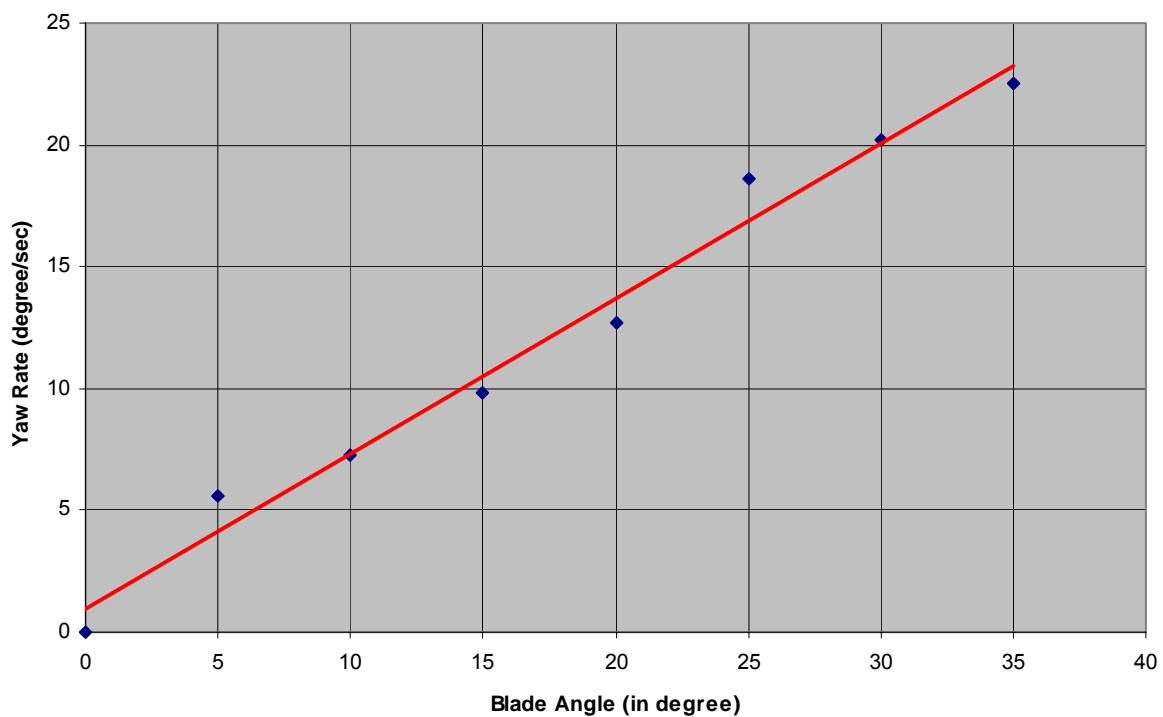


Figure 4.8: Main rudder identification graph

4.1.4 Bow thruster Identification

The bow thruster establishes a constant force in bow of the AUV. The AUV turns around the stern rudder. Instead of generating the thrust with a propeller this system works with a gear-pump, located inside of the AUV. The idea behind this thruster is, to increase manoeuvrability in small areas and to turn independent from the stern thruster. Figure 4.9 shows the location of the bow thruster system, the direction of force and the estimated movement.

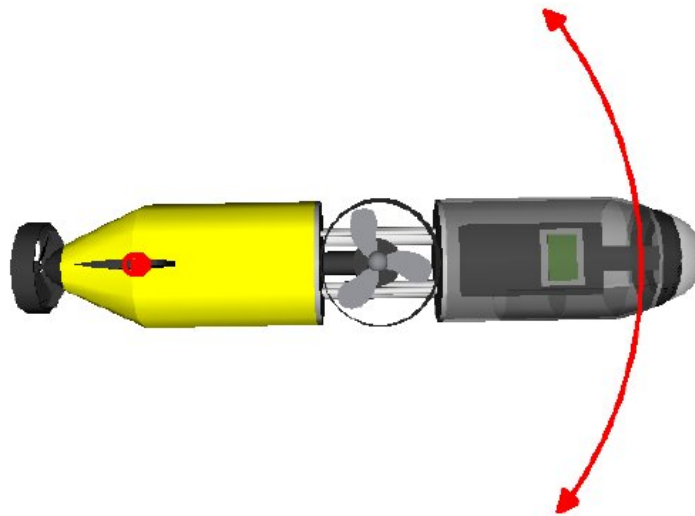


Figure 4.9: Bow thruster force direction

There is no graph of forces at different motor-speed values because it is only possible to set it star-, backboard direction or off. The generated thrust is 0.42 N and turns the AUV with a rate of 7-degree per second.

4.2 Sensor Suite Identification and Calibration

Two important concepts to understand when analysing any sensor are sensitivity and range. Sensitivity is a measure of the degree to which the output signal changes as the measured quantity changes within its range.

The Sensor Suite has to be calibrated. Sensors have limitations not only in their accuracy, also in their design.

Several sensors are only able to measure a specific value:

- Compass only yaw not pitch or roll
- PSD only from 0.2 up to 1.40 m to front, sides and downward
- Accelerometer only acceleration in 3 axis
- Depth sensor only depth in water

4.2.1 PSD Sensor

All four ranging PSD-Sensors needs to be tested if proper working in water and what values they generate at which range to a wall or subject. Proper working includes test with different colours and different moving obstacles.

The Sharp PSDs are intended for applications in air. Due to the triangulation measurement method and measurement through the AUV hull, light refraction and water absorption affect the range and the values measured at certain ranges.

This problem is minimized at the side and bottom PSDs by having a flat wall in front of them. A problem was occurs with the front PSD due to the round window in front of it. This window breaks the light and terribly wrong measurements are the result. However by calibrating the front PSD values it can still be used. However, the range is extremely limited. Figure 4.10 shows this problem.

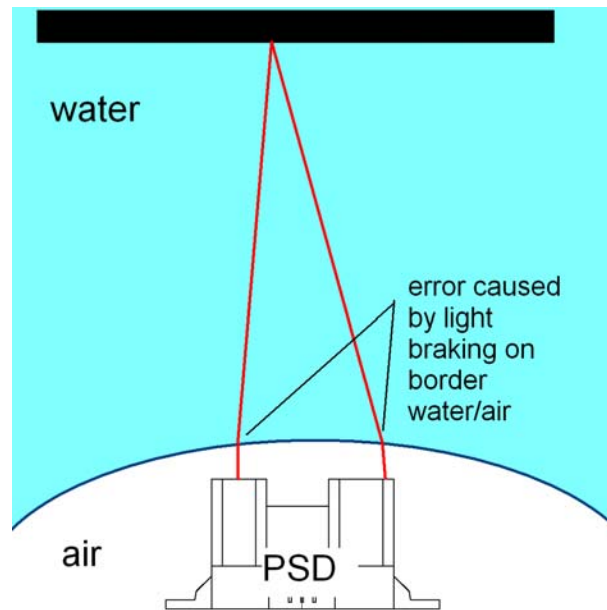


Figure 4.10: Front PSD triangulation problem

Experiments were performed to see if measurement through the hull affects any changes to the results without hull.

The next important step was the measurement in water, which comes along with the difficulty of light refraction on the border to the water and the absorption of light waves in the low infrared light. Experiments were performed in a pool at different depth. Detection object was the white wall of the pool. There were changes to air-measurements in range and output voltage measurable. Varying the depth affected no more changes.

I also had the chance to perform a test in very cloudy water. The visibility in this water was about 0.60m. This pool was very dirty and a gage was swimming around. The AUV was in 0.50m depths. The results of these tests can be seen in Figure 4.11.

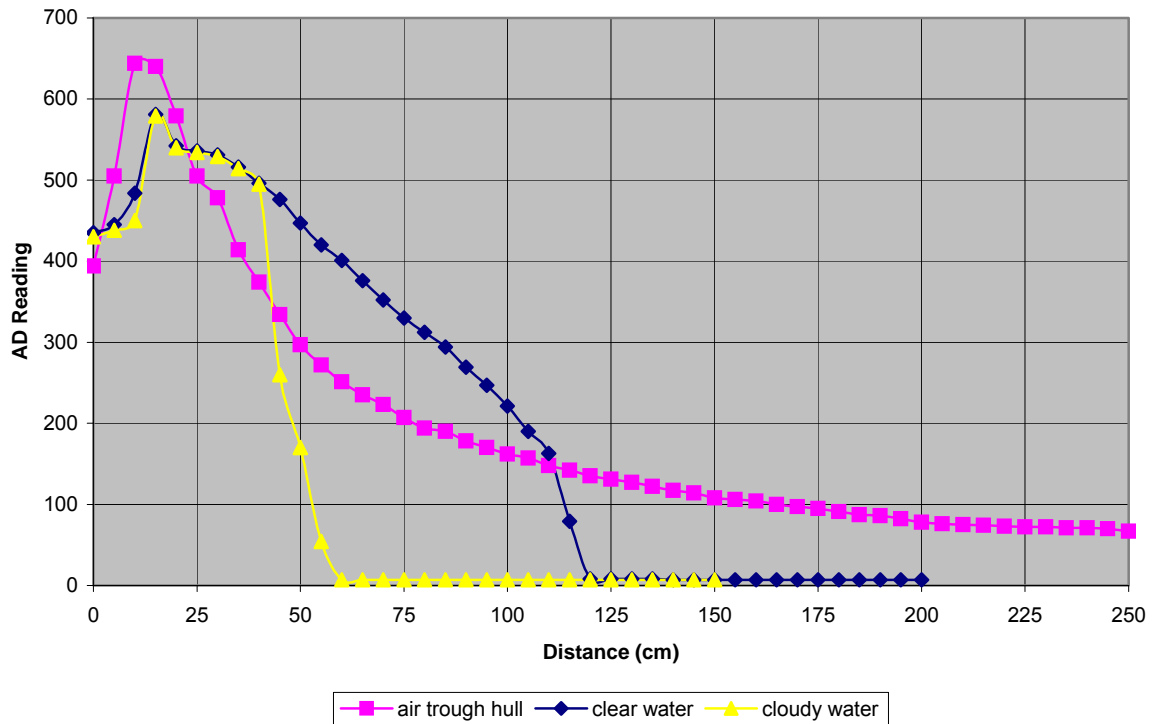


Figure 4.11: PSD calibration distance to output at various conditions

PSDs are using a modulated infrared light beam for their triangulation process. This makes them insensitive against environmental effects. However sunlight contains a huge amount of infrared light. This can saturate the sensor. In this case the output voltage V_{Out} drops to 0.0 Volt.

Changes of the PSD behaviour in various depths could not be measured. Particles and poor visibility could affect the accuracy of PSDs, but they can be negligible in the pool area.

4.2.2 Compass

The compass utilized in this project has a very high degree of accuracy. During usage some noise in its readings has been arbitrated, however the average is very exact.

Mounting the compass close to different electronics devices causes several problems. Although the compass was calibrated, an accuracy check must also be done to ensure external influences are identified. This is particularly important when dealing with underwater environment when actuators can cause changes in magnetic field due to the high currents involved. The digital compass comes with a calibration routine implemented in the RoBios. This process is accessible through the HDT. In this menu, the compass must be selected and the calibrating process commenced. It needs to turn the compass (so the whole vehicle) to 0 degree, and then confirm. It then must be rotated to 180 degree and again confirmed by pressing a button. This calibration process takes into account all the deviations.

A thermal drift test was performed on the V2XG; the result is shown in Figure 4.12. The test involved activating the V2XG in a constant position for approximately 6 hours whilst analysing associated output. Looking at the outputs there is no real drift to speak of. The yaw angle remained fairly constant aside from a little movement at the beginning, which could be attributed to the apparatus moving.

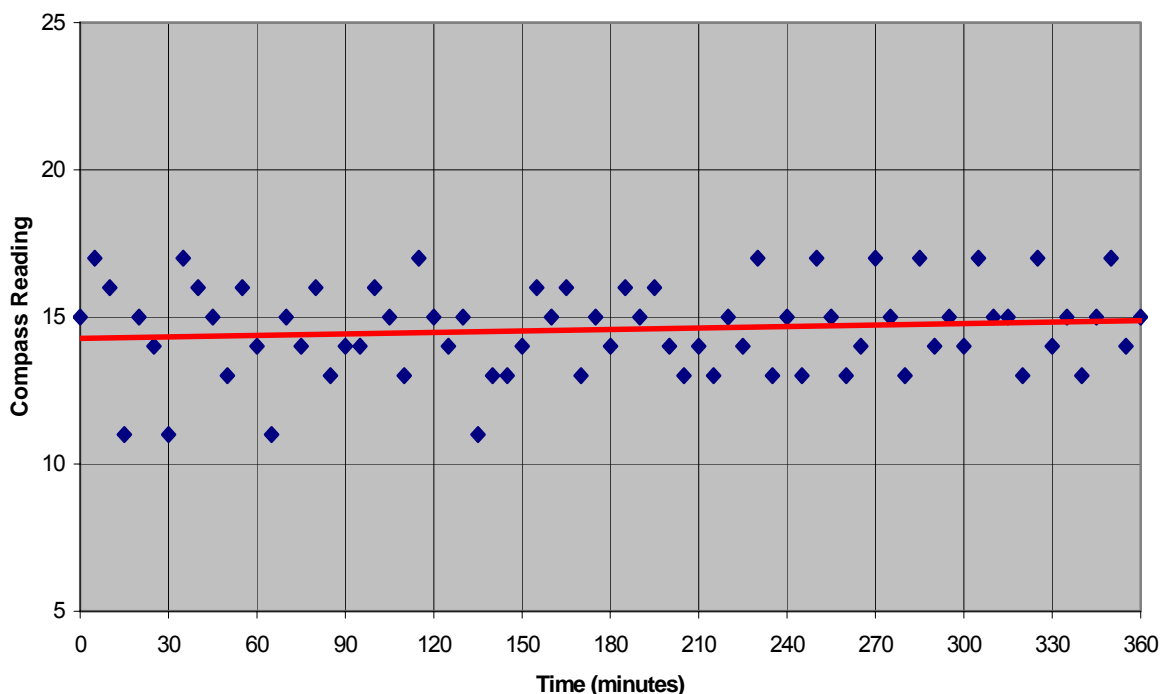


Figure 4.12: Thermal drift of compass

The compass is very sensitive to changes in its level. For accurate measurement it must be level. The V2XG has a dynamic tilt area of ± 15 degree. The heavy bottom design of the should eliminate roll and pitch movement. However, the accuracy of the compass in the case of tilt movement must be verified. Figure 4.13 represents a measurement of the deviation at different tilt angles.

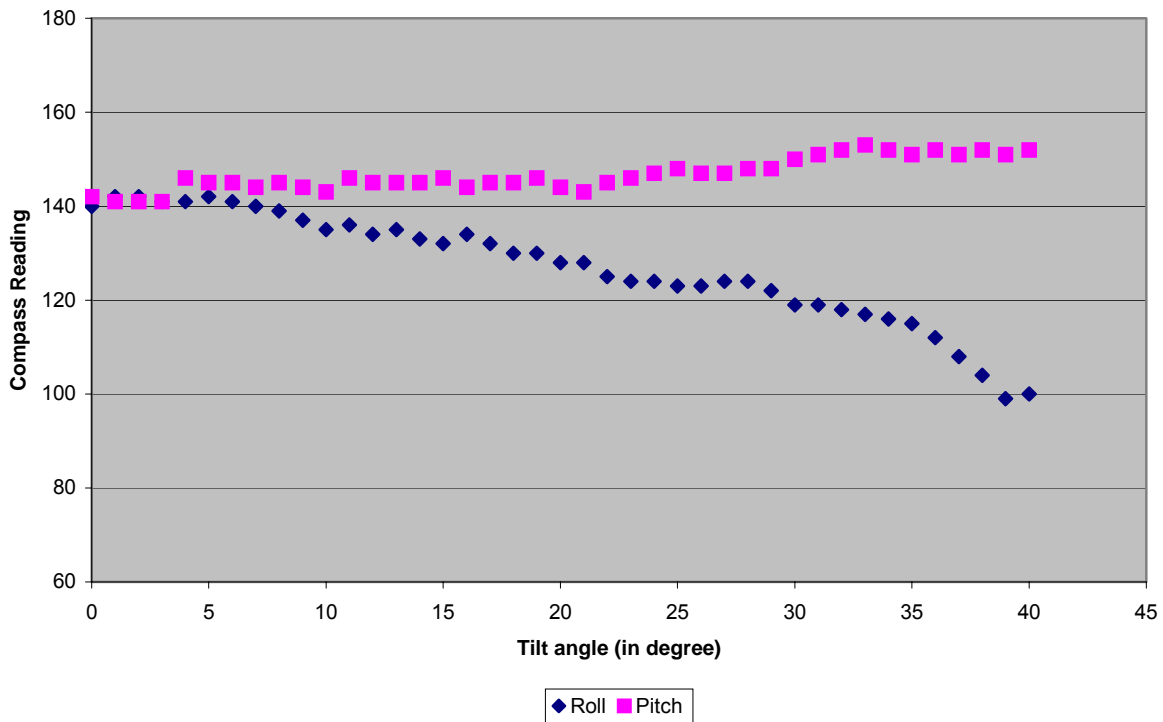


Figure 4.13: The tilt influence on the compass

Metal and electronic devices can influence the magnetic field and therefore affect the compass readings. This is particularly evident when in the laboratory suspicious readings result just from walking around.

4.2.3 Accelerometer

The accelerometer is a discrete unit and comes along with its own microprocessor, 10 Bit AD converter and a RS232 Interface. The circuit generates its own power from the serial port. It also has an onboard one pole filter to cut noise.

The SerAccel module comes with calibration values programmed within the on board non-volatile memory on the PIC16LF88. For recalibrating purposes it is the simplest way to connect the module with a cable to the serial port of a computer. To access the configuration menu open a terminal program and press “Ctrl-S”.

Pressing “1” from this menu will start the calibration routine. Calibration is done using the force of gravity as a reference. On screen commands step through the process:

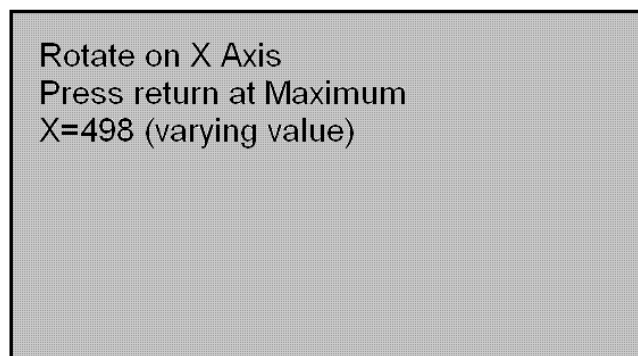


Figure 4.14: Screen on accelerometer calibration process

Rotating the SerAccel increases or decreases the various values. The SerAccel must be turned so the board is perpendicular to the earth’s surface and the on-screen value is at a maximum. Although the jitter, the surrounding environment will prevent this from happening: the Calibration routine takes this into account. Return is to be pressed when the value are ok. Repeat this process for the Y and Z-Axis as well.

These calibration values are recorded to the non-volatile EEPROM on board the PIC micro controller. Every time the SerAccel is activated these calibration values are read from the memory and will be used in the main routine. Therefore, recalibration is not necessary every time when activated. The supplier recommends that calibration is only necessary in sensitive applications if the temperature changes more than 5 degrees since the last calibration.

The accelerometer measures with its z-axis the gravitation. In the case of a tilt movement, the other axis begins measuring the gravitation as well (parts of). The bottom heavy design of the AUV should prevent the accelerometer from measuring the gravitation with its other axis, as this can cause a heavy error.

An experiment was performed to see the connection between tilt and gravitation measurement error.

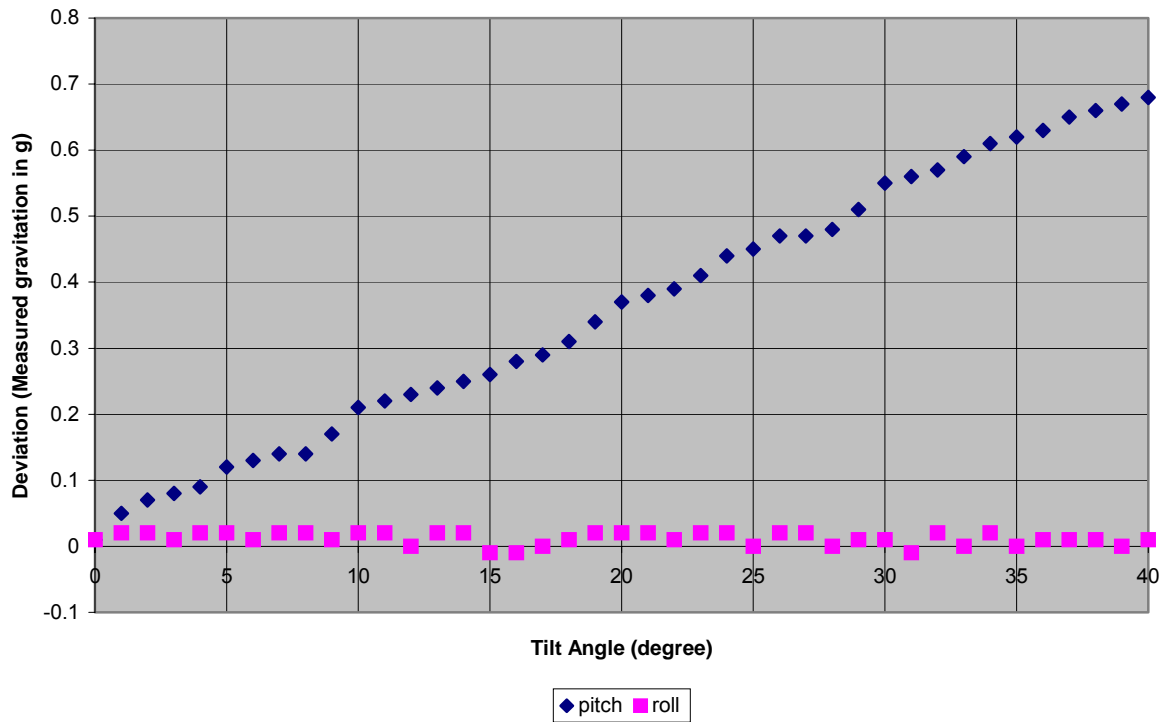


Figure 4.15: Error caused by tilt

The acceleration signal output by the sensor is doubly integrated with time, which yields the travelled distance. Bias offset drift exhibited in the acceleration signal is accumulative and the accuracy of the distance measurement deteriorates with time due to the integration. This problem can be rectified through by periodic recalibration and the use of external measurements on position, velocity, and attitude. These may be compared with the corresponding quantities calculated by the inertial system.

4.2.4 Depth Sensor

The depth sensor is a complex system consisting of several parts. Initially the amplifier board itself must be calibrated. This procedure requires a syringe, a multimeter and tuning four blue spindle potentiometers. As seen in figure 3.31, three are marked with black lines. These are required to adjust the common mode rejection ratio (CMRR), offset voltage (V_{offset}) and also the reference voltage (V_R) of the amplifier. The final unmarked potentiometer adjusts the span of the output voltage. This potentiometer, allows changing the sensitivity of the pressure sensor; the output span can be changed from 0-4.9V to 0-10V, giving the pressure sensor a more accurate output over half its maximum pressure when sampled by the 0-4.9V EyeBot.

Referring to the Sensym application sheet [Sensortech, 2004] the following calibrating procedure for setting the four potentiometers applies:

1. Set the Common Mode Rejection Ratio by shortening the points A and B. Adjust the CMMR potentiometer until voltage is 0.00V between V_X and V_R .
2. Set the Offset Voltage by removing the short from A and B and adjust the V_{OS} potentiometer until the digital multimeter between V_X and V_R again displays 0.00V.
3. Set the Output Reference Voltage by adjusting the output reference V_R potentiometer until the output voltage V_O is equals 1.00V.
4. Set the Output Span by using a syringe to apply full-scale pressure to the sensor. Then adjust the output span potentiometer, R_P , until the output voltage is at desired maximum. (for example 4.9V for 0-10m).

Note that after initial calibration these first three potentiometers should remain consistent. The fourth output span potentiometer could be used to alter the maximum depth or sensitivity of the pressure sensor. The lookup table must then be updated (or translating algorithms in the controller) to translate the 10 bit AD converter reading to an appropriate AUV depth in mm.

The first experiment took place on the Lab-Table. A syringe with a valve were connected to the pressure sensor input port. Each time the syringe plunger was pushed in by one notch, the sensor output voltage was recorded.

Using the volume of the silicone hose, volume of the syringe and current atmospheric pressure, the simulated depth was calculated according to the equation of Boyle's Law:

$$p_1V_1 = p_2V_2$$

Where,

$$p_1 = 101.3kPa$$

$$V_1 = 1.04 * \pi(0.005)^2 + 10 * 10^{-6} m^3$$

$$= 6.228 * 10^{-5} m^3$$

$$p_2 = \rho gh + p_{atmospheric} = d \times 9.8 + 101.325kPa$$

$$V_2 = 1.04 \times \pi(0.005)^2 + \frac{i}{50} * 10^{-5} m^3$$

and i is the syringe notch number (0 to 50) and d is the depth in meters below sea level. Figure 4.13 shows the results of this test.

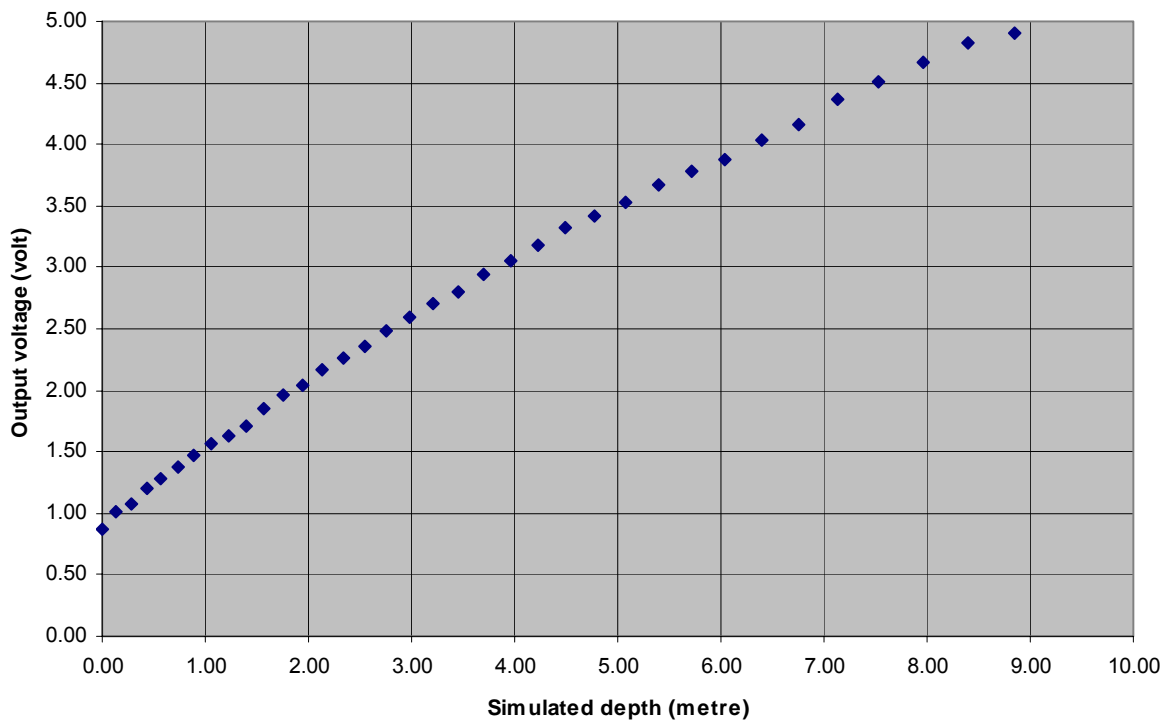


Figure 4.16: Calibration graph with syringe

The second experiment was performed in the pool. A measure tape was attached to a stick used to measure the depth of the AUV, which was pushed down to various depths by hand to obtain the desired measurements. The process was repeated five times. Figure 4.17 shows the results of this test.

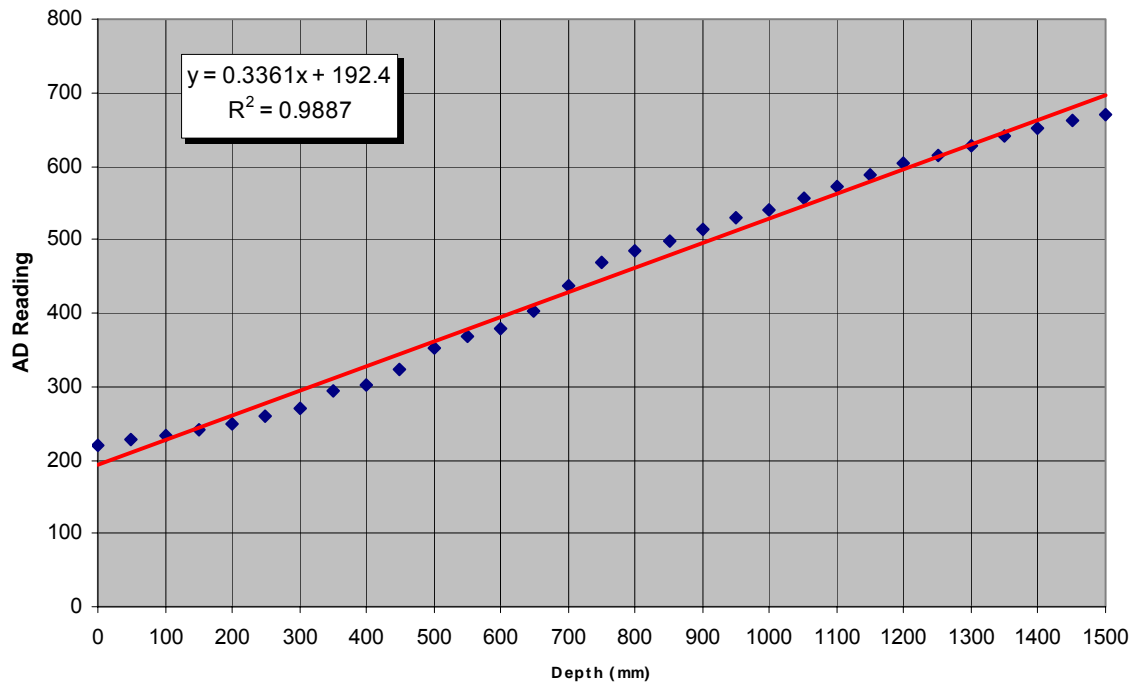


Figure 4.17: Pool depth sensor calibration graph

A resolution test showed the sensor to be sensitive to changes of 1cm in depth. In most situations, the surface waves have an amplitude of 1cm or more. Thus, this resolution is more than adequate.

To gauge the hysteresis of this sensor system it was placed in the water and output readings taken for every 5cm increment in depth. Readings were taken for increasing and decreasing values of depth to check for hysteresis effects. Readings taken for increasing depth show no sizeable hysteresis effects.

4.2.5 Battery Gauge

The battery gauge requires an initial calibration before first use. A variable voltage supply is necessary for this procedure.

The voltage supply has to be adjusted to 13,5 Volt. The variable spindle potentiometer P_1 has to be tuned until LED Nr. 10 is alight. Following this, the supply voltage must be decreased to 10 Volt. The spindle potentiometer P_2 has to be tuned that now LED Nr. 3 is lit. This process Should be repeated because of mutual influence between P_1 and P_2 .

4.2.6 Colour Camera

For optimal use, the camera which is usually intended for usage in air needs to be adjusted and calibrated for tasks as recognizing obstacles, pipeline following and more. The camera allows adjustments of values for the RGB. It is also possible to do some basic navigation with the camera, such as pipeline following or more. According to the obstacle recognition code, and red golf-ball test, the optimal distance to recognise an obstacle has been found to be 0.60m.

4.3 Body Identification

The body of the vehicle and its behaviour in water have to be identified for proper navigating and acting. An experiment was established to obtain the velocity at various motor controller speeds. The pool was divided into several areas, forming a test-way for speed measurement.

The speed test-way consists of 4 parts:

1. 5 metres to accelerate
2. 1 meter for the first measurement
3. 1 meter for the second measurement
4. 2 metres stopping.

The AUV was set to the desired speed and when the motor started it was released. It passed the acceleration area, the two measurement areas and was then stopped by a person at the end of the pool. The measurement was recorded with a video camera and red bottles on the other side of the pool. With the help of the time-code, the time passing the one-meter distance could calculate back to the speed. Figure 4.18 shows a scheme of the pool measurement setup.

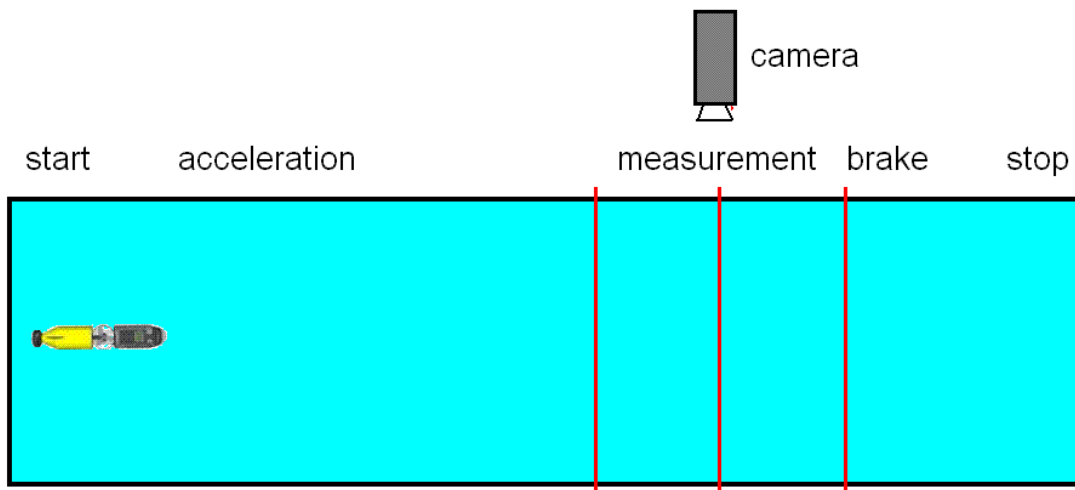


Figure 4.18: Pool configuration

Figure 4.19 shows the results of this test.

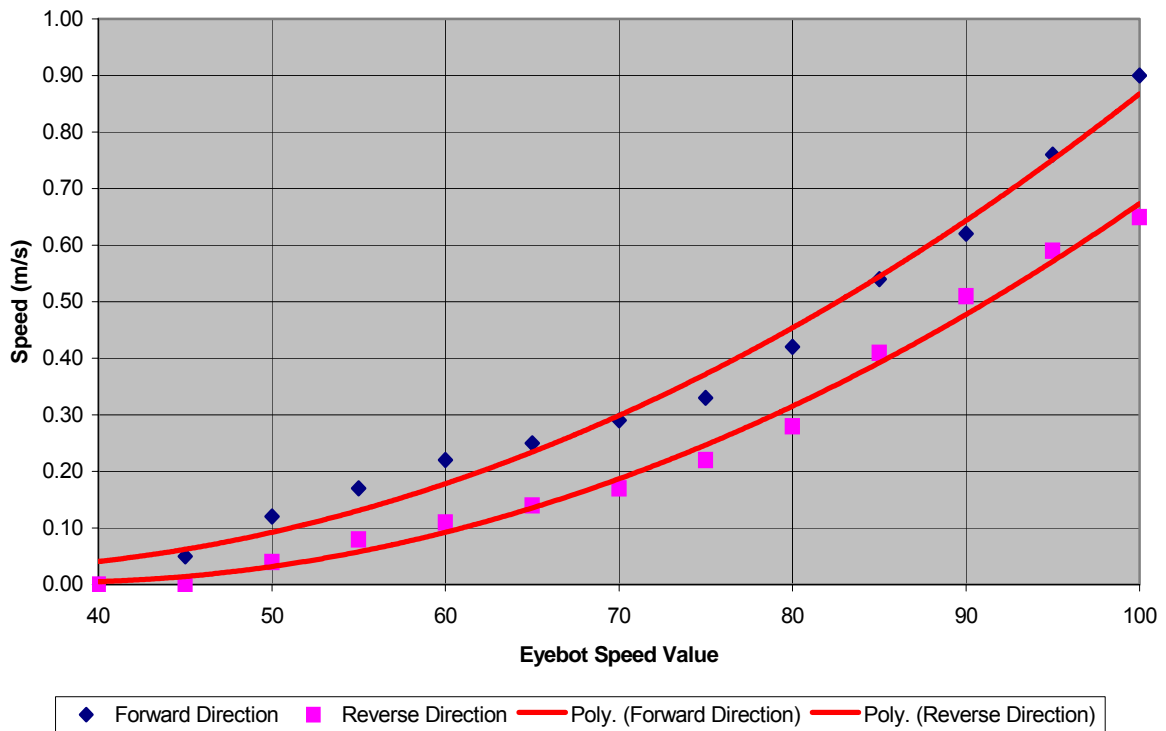


Figure 4.19: Velocity vs. Eyebot speed of the AUV



Figure 4.20: Calculating times using a video tape and time code

4.4 Environment and Equipment

The experiment environments were two standard swimming pools, filled with chlorine water. Both had the dimensions of 4 meter to 10 meter. Maximum depth was 2.50m on one and 0.70m on the other end. One of the pools was very cloudy (visibility average: 0.60m), providing an interesting parameter for testing the vision based sensors such as camera and PSDs. Most tests were performed in the evening where light conditions were dimming. The load-cell shown in Figure 4.21 was used to measure the thrust. Its display was calibrated and it was equipped with an interface as well. It could measure from 0 to 1kg with an accuracy of 0.001kg.

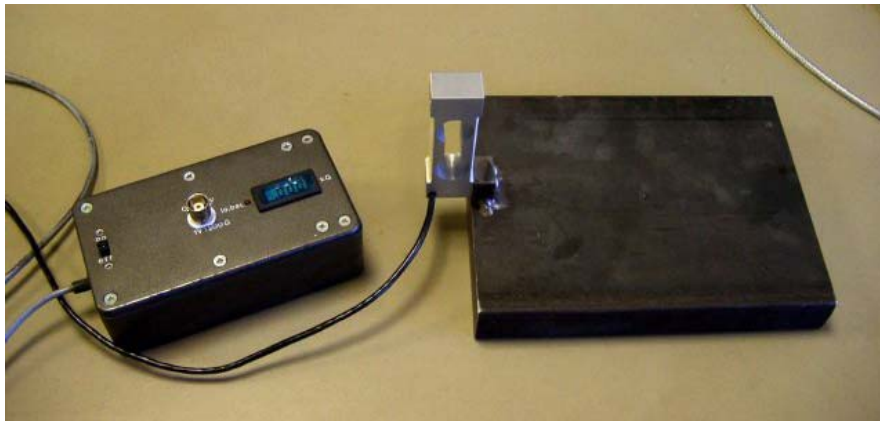


Figure 4.21: The load cell

A digital JVC mini-DV video camera was used to record the experiments. Besides small tools as a measuring tape, a stick or red coke-bottles were useful utilities.

4.5 Summary

Several experiments were performed to get the real vehicle behaviour, force and coupled effects of actuators. Problems with the heave thruster turning the AUV, a big turning diameter with the main rudder and a bow thruster with less power have been addressed.

Sensors were identified, defined and calibrated in this chapter. Most of the sensors work fine, problems raised with the front-PSD and the accelerometer. The front-PSD is sitting in front of a curved wall, which is amplifying light refraction effects trough hull to water that results in wrong readings and a highly reduced range. The accelerometer gives wrong readings due to a tilt movement of the AUV when changing the depth rapidly.

5 Controlling and Navigation of USAL

Once modelling has been undertaken, a control system can be designed for the underwater vehicle. Control systems are required to provide signals to the actuators in order to achieve the desired positions and velocities for the vehicle. Controlling underwater vehicles differs from controlling other vehicles due to the nature of underwater dynamics. The controlling device is an Eyebot-controller with modified software. The controller is primarily formed with PID algorithms to control the actuators via PWM signal according to the desired values and measurements. Various sensors and a camera generated input.

The USAL-AUV INS has a sensor suite that contains sensors that measure the required state variables. It also contains a dynamic model of the USAL-AUV system and thus, given the values for the thrusters inputs, the resulting system reaction can be calculated. All of this information, i.e. the sensor readings, thrusters inputs and dynamic model calculations need to be collated to give an output of USAL-AUV's state. However, the problem of state variables exceeding measurement sensors also has to be addressed.

5.1 Simplifications in Dynamics

Due to the symmetrical shape and bottom heavy construction some simplifications in dynamics can be considered. The following assertions are made, to simplify dynamics:

- Considered symmetrical
- Roll and pitch is negligible which means during all manoeuvres the vehicle remains in a horizontal position.
- Sway (movement in y-Axis) is negligible.
- The vehicle degrees of freedom are decoupled (especially on low speed)
- Low speed AUV

The USAL AUV can be seen fairly to be symmetric about its three planes. Only the blades in the stern deviate from this slightly. The dynamic matrices of the AUV can be simplified without loss of information by doing this assumption.

Due to the choice of the bottom heavy design movement like pitching or rolling can be negligible, because the AUV is not intended to do these movements. They cannot be controlled actively.

The USAL-AUV is rated as low speed AUV. Thrust power increases very quickly with speed. Doubling the speed requires eight times more power. The Explorer AUVs are designed for a nominal cruise speed of 2.0 m/s and a design maximum speed of 2.5 m/s. Greater speeds can be achieved if required at the expense of larger and heavier thruster components. Because the amount of energy the AUV can carry on-board is limited, the efficiency of the propulsion system is critical to minimize the amount of electronics power consumed. In addition lower speed enables more precision. [Wettergreen, 1995] As the AUV standard task location is a swimming pool, external non-linear environmental forces can be controlled and neglected.

5.2 Motion Control

In developing a control system for an AUV, the aim is for the vehicle to be able to accurately follow a desired trajectory, regardless of the complexities of its own dynamics or the disturbances it experiences.

In Chapter 4 model values of the USAL-AUV has been achieved. Due to its under-actuated design it can move surge, heave and yaw directions but not in sway, pitch, roll. Due to the thruster configuration. Yaw it is highly coupled to movement in x direction due the additional front rudder system also provides more flexibility. It is quite common to use PID controllers for each DOF are used in AUVs due to the simplicity of implementation.

5.2.1 On/Off Hysteresis Control

The on/off hysteresis control algorithm was the first control tested for the AUV, because it is very easy to implement. There is no special tuning necessary: just implementing a hysteresis around the desired value.

Because of the sluggish behaviour and slow reaction of the vehicle body this type of controller promised good results in simulation. However switching the motors from 0 to 100 and reverse the motion from 0 to 100 causes very high current spikes and high wear on the mechanics. The ineffective energy transformation causes a high loss of limited energy.

5.2.2 PID Tracking Control

An alternate solution is the PID-Controller. Adapted to the vehicle dynamics, it has the possibility to give accurate movement. Precondition is a real-time or constant processing of all the data. To setup the variables K_p , K_I and K_D a simulation using the vehicle parameters was archived. This simulation using the program “WinFact98” took the vehicle behaviour as control path. Figure 5.1 shows a screenshot of the simulation interface.

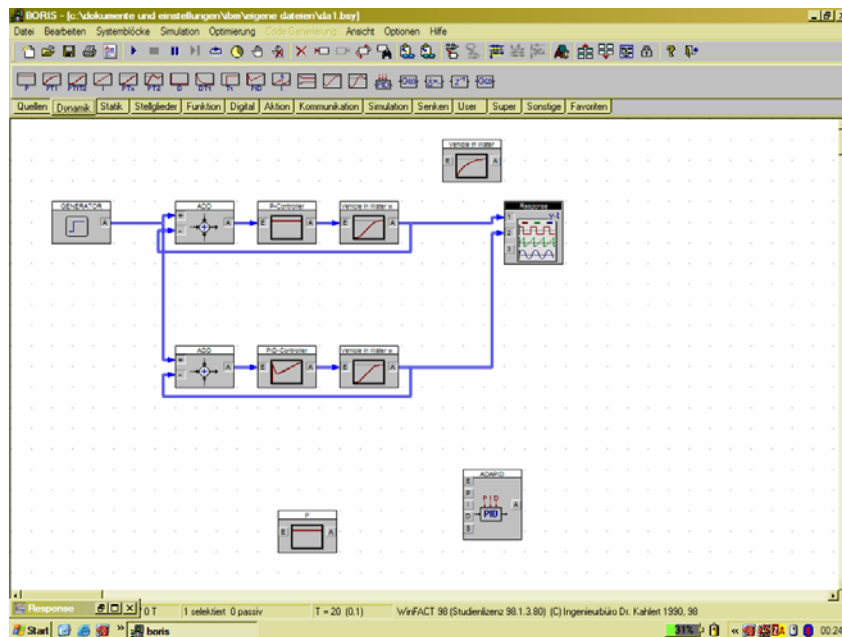


Figure 5.1: Simulating the AUV using WinFact98

Measurements should fine-tune these variables, however these measurements were omitted due to time constraints.

5.3 Sensor Data

To achieve truly autonomous behaviour, an autonomous underwater vehicle (AUV) must be able to navigate accurately within an area of operation. In order to achieve this, an AUV needs to employ a navigation sensor with a high level of accuracy and reliability. However, in practice, a single sensor alone may not be sufficient to provide a suitable navigation system, as it can only operate efficiently under certain conditions or has inherent limitations when operating in underwater environments.

Basic environmental information is gained from the PSD-ranging sensors, which are the most important sensors in the small world of the pool to navigate and to avoid hitting any walls or obstacles.

The accelerometer needs additional CPU-power to return velocity and distance information. Other sensors like the compass or the depth-sensor can return rate or tendency information with simple functions.

The PSDs and the depth sensor are connected via the ADC to the Eyebot. A translation table becomes necessary to transform the AD reading to the measured value. With the help of linear regression [Buenger, 2004] it is possible to translate the AD reading within a simple row to the value. A significant amount of noise was measured, although a one-pole filter was installed. To reduce this noise the controller takes the average of 5 readings. The compass is connected via digital input. Accessing these data is very easy due to the operations system implemented routines. To get the accelerometer data, which is connected to serial port two was not easy. It provides values in a row of ASCII-characters. Reading from the port and translating the characters to INT-values is solved by a special routine.

5.4 Controller Implementation

The hierarchical architecture as described by Valavanis [Valavanis et al, 1997] uses a top-down approach to divide the system in levels. The higher levels are responsible for the overall mission goals, and lower levels are responsible for solving particular problems to accomplish the mission. It is a serial structure where direct communication is possible only between two adjacent levels. The higher level sends commands to the lower level and, as a result, receives sensory information back from the lower level. The information flow decreases from the bottom to the top of the hierarchy.

This makes it easier to verify controllability and stability, i.e., performance evaluation of the architecture is feasible. The disadvantage of this scheme is a lack of flexibility, and, as a result, an attempt to modify some functionality requires significant modifications of the whole system. Since there is no direct communication between high-level control and low-level peripherals (sensors, actuators), response time (sensor input-system action) is long, and sensor integration/fusion is difficult.

5.4.1 Control System Structure

The control system itself consists of three PID controllers dedicated one by one to each degree of freedom. Gaining information from the sensor suite each controller has its own actuator that acts on the vehicle. The structure is shown on Figure 5.2 below.

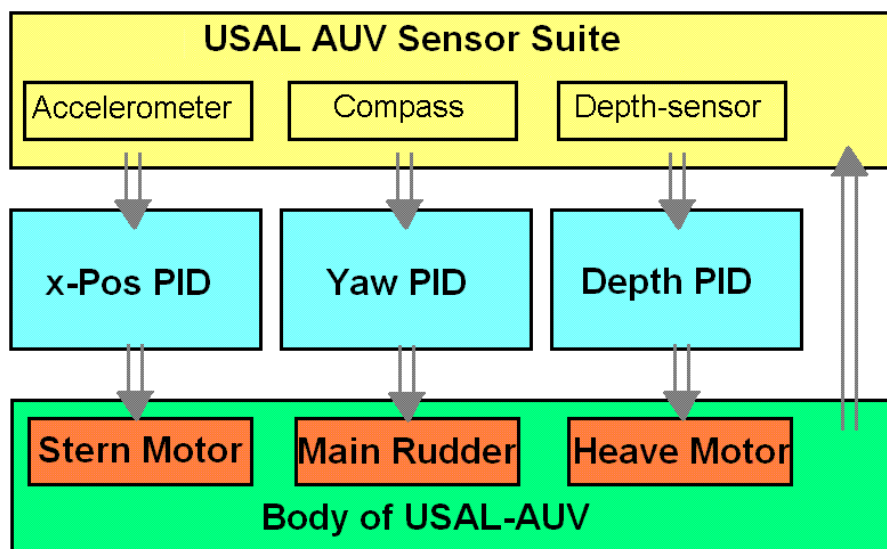


Figure 5.2: Control system structure

5.4.2 Software Structure

The software structure is pretty similar to the control structure. It is organized as three-layer software as shown in Figure 5.3.

Planning Layer:

The upper layer acts as main task area. The desired tasks, navigation and obstacles recognizing is processed in this level.

Control Layer:

Control functions and tracking algorithms are implemented in the manoeuvres level. This level gains information from the execution layer and provides instructions for the actuator-classes motors and servos.

Execution Layer:

This layer is responsible for interfacing between vehicle hardware, comprised of the sensor group and the actuator group. Sensors are accessed by the controllers of the upper layer and by the remains of the architecture components. The actuator group is responsible for interfacing with the hardware actuators.

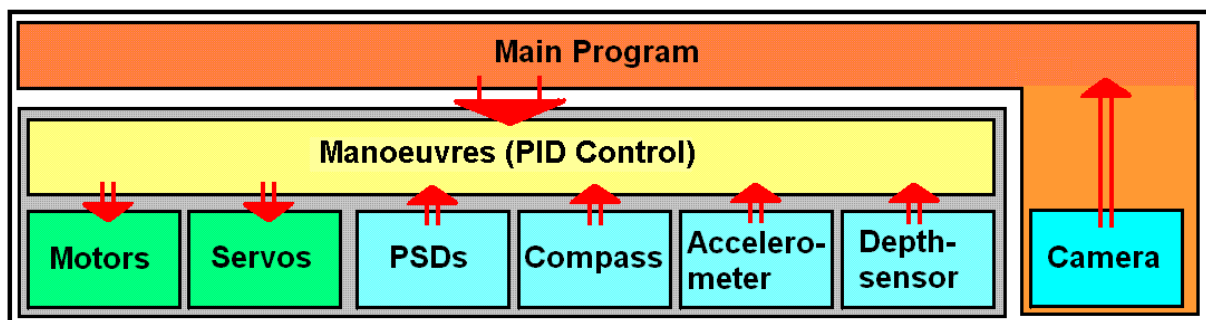


Figure 5.3: Three layer software structure

The complete program structure contains of the following classes and functions.

Main Program (main.cc)

This module contains the mission task and navigation. In this layer picture processing, obstacle recognition and map building is implemented. Navigation commands go straight to manoeuvres.cc.

Manoeuvres (manoeuvres.cc)

This module contains the PID-controller and some basic functions to control the movement of the vehicle.

Motors (motors.cc)

The motors module is responsible for providing intensity and direction of thrust from the motors. Its rate of change is limited to protect the motors and to reduce current spikes.

Servos (rudder.cc)

This module is responsible for change of yaw by controlling the two rudder systems.

Accelerometer (acce.cc)

This module manages the communication with the accelerometer unit which is attached on COM2. It also translates the ASCII character coming from the accelerometer into INT values. In addition to this it provides via integration the speed and the distance value.

PDSs (psd.cc)

This module provides the distance value from the various PSD sensors mounted in the vehicle. With the help of an algorithm it translates the AD reading to distance value.

Compass (compass.cc)

The compass module provides the 0-360 degree heading from the compass module and calculates yaw-rate (in degree per second).

Depth-sensor (depth.cc)

The depth module does pretty much the same as the PSD module. It translates the AD reading from the channel of the depth sensor with a specific algorithm to the depth value.

5.5 Subsim simulator

A simulator for AUVs called 'Subsim' was developed in the Mobile Robotics Lab. The data achieved from the construction and identification process of USAL-AUV was implemented into a vehicle-file to be used in this simulator. This makes possible to simulate the behaviour of the AUV or programs without the need of a real pool. A controller program can be checked for proper working before uploaded to the AUV and before tested in a pool. This could save plenty of time. Figure 5.4 shows a screenshot of the simulator. The controller display is displayed on the left and on the main window presents the AUV in its world. The simulation time can be increased or decreased, a variable view angle and visualisation of sensors is possible as well as 3D stereo view. The simulator is able to simulate AUVs in various worlds, for example in a pool or a rock environment. [Braeunl et al, 2004]

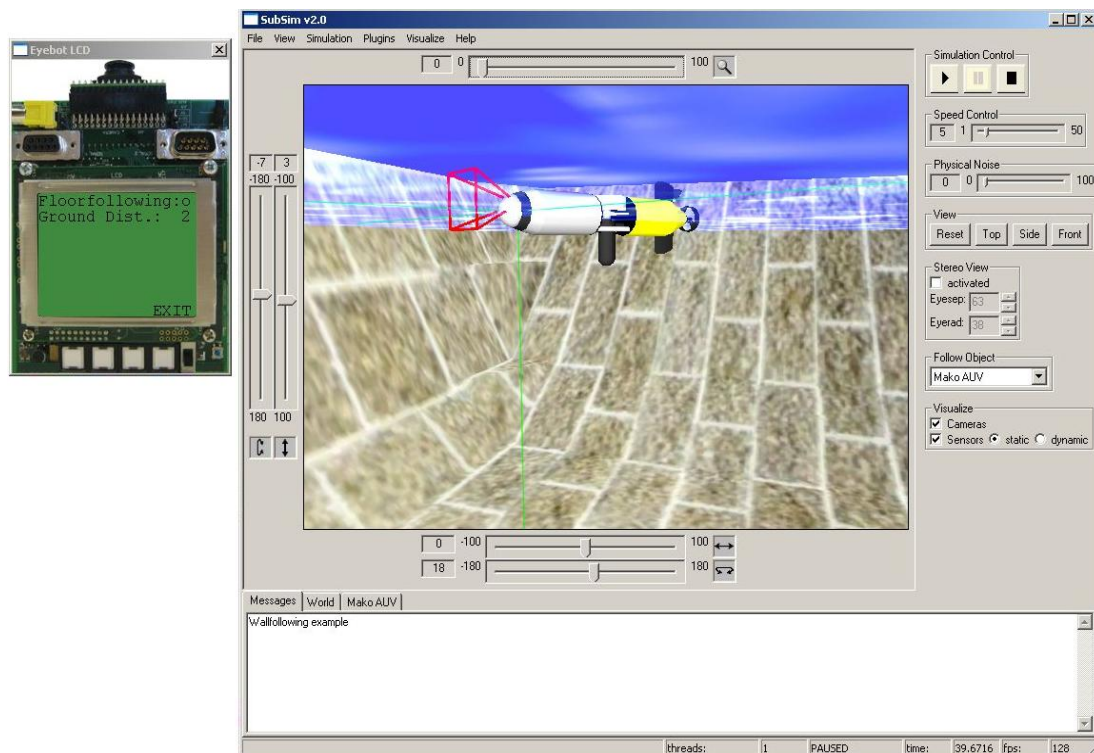


Figure 5.4: The Subsim simulator

5.6 Wall following task

The wall following task is a typical procedure for AUVs. In this task, the AUV follows a wall, generally the wall of the pool in a certain distance. It continuously measures the distance between wall and vehicle with its side-PSD and corrects deviation with the main rudder system. If the distance decreasing the AUV turns away from the wall, otherwise if the distance increasing it turns towards the wall.

Different types of controllers can be used for this application, but mainly a PID controller is well suitable to achieve the correct control signals.

At this stage the wall following task is not implemented in the standard manoeuvres class because it is a special task. The planning layer gets the information directly from PSD-class (distance in metres) and controls the actuators with the help of manoeuvres class (speed and steering).

5.7 Summary

This chapter spotlights the development and considerations concerning the vehicle controller and the software on the controller. PID controllers are easy to implement and in this case the most suitable solution. A short introduction into the program structure is given, for more information have a look in the classes to see which functions they offer.

6 Conclusion

This thesis has given an overview over the development of the USAL-AUV. Various strategies, techniques and theories relating from basic electronic circuits up to motion, navigation and location control for autonomous underwater vehicle has been considered. It shows how different sensors work and how they can be combined to an effective navigation system. This relative small AUV was a high challenge in using space and energy on the most effective way.

6.1 Contributions of the Thesis

The following contributions were made in the thesis. Development of the electronics system of an AUV providing:

- Supply of different voltages
- Energy control and recharge possibility
- Water leakage detection and electronics protection
- Communication
- Easy and reliable design
- All controller values soft coded for easy modifications
- Efficient energy use

Development of a basic motion controller capable of:

- Controlling power delivered to a motor through PWM.
- Controlling the thrust and direction of a motor.
- Limiting thrust rate of change to reduce mechanical wear on motors.
- Controlling the rudder blades.
- Proportional depth and yaw control.
- Modularity, simplifying future software development.

Development of the Sensor Suite capable of:

- Providing navigation, mission and preceptive sensors
- Being small and light-weight and having low power requirements
- Sampling rate greater than 20Hz

Identification of Actuators and Sensors

6.2 Discussions of the Outcomes

A discussion of the outcomes in this thesis is presented in this section.

6.2.1 Electronics System

An electronic system was archived to provide voltage supply, motion control and energy management. The whole design is very effective and reliable. Integrated noise filter stops devices interfering each other. The dual motor driver, which was reason for delay in manufacturing, works now very well. Communication to a host computer is provided via a Bluetooth device.

6.2.2 Sensor Suite

The sensor suite is pretty well equipped for all navigation and mission purposes. Compass and depth sensor are working really fine and accurate.

The PSD sensors are intended for use in air and due to water refraction and infrared wave absorption the range of these sensors decreases in water. However, it's a very small compact solution for distance measurement. An so far unsolved problem with the front-PSD arised from the curved hull in the front.

The AUV was designed to be stable in the water and not to do any rolling and pitching, but experiments have shown that it tend to roll when diving. This is problematic for the accelerometer, because it starts measuring the earth gravity.

During the experiments a lot of random noise was noticed in the values. Taking average of five readings improved the results a lot and calmed down the random noise.

6.2.3 Controller

Simple PID algorithms were implemented. Two controllers for yaw and depth do position tracking. The third controller could not be implemented so far due to problems with the accelerometer.

The control system is built in a three level guidance. The top level does the task, navigation and path planning; the tracking controllers are located in the second level and the low level includes the hardware driver. The controllers are limited in their speed change rate to reduce current spikes and mechanical wear on the motors.

6.2.4 Improvement on the mechanical design

The mechanical design required some modifications. During the first watering it was realized that the bow weight rack was not required.

But due to the lack of manoeuvrability a bow thruster system needs to be implemented. The electronic circuits and sensors were mounted on a special rack to guarantee that sensors hold the right position and direction.

6.3 Recommendations and Future Work

This section presents some suggestions for further research or improvement.

6.3.1 Electronics System

The electronic system is a very economic, effective and stable system. An improvement could be a waterproof connector in the stern hull for providing serial and power connect even when dived for special experiments. But this is not really necessary, due to the fact that the EyeBot is a powerful controller with enough memory to log all events.

6.3.2 Sensor Suite

The sensor suite is nearly complete. Due to the problems with the accelerometer it is recommended to implement a velocity measurement system based on pressure difference measurement system.

The accelerometer is used at the moment only to measure x-axis movement. This sensor needs improved algorithms and is able to measure more axes. Another problem occurred with the front PSD. This PSD needs some modifications to measure properly through the hull or maybe replaced by another system.

6.3.3 Controller Software

The controller software is at the moment on a very basic level. The PID-values are based on a very simple simulation. Due to technical problems only a few tests could be achieved. New control algorithms maybe integrating fuzzy logic could help the improve accuracy and to save energy.

The communication system is at this stage only used to upload programs to the controller. With the help of a control program on a host computer is could be upgraded to a full bi-directional control system.

6.3.4 Mechanical System

The heading and stability values of the AUV have been observed could be increased. Additional paddles attached on the front hull in the same way as the paddles on the stern hull could improve behaviour of the whole vehicle.

During measurements the bow thruster system was seen as a very effective control for yaw. The only problem was lack of power. This comes from the space restriction in the initial design. The pump, which is used, is a small high performance water pump, imported from Germany. In a second revision it was realized that there is the possibility to track easily the pressure-hoses from the bow to the stern hull. This enables to mount a bigger pump in the stern hull maybe on the top of the motor-driver that is attached on the heave. This would reduce weight and space problems in the bow hull.

Another consideration is to replace the heave thruster by a buoyancy control system. There are a number of easy to handle and easy to integrate systems available on the market. Two systems are presented in appendix E. A buoyancy control system would save a lot of energy because it only needs energy for a change in depth. In the actual design the vehicle is positive buoyant and the heave thruster needs energy all the time to push it under water.

During tests a pitching movement has be observed. The AUV is unstable due to the fact that only one thruster controls it. A second control thruster to control – pitch movement would make the system better.

6.4 Final Word

This project performed an AUV that provides an ideal base for further research and for participating in AUV competitions. An effective control system suitable for demonstrating the capabilities of the USAL-AUV platform was implemented, providing a foundation for its future expansion. Some problems have been addressed and can be handled by the following students. This AUV represents a field of research that is at the forefront of innovation at universities around the world.

References

- [Abbot, 1999] E. Abbott and D. Powell,
'*Land-vehicle navigation using GPS*',
Proc. IEEE, vol. 87, pp. 145–162, Jan. 1999.
Available from: IEEE Xplore [13/10/2005]
- [AUVISI, 2005] AUVSI. Association for Unmanned Vehicle Systems International
Available: <http://www.auvsi.org/> [online; checked 21/12/2005]
- [Bachmayer et al, 2000] Ralph Bachmayer, Louis L. Whitcomb, and M. A. Grosenbaugh,
'*An accurate four-quadrant nonlinear dynamical model for marine thruster:
Theory & experimental validation*',
IEEE Journal of Oceanic Engineering, 25(1), January 2000.
Available from: IEEE Xplore [26/11/2005]
- [Balasuriya et al, 1997] Balasuriya, B.A.A.P.; Takai, M.; Lam, W.C.; Ura, T.; Kuroda, Y. 1997;
'*Vision based autonomous underwater vehicle navigation: underwater cable tracking*',
Conference Proceedings OCEANS '97. MTS/IEEE
Volume 2, 6-9 Oct. 1997 Page(s):1418 - 1424 vol.2 [online]
Digital Object Identifier 10.1109/OCEANS.1997.624205,
- [Barshan and Durrant-Whyte, 1993] B. Barshan and H. F. Durrant-Whyte,
'*An inertial navigation system for a mobile robot*',
in Proc. Int. Conf. Intelligent Robots and Systems, Yokohama, Japan, 1993, pp. 2243–2248.
Available from: IEEE Xplore [26/11/2005]
- [Barshan and Durrant-Whyte, 1995] Barshan, B.; Durrant-Whyte, H.F. 1995;
'*Inertial navigation systems for mobile robots*',
IEEE Transactions on Robotics and Automation, Volume 11, Issue 3, June 1995 pp:328 - 342
Digital Object Identifier 10.1109/70.388775, Available from: IEEE Xplore [01/09/2005]
- [Braeunl et al, 2004] Thomas Braunl, Adrian Boeing, Louis Gonzales, Andreas Koestler, Minh
Nguyen, Joshua Pettitt
'*The Autonomous Underwater Vehicle Initiative ? Project Mako*'
2004 IEEE Conference on Robotics, Automation, and Mechatronics (IEEE-RAM), Dec. 2004,
Singapore, pp. 446-451 (6)
- [Braeunl et al, 2005] T. Bräunl. Eyebot MK4 features, 2005
Available: <http://robotics.ee.uwa.edu.au/eyebot/index.html> [Online; checked 26/12/05]
- [Brown and Buzinski, 1997] R. G. Brown and P. Y. C. Hwang,
'*Introduction to Random Signals and Applied Kalman Filtering*',
3rd ed. New York: Wiley, 1997, p. 219.

- [Buzinski et al, 1992] Buzinski, M.; Levine, A.; Stevenson, W.H. 1992;
'Performance characteristics of range sensors utilizing optical triangulation',
Proceedings of the IEEE 1992 National Aerospace and Electronics Conference, 1992.
NAECON 1992, 18-22 May 1992 Page(s):1230 - 1236 vol.3 [online]
Digital Object Identifier 10.1109/NAECON.1992.220581
Available from: IEEE Xplore [26/08/2005]
- [Chaplin, 2005] Martin Chaplin, London South Bank University
'Molecular Vibration and Absorption' [online]
Available: <http://www.lsbu.ac.uk/water/vibrat.html>
- [Chong-moo et al, 2003] Chong-moo Lee; Seok-Won Hong; Woo-Jae Seong 2003;
'An integrated DVL/IMU system for precise navigation of an autonomous underwater vehicle',
Proceedings OCEANS 2003, Volume 5, 22-26 Sept. 2003 Page(s):2397 Vol.5 [online]
Digital Object Identifier 10.1109/OCEANS.2003.1282917,
Available from: IEEE Xplore [01/09/2005]
- [Craig, 1989] John J. Craig,
'Introduction to Robotics: Mechanics and Control',
Addison-Wesley, second edition, 1989.
- [Cowling and Corfield, 1995] Cowling, D.; Corfield, S.J. 1995;
'Control functions for autonomous underwater vehicle on-board command and control
systems',
IEEE Colloquium on Control and Guidance of Remotely Operated Vehicles,
6 Jun 1995 Page(s):3/1 - 3/8 [online], Available from: IEEE Xplore [26/08/2005]
- [Everett, 1995] Everett, H.R.,
'Sensors for Mobile Robots: theory and application',
Wellesley, Mass : A.K. Peters, 1995
- [Fryxell et al, 1994] Fryxell, D.; Oliveira, P.; Pascoal, A.; Silvestre, C. 1994;
'An integrated approach to the design and analysis of navigation, guidance and control
systems for AUVs',
Proceedings of the 1994 Symposium on 19-20 July 1994 Autonomous Underwater Vehicle
Technology, 1994. Page(s):208 - 217 [online]
Digital Object Identifier 10.1109/AUV.1994.518627, Available from: IEEE Xplore [28/08/2005]
- [Grenon et al, 2001] Grenon, G.; An, P.E.; Smith, S.M.; Healey, A.J. 2001;
'Enhancement of the inertial navigation system for the Morpheus autonomous underwater
vehicles',
IEEE Journal of Oceanic Engineering, Volume 26, Issue 4, Oct. 2001 Page(s):548 - 560
Digital Object Identifier 10.1109/48.972091, Available from: IEEE Xplore [28/08/2005]
- [Kalyan et al, 2004] Kalyan, B.; Balasuriya, A.; Ura, T.; Wijesoma, S. 2004;
'Sonar and vision based navigation schemes for autonomous underwater vehicles',
Control, Automation, Robotics and Vision Conference, 2004. ICARCV 2004 8th
Volume 1, 6-9 Dec. 2004 Page(s):437 - 442 Vol. 1 [online]
Digital Object Identifier 10.1109/ICARCV.2004.1468865,
Available from: IEEE Xplore [01/09/2005]

- [Kaplan, 1996] E. D. Kaplan,
Understanding GPS: Principle and Applications,
1st ed. Boston, MA: Artech House, 1996, p. 39.
- [Kondo and Ura, 2002] Kondo, H.; Ura, T. 2002;
'Underwater structure observation by the AUV with laser pointing device',
Proceedings of the 2002 International Symposium on Underwater Technology, 2002,
16-19 April 2002 Page(s):178 - 183 [online]
Digital Object Identifier 10.1109/UT.2002.1002423, Available from: IEEE Xplore [29/08/2005]
- [Korba et al, 1994] Korba, L.; Elgazzar, S.; Welch, T. 1994;
'Active infrared sensors for mobile robots',
IEEE Transactions on Instrumentation and Measurement,
Volume 43, Issue 2, Apr 1994 Page(s):283 - 287 [online]
Digital Object Identifier 10.1109/19.293434 Available from: IEEE Xplore [31/08/2005]
- [Lewis et al, 1993] Frank L. Lewis, Chaouki T. Abdallah, and D.M. Dawson.
Control of Robot Manipulators,
Macmillan, 1993.
- [Li et al, 2004] Li, T.-H.S.; Shih-Jie Chang; Wei Tong 2004;
'Fuzzy target tracking control of autonomous mobile robots by using infrared sensors',
IEEE Transactions on Fuzzy Systems,
Volume 12, Issue 4, Aug. 2004 Page(s):491 - 501 [online]
Digital Object Identifier 10.1109/TFUZZ.2004.832526,
Available from: IEEE Xplore [01/09/2005]
- [MIT, 2005] Massachusetts Institute of Technology
'MIT Project ORCA '
Available: <http://web.mit.edu/orca/www/> [09/01/06]
- [Mostov, 2005] K. Mostov,
'Method for correction of systematic inertial sensor error',
Web Page of PATH, Univ. California, Berkeley. [Online].
Available: <http://www.path.berkeley.edu/~webed/sensor/papers.html> [12/11/2005]
- [National, 2005] National Semiconductors
'LM3914 Datasheet '
Available: www.national.com [10/11/05]
- [Loebis et al, 2002] Loebis, D., R. Sutton and J. Chudley,
'Review of Multisensor Data Fusion Techniques and Their Application to Autonomous Underwater Vehicle Navigation',
Journal of Marine Engineering and Technology, no. A1, pp. 3-14. (2002)
- [Loebis et al, 2003] D. Loebis, J. Chudley and R. Sutton,
'A Fuzzy Kalman Filter Optimized Using a Genetic Algorithm for Accurate Navigation of an Autonomous Underwater Vehicle',
Submitted to the MCMC2003, Girona, Spain (2003).

- [Padi, 2004] Padi Inc.
'Advanced Open Water Diver Manual'
Padi, 2004
- [Papoulias, 1993] F. A. Papoulias,
'On the Nonlinear Dynamics of Pursuit Guidance for Marine Vehicles',
Journal of Ship Research, Vol. 37, No. 4, 1993, pp. 342-353.
- [Papoulias, 1994] F. A. Papoulias,
Cross Track Error and Proportional Turning Rate Guidance of Marine Vehicles,
Journal of Ship Research, Vol. 38, No. 2, 1994, pp. 123-132.
- [Pettersen et al, 1996] Pettersen, K.Y.; Egeland, O. 1996;
'Position and attitude control of an underactuated autonomous underwater vehicle',
Proceedings of the 35th IEEE Decision and Control, 1996,
Volume 1, 11-13 Dec. 1996 Page(s):987 - 991 vol.1
Digital Object Identifier 10.1109/CDC.1996.574614, Available from: IEEE Xplore [29/08/2005]
- [Sensortech, 2004] SenSym Sensortech
'SX-052 General Description of SX Series'
Available: www.sensortech.com [24/11/05]
- [Sparkfun, 2005] Sparkfun Electronics
'SerAccel V5, A self contained triple axes accelerometer'
Available: www.sparkfun.com [28/10/05]
- [UoF, 2005] University of Florida Machine Intelligence Laboratory
'Subjugator Website'
Available: www.subjugator.org [09/01/06]
- [UWA, 2005] University of Western Australia
'Autonomous Underwater Vehicles'
Available: <http://robotics.ee.uwa.edu.au/auv/> [08/01/06]
- [Valavanis et al, 1997] Valavanis, K.P.; Gracanin, D.; Matijasevic, M.; Kolluru, R. 1997;
'Control architectures for autonomous underwater vehicles',
Control Systems Magazine, IEEE Volume 17, Issue 6, Dec. 1997 Page(s):48 - 64
Digital Object Identifier 10.1109/37.642974, Available from: IEEE Xplore [01/09/2005]
- [Wettergreen et al, 1998] D. Wettergreen, C. Gasket, A. Zelinsky,
'Development of a Visually-Guided Autonomous Underwater Vehicle',
Research School of Information Sciences and Engineering,
Australian National University, 1998.
- [Wettergreen et al, 1999] David Wettergreen, Chris Gaskett, and Alex Zelinsky
'Autonomous Control and Guidance for an Underwater Robotic Vehicle',
Proceedings of the International Conference on Field and Service Robotics (FSR'99),
(Pittsburgh, USA, September 1999)

[Wikipedia stability, 2005]

Available: <http://en.wikipedia.org/wiki/Stability> [03/12/05]

[Wikipedia buoyancy, 2005]

Available: <http://en.wikipedia.org/wiki/Buoyancy> [02/12/05]

[Wikipedia PID, 2005]

Available: http://en.wikipedia.org/wiki/PID_controller [11/01/06]

[Xiaoping et al, 2000] Xiaoping Yun; Bachmann, E.R.; Arslan, S. 2000;

'An inertial navigation system for small autonomous underwater vehicles',

Proceedings, ICRA '00, IEEE International Conference on Robotics and Automation 2000, Volume 2, 24-28 April 2000 Page(s):1781 - 1786 vol.2

Digital Object Identifier 10.1109/ROBOT.2000.844853,

Available from: IEEE Xplore [30/08/2005]

[Yoerger and Slotine, 1985] D. Yoerger and J-J. Slotine,

'Robust trajectory control of underwater vehicles',

IEEE Journal of Oceanic Engineering, OE-10(4):462-470, October 1985.

[Yoerger et al, 1990] D. Yoerger, J. Cooke, and J-J. Slotine,

'The influence of thruster dynamics on underwater vehicle behaviour and their incorporation into control system design',

IEEE Journal of Oceanic Engineering, 15(3): 167-178, July 1990.

[Yuh, 1995] J. Yuh,

'Underwater Robotic Vehicles: Design and Control',

Workshop on Future Research Directions in Underwater Robotics, 1994.

TSI Press, 1995.

[Yuh, 2001] J. Yuh.

'Design and control of autonomous underwater robots: A survey', [online], 2001

Available: http://neuronai.tuke.sk/_hudecm/pdf_papers/

DesignAndControlOfAutonomousUnderwaterrobotsASurvey.pdf [29/10/2005]

[Zhang et al, 1997] Zhang Rubo; Gu Guochang; Zhang Guoyin 1997;

'AUV obstacle-avoidance based on information fusion of multi-sensors',

IEEE International Conference on Intelligent Processing Systems, 1997. ICIPS '97.

Volume 2, 28-31 Oct. 1997 Page(s):1381 - 1384 vol.2 [online]

Digital Object Identifier 10.1109/ICIPS.1997.669232, Available from: IEEE Xplore [02/09/2005]

Appendix

A Test Results

This chapter includes tables of all series of measurements.

A.1 Actuator Identification

This chapter includes all the testing results of the actuators.

A.1.1 Stern Thruster Identification

Forward Direction

Backward Direction

Speed Value	Thrust Force (kg)	Thrust Force (N)		Speed Value	Thrust Force (kg)	Thrust Force (N)
1	0.00	0		1	0.00	0
2	0.00	0		2	0.00	0
...
40	0.00	0		40	0.00	0
41	0.00	0		41	0.00	0
42	0.00	0		42	0.00	0
43	0.00	0		43	0.00	0
44	0.02	0.1962		44	0.00	0
45	0.02	0.1962		45	0.00	0
46	0.02	0.1962		46	0.00	0
47	0.02	0.1962		47	0.02	0.1982
48	0.02	0.1962		48	0.02	0.1982
49	0.03	0.2943		49	0.04	0.3964
50	0.04	0.3924		50	0.05	0.4955
51	0.05	0.4905		51	0.06	0.5946
52	0.07	0.6867		52	0.07	0.6937
53	0.08	0.7848		53	0.08	0.7928
54	0.10	0.981		54	0.09	0.8919
55	0.10	0.981		55	0.10	0.991
56	0.11	1.0791		56	0.10	0.991
57	0.12	1.1772		57	0.11	1.0901
58	0.13	1.2753		58	0.12	1.1892
59	0.13	1.2753		59	0.12	1.1892
60	0.14	1.3734		60	0.13	1.2883
61	0.14	1.3734		61	0.13	1.2883
62	0.15	1.4715		62	0.13	1.2883

Electronics and sensor design for an autonomous underwater vehicle

63	0.15	1.4715		63	0.14	1.3874
64	0.16	1.5696		64	0.15	1.4865
65	0.17	1.6677		65	0.16	1.5856
66	0.18	1.7658		66	0.16	1.5856
67	0.18	1.7658		67	0.17	1.6847
68	0.19	1.8639		68	0.17	1.6847
69	0.19	1.8639		69	0.18	1.7838
70	0.20	1.962		70	0.18	1.7838
71	0.20	1.962		71	0.19	1.8829
72	0.21	2.0601		72	0.19	1.8829
73	0.21	2.0601		73	0.20	1.982
74	0.22	2.1582		74	0.21	2.0811
75	0.23	2.2563		75	0.22	2.1802
76	0.24	2.3544		76	0.23	2.2793
77	0.24	2.3544		77	0.24	2.3784
78	0.25	2.4525		78	0.24	2.3784
79	0.25	2.4525		79	0.25	2.4775
80	0.25	2.4525		80	0.26	2.5766
81	0.26	2.5506		81	0.26	2.5766
82	0.27	2.6487		82	0.26	2.5766
83	0.28	2.7468		83	0.27	2.6757
84	0.31	3.0411		84	0.28	2.7748
85	0.32	3.1392		85	0.28	2.7748
86	0.33	3.2373		86	0.29	2.8739
87	0.35	3.4335		87	0.30	2.973
88	0.35	3.4335		88	0.31	3.0721
89	0.36	3.5316		89	0.32	3.1712
90	0.37	3.6297		90	0.32	3.1712
91	0.37	3.6297		91	0.33	3.2703
92	0.38	3.7278		92	0.33	3.2703
93	0.39	3.8259		93	0.34	3.3694
94	0.39	3.8259		94	0.35	3.4685
95	0.39	3.8259		95	0.35	3.4685
96	0.40	3.924		96	0.36	3.5676
97	0.40	3.924		97	0.36	3.5676
98	0.41	4.0221		98	0.37	3.6667
99	0.42	4.1202		99	0.37	3.6667
100	0.42	4.1202		100	0.37	3.6667

A.1.2 Heave Thruster Identification

Downward Direction

Upward Direction

Speed Value	Thrust F. (kg)	Thrust F. (N)		Speed Value	Thrust F. (kg)	Thrust F. (N)
1	0.00	0.00		1	0.00	0.00
2	0.00	0.00		2	0.00	0.00
...
65	0.00	0.00		65	0.00	0.00
66	0.00	0.00		66	0.00	0.00
67	0.00	0.00		67	0.00	0.00
68	0.08	0.78		68	0.00	0.00
69	0.08	0.78		69	0.02	0.20
70	0.09	0.88		70	0.02	0.20
71	0.10	0.98		71	0.02	0.20
72	0.10	0.98		72	0.02	0.20
73	0.12	1.18		73	0.03	0.29
74	0.12	1.18		74	0.03	0.29
75	0.14	1.37		75	0.03	0.29
76	0.14	1.37		76	0.03	0.29
77	0.15	1.47		77	0.04	0.39
78	0.17	1.67		78	0.04	0.39
79	0.18	1.77		79	0.05	0.49
80	0.19	1.86		80	0.05	0.49
81	0.21	2.06		81	0.05	0.49
82	0.23	2.26		82	0.05	0.49
83	0.25	2.45		83	0.06	0.59
84	0.27	2.65		84	0.06	0.59
85	0.28	2.75		85	0.06	0.59
86	0.30	2.94		86	0.06	0.59
87	0.32	3.14		87	0.07	0.69
88	0.33	3.24		88	0.07	0.69
89	0.35	3.43		89	0.07	0.69
90	0.36	3.53		90	0.07	0.69
91	0.38	3.73		91	0.08	0.78
92	0.41	4.02		92	0.08	0.78
93	0.43	4.22		93	0.08	0.78
94	0.44	4.32		94	0.09	0.88
95	0.46	4.51		95	0.09	0.88
96	0.48	4.71		96	0.09	0.88
97	0.49	4.81		97	0.10	0.98
98	0.51	5.00		98	0.10	0.98
99	0.53	5.20		99	0.11	1.08
100	0.54	5.30		100	0.11	1.08

A.1.3 Main Rudder Identification

Angle	Yaw Rate
0	0
5	5.6
10	7.3
15	9.8
20	12.7
25	18.6
30	20.2
35	22.5

A.1.4 Bow thruster Identification

Clockwise

Anticlockwise

Speed Value	Thrust F. (kg)	Thrust F. (N)		Speed Value	Thrust F. (kg)	Thrust F. (N)
0	0	0		0	0	0
100	0.04	0.39		100	0.04	0.39

A.2 Sensor Identification

This chapter includes all the testing results of the sensors.

A.2.1 PSD sensors

The PSD table include three different series of measurements.

PSD through hull

PSD trough hull clear water

PSD trough hull cloudy water

DistAir	V-Out	AD-Reading		DistWater	AD-Reading		DistDirtWater	AD-Reading
0	1.611	394		0	435		0	430
5	2.039	505		5	445		5	438
10	2.559	644		10	484		10	450
15	2.572	640		15	581		15	579
20	2.332	579		20	542		20	540
25	2.039	505		25	536		25	534
30	1.941	478		30	531		30	529
35	1.681	414		35	516		35	514
40	1.514	374		40	496		40	495
45	1.336	334		45	476		45	260
50	1.194	297		50	447		50	170
55	1.081	272		55	420		55	54
60	1.007	251		60	401		60	7
65	0.944	235		65	376		65	7
70	0.899	223		70	352		70	7
75	0.841	207		75	330		75	7
80	0.791	194		80	312		80	7
85	0.761	190		85	294		85	7
90	0.721	178		90	269		90	7
95	0.684	170		95	247		95	7
100	0.663	162		100	221		100	7
105	0.622	157		105	190		105	7
110	0.591	148		110	163		110	7
115	0.579	142		115	79		115	7
120	0.551	135		120	8		120	7
125	0.523	131		125	8		125	7
130	0.512	127		130	8		130	7
135	0.501	122		135	8		135	7
140	0.461	117		140	7		140	7
145	0.459	114		145	7		145	7
150	0.44	108		150	7		150	7
155	0.432	106		155	7			
160	0.412	104		160	7			
165	0.401	100		165	7			
170	0.391	97		170	7			
175	0.382	95		175	7			
180	0.362	91		180	7			
185	0.351	87		185	7			

Electronics and sensor design for an autonomous underwater vehicle

190	0.332	86		190	7			
195	0.331	82		195	7			
200	0.32	78		200	7			
205	0.319	76						
210	0.319	75						
215	0.316	74						
220	0.316	73						
225	0.307	72						
230	0.305	72						
235	0.289	71						
240	0.289	71						
245	0.285	70						
250	0.271	67						
255	0.251	65						
260	0.237	61						
265	0.23	59						
270	0.213	56						
275	0.207	54						
280	0.203	52						
285	0.186	45						
290	0.172	43						
295	0.165	40						
300	0.161	39						
305	0.159	38						
310	0.158	37						
315	0.153	34						
320	0.152	33						
325	0.152	32						
330	0.152	32						
335	0.152	32						
340	0.152	32						
345	0.15	32						
350	0.15	32						

A.2.2 Compass

These measurements include the tilt and the time drift measurement of the compass.

Tilt influence

Tilt X	Test 1	Test 2	Test 3		Tilt Y	Test 1	Test 2
0	50	140	260		0	50	142
1	49	142	261		1	42	141
2	48	142	259		2	44	141
3	48	141	259		3	43	141
4	47	141	259		4	44	146
5	46	142	259		5	46	145
6	47	141	259		6	46	145
7	47	140	260		7	47	144
8	46	139	260		8	46	145
9	47	137	257		9	46	144
10	49	135	259		10	45	143
11	47	136	257		11	47	146
12	45	134	259		12	46	145
13	44	135	258		13	49	145
14	43	133	257		14	51	145
15	42	132	257		15	50	146
16	43	134	258		16	48	144
17	41	132	257		17	47	145
18	40	130	262		18	44	145
19	39	130	259		19	45	146
20	40	128	257		20	42	144
21	39	128	260		21	44	143
22	39	125	259		22	43	145
23	38	124	257		23	42	146
24	38	124	258		24	44	147
25	37	123	259		25	46	148
26	37	123	257		26	42	147
27	38	124	258		27	38	147
28	38	124	257		28	35	148
29	39	122	256		29	32	148
30	39	119	257		30	28	150
31	39	119	255		31	27	151
32	37	118	257		32	24	152
33	38	117	259		33	19	153
34	37	116	257		34	14	152
35	38	115	256		35	11	151
36	37	112	254		36	3	152
37	36	108	249		37	359	151
38	38	104	251		38	355	152
39	37	99	252		39	353	151
40	38	100	248		40	350	152

Time drift measurement

Time (min)	Test 1	Test 2
0	15	271
5	17	269
10	16	272
15	11	268
20	15	271
25	14	269
30	11	271
35	17	272
40	16	270
45	15	271
50	13	268
55	16	272
60	14	269
65	11	268
70	15	270
75	14	272
80	16	272
85	13	269
90	14	272
95	14	270
100	16	270
105	15	269
110	13	270
115	17	272
120	15	269
125	14	271
130	15	270
135	11	272
140	13	270
145	13	268
150	14	272
155	16	273
160	15	270
165	16	271
170	13	272
175	15	272
180	14	270
185	16	271
190	15	269
195	16	272

Test 1	Test 2	Time (min)
200	14	270
205	13	272
210	14	269
215	13	170
220	15	272
225	14	271
230	17	269
235	13	268
240	15	272
245	13	268
250	17	270
255	15	272
260	13	269
265	14	268
270	17	272
275	15	270
280	13	271
285	17	272
290	14	269
295	15	268
300	14	271
305	17	268
310	15	270
315	15	271
320	13	269
325	17	268
330	14	270
335	15	272
340	13	269
345	15	271
350	17	270
355	14	269
360	15	271

A.2.3 Accelerometer

These measurements include the tilt and the time drift of the accelerometer.

Tilt drift

Angle	Test 1 (avg) X	Test 2 (avg) Y
0	0.01	0.01
1	0.05	0.02
2	0.07	0.02
3	0.08	0.01
4	0.09	0.02
5	0.12	0.02
6	0.13	0.01
7	0.14	0.02
8	0.14	0.02
9	0.17	0.01
10	0.21	0.02
11	0.22	0.02
12	0.23	0
13	0.24	0.02
14	0.25	0.02
15	0.26	-0.01
16	0.28	-0.01
17	0.29	0
18	0.31	0.01
19	0.34	0.02
20	0.37	0.02
21	0.38	0.02
22	0.39	0.01
23	0.41	0.02
24	0.44	0.02
25	0.45	0
26	0.47	0.02
27	0.47	0.02
28	0.48	0
29	0.51	0.01
30	0.55	0.01
31	0.56	-0.01
32	0.57	0.02
33	0.59	0
34	0.61	0.02
35	0.62	0
36	0.63	0.01
37	0.65	0.01
38	0.66	0.01
39	0.67	0
40	0.68	0.01

Time Drift

Time	Test (avg)
0	0.01
5	-0.01
10	0.01
15	0.01
20	0
25	0.01
30	0.01
35	0
40	0.01
45	0.01
50	0
55	0.01
60	-0.01
65	0.01
70	0
75	0.01
80	0.01
85	0.01
90	0
95	0.01
100	0.01
105	0.01
110	-0.01
115	0.01
120	0.01
125	0.01
130	0
135	0
140	0.01
145	0.01
150	0
155	0.01
160	0.01
165	0.01
170	0.01
175	0.01
180	0.01
185	0.01
190	0.01
195	0.01
200	0.01
205	0.01
210	0.01
215	0.01

Time	Test (avg)
220	0.01
225	0.01
230	0.01
235	0.01
240	0.01
245	0.01
250	0.01
255	0.01
260	0.01
265	0.01
270	0
275	0.01
280	0.01
285	0.01
290	0.01
295	0
300	0.01
305	0.01
310	0.01
315	0
320	0
325	0.01
330	0
335	0.01
340	0.01
345	0.01
350	0
355	0.01
360	0.01

A.2.4 Pressure Sensor

The pressure sensor tables include three different series of measurements.

Calibration with Syringe

Notch	Pressure	Sim Depth	Vout
0	101.30	0.00	0.87
1	102.65	0.14	1.01
2	104.04	0.28	1.08
3	105.47	0.43	1.20
4	106.94	0.58	1.28
5	108.45	0.73	1.37
6	110.00	0.89	1.47
7	111.59	1.05	1.56
8	113.24	1.22	1.63
9	114.93	1.39	1.72
10	116.67	1.57	1.85
11	118.47	1.75	1.97
12	120.33	1.94	2.04
13	122.24	2.14	2.16
14	124.22	2.34	2.27
15	126.26	2.55	2.36
16	128.36	2.76	2.48
17	130.54	2.98	2.60
18	132.80	3.21	2.71
19	135.13	3.45	2.80
20	137.55	3.70	2.95
21	140.06	3.95	3.05
22	142.66	4.22	3.18
23	145.35	4.50	3.32
24	148.16	4.78	3.42
25	151.07	5.08	3.53
26	154.10	5.39	3.68
27	157.25	5.71	3.79
28	160.53	6.04	3.88
29	163.96	6.39	4.03
30	167.53	6.76	4.16
31	171.26	7.14	4.37
32	175.16	7.54	4.52
33	179.25	7.95	4.67
34	183.53	8.39	4.83
35	188.02	8.85	4.90

Depth Calibration

Depth	Reading
0	221
50	227
100	234
150	241
200	248
250	259
300	271
350	293
400	301
450	324
500	351
550	368
600	378
650	402
700	437
750	469
800	486
850	499
900	513
950	529
1000	540
1050	556
1100	572
1150	589
1200	604
1250	614
1300	627
1350	640
1400	651
1450	663
1500	671

Hysteresis Measurement

Depth	Reading
150	242
200	248
250	259
300	270
250	259
200	248
150	241
200	249
150	241
200	248
250	259
200	249
150	241
200	248
250	259
200	248
150	241
200	248
250	259
200	249
150	241

A.3 Body Measurements

This chapter includes all the testing results concerning the vehicle body and its behaviour. Static behaviour as achieved velocity after dying out all dynamic oscillations during acceleration.

Vehicle Surge

Forward Direction

Backward Direction

Eyebot Speed Value	Thrust F. (N)	Speed		Eyebot Speed Value	Thrust F (N)	Speed
40	0.00	0.00		40	0.00	0.00
45	0.1962	0.05		45	0.00	0.00
50	0.3924	0.12		50	0.4955	0.04
55	0.981	0.17		55	0.991	0.08
60	1.3734	0.22		60	1.2883	0.11
65	1.6677	0.25		65	1.5856	0.14
70	1.962	0.29		70	1.7838	0.17
75	2.2563	0.33		75	2.1802	0.22
80	2.4525	0.42		80	2.5766	0.28
85	3.1392	0.54		85	2.7748	0.41
90	3.6297	0.62		90	3.1712	0.51
95	3.8259	0.76		95	3.4685	0.59
100	4.1202	0.9		100	3.6667	0.65

Main Rudder

Angle	Yaw Rate
0	0
5	5.6
10	7.3
15	9.8
20	12.7
25	18.6
30	20.2
35	22.5

B Technical Data

B.1 Main Controller

Type:	Eyebot MK4
Manufacturer:	Joker Robotics
Voltage requirement:	7 V - 9 V DC
Power consumption:	Eyebot controller only: 235 mA Eyebot controller with EyeCam CMOS camera: 270 mA
Size:	10.6 cm x 10.0 cm x 2.8 cm (width x height x depth)
Weight:	190 g

Main Features:

- 25MHz 32bit Controller (Motorola 68332)
- 2 MB RAM
- 512KB ROM (for system + user programs!)
- Motor drivers for 2 DC motors included in board (L293D)
- Background debugger BDM circuit included in board
- 16 timing processor I/Os (programmable as input or output)
- Single compact PCB, almost same size as old EyeBot
- Large graphics LCD (128x64 pixels)

In- and Outputs:

- 1 digital colour and greyscale camera input (allows real time on-board image processing)
- 1 parallel port
- 2 serial ports
- 8 digital inputs
- 8 digital outputs
- 8 analogue inputs
- 12 servos

Others:

- 4 input buttons
- Reset button, power switch
- Speaker for audio output
- Microphone for audio input
- Battery level indication

Limitations:

Total power limit is 3amps. A polyswitch protects the board, however, high voltage or reverse polarity may damage the board
Total servo current must not exceed 3 A
DC motor current must not exceed 1 A each
Unregulated controller input voltage is supplied to motors
Encoder feedback must not exceed 5 V

B.2 Energy System

B.2.1 Battery

Type:	Lead battery Xinshun 6-FM-7
Manufacturer:	Xinshun
Voltage:	12 V
Current:	7 Ah
Volume:	95x61x150 mm
Weight:	2,24 kgs

B.2.2 Switching Voltage Regulator

Type:	LM2576 ADJ
Manufacturer:	National Semiconductors

The LM2576 series of regulators are monolithic integrated circuits that provide all the active functions for a step-down (buck) switching regulator, capable of driving 3A load with excellent line and load regulation. These devices are available in fixed output voltages of 3.3V, 5V, 12V, 15V, and an adjustable output version. Requiring a minimum number of external components, these regulators are simple to use and include internal frequency compensation and a fixed-frequency oscillator.

The LM2576 series offers a high-efficiency replacement for popular three-terminal linear regulators. It substantially reduces the size of the heat sink, and in some cases no heat sink is required. A standard series of inductors optimised for use with the LM2576 are available from several different manufacturers. This feature greatly simplifies the design of switch-mode power supplies.

Other features include a guaranteed $\pm 4\%$ tolerance on output voltage within specified input voltages and output load conditions, and $\pm 10\%$ on the oscillator frequency. External shutdown is included, featuring 50 μ A (typical) standby current. The output switch includes cycle-by-cycle current limiting, as well as thermal shutdown for full protection under fault conditions.

B.2.3 Battery Gauge

Type:	LM2576 ADJ
Manufacturer:	National Semiconductors
Supply Voltage:	max 25V
Max Voltage on Output Drivers	25V
Max Input Signal Voltage	(Note 4) $\pm 35V$
Divider Voltage:	-100 mV to V+
Reference Load Current:	10 mA

Functional Description:

The simplified LM3914 block diagram is to give the general idea of the circuit's operation. A high input impedance buffer operates with signals from ground to 12V, and is protected against reverse and over-voltage signals. The signal is then applied to a series of 10 comparators; each of which is biased to a different comparison level by the resistor string.

In the example illustrated, the resistor string is connected to the internal 1.25V reference voltage. In this case, for each 125mV that the input signal increases, a comparator will switch on another indicating LED. This resistor divider can be connected between any 2 voltages, providing that they are 1.5V below V+ and no less than V-. If an expanded scale meter display is desired, the total divider voltage can be as little as 200mV. Expanded-scale meter displays are more accurate and the segments light uniformly only if bar mode is used. At 50mV or more per step, dot mode is usable.

B.2.4 Battery Charger

Type:	Battery Fighter Junior
Manufacturer:	Asia Bright Industrial Co., Ltd.
Distributor:	Master Instruments Pty Ltd
Input Voltage:	230 – 240 V AC
Nominal Output Voltage:	12 V DC
Nominal Output Current:	0.75 Ah
Maximal Output Voltage:	14.4 V DC
Maximal Output Current:	0.75 Ah
Float Voltage:	13.2 V DC
Features:	Short Circuit Protection, Reverse Polarity Protection, Spark Proof
Volume:	58x50x83 mm
Weight:	0.45 kgs

B.3 Actuators

B.3.1 Stern Motor Thruster

Type:	12 Volt Brushed Motor Johnson HC970
Manufacturer:	Son Kong
Distributor:	Johnson
Power requirement:	12 Volt DC
Max. RPM:	5000 t/min
Max. Thrust:	4.12 N forward / 3.67 N backward
No Load Current:	0.7 amp
Max Current:	3.8 amp
Size: (L x Ø):	75 x 50 Ø mm
Weight of Motor:	0.6 kgs

B.3.2 Heave Motor Thruster

Type:	12 Volt Brushed Boat Motor
Manufacturer:	Springstar Co. Ltd. Taiwan
Importer:	Sevyor U.S.A. Inc
Power requirement:	12 Volt DC
Max Thrust in AUV:	5.30 N forward / 1.08 N backward
No Load Current:	0.9 amp
Low Speed Current:	5.8 amp
Weight of Motor:	1.6 kgs
Low Speed RPM:	3.390
High Speed RPM:	3.580
Low Speed Thrust:	5lbs (2.268kg; 22.2N)
High Speed Thrust:	13lbs (5.90kg; 57.8N)
No Load Current Draw:	0.9AMP
Full Load Low Speed:	5.8AMP
Full Load High Speed:	12.5AMP

B.3.3 Main Rudder Servo

Type:	High Torque Servo HS 645 MG
Manufacturer:	HiTec
Power requirement:	4.8-7.2 Volt DC
Max Current:	2.4 amps
Features:	Dual Ball Bearings, Metal Gears
Torque (6V):	3.5kg/cm
Transit Speed:	0.14 sec/60°
Size (L x W x H):	29 x 13 x 30mm
Weight:	19.2g

B.3.4 Bow thruster Pump

Type:	12 Volt Gear Pump Graupner 1951
Manufacturer:	Graupner
Power requirement:	12 Volt DC
No Load Current:	0.8 amps
Max Current:	2.8 amps
Flow rate:	1200 ml/min
Size (L x Ø):	58 x 32 Ø mm
Weight:	85 g

B.3.5 Camera Servo

Type:	Mini Servo HS-85BB MIGHTY MICRO
Manufacturer:	HiTec
Power requirement:	4.8-7.2 Volt DC
Max Current:	0.9 amps
Torque (6V):	3.5kg/cm
Transit Speed:	0.14 sec/60°
Size (L x W x H):	29 x 13 x 30mm
Weight:	19.2g

B.4 Sensors

B.4.1 PSD

Type:	GP2Y0A02YK
Manufacturer:	Sharp
Power requirement:	4.8-7.2 Volt DC
Range:	20-150cm
Output:	Analogue
Size (L x W x H):	29 x 13 x 30mm
Weight:	19.2g

B.4.2 Compass

Type:	Vector 2XG
Manufacturer:	Precision Navigation, Inc.
Power requirement:	5-volt (regulated) supply
Accuracy:	2°
Low resolution output:	5 Hz
High resolution output:	2.5Hz
Input voltage on all I/O ports:	-0.3 to VDD +0.3 volts
Output voltage on all I/O ports:	-0.3 to VDD +0.3 volts
Output ports can source or sink	5mA
Features:	Hard iron calibration, Polled or continuous mode Master or slave capability for data clock generation
Operating temperature range:	-20°C to 70°C
Size (L x W x H):	29 x 13 x 30mm 1.50" x 1.30" x 0.39"; 0.3oz
Weight:	19.2g

B.4.3 Accelerometer

Type:	Sparkfun V5
Manufacturer:	Freescale
Power requirement:	Generates Power from RS232 Interface
Current:	Measuring Consumption: 500 μ A Sleep Mode: 3 μ A
Range:	$\pm 1.5g - 6g$ Three Axis Low-g (Range Select)
Accuracy:	High Sensitivity (800 mV/g @1.5 g)
Features:	1-pole low pass filter, temperature compensation, Sleep Mode, Robust Design, High Shocks Survivability
Size (L x W x H):	6mm x 6mm x 1.45mm
Weight:	32.6g

B.4.4 Pressure Sensor

Type:	Sensym SX15AD2 (absolute gage device)
Manufacturer:	Honeywell
Operating Pressure:	0-15 psi
Operating temperature:	-40 C - +85 C
Features:	high impedance bridge
Size (L x W x H):	6mm x 6mm x 1.45mm
Weight:	32.6g
Amp Power requirement:	12 V DC
Amp Range:	0-10 meter (adjustable)
Amp Features:	voltage regulation, temperature compensation

B.4.5 Camera

Type:	CMOS VGA Colour Digital Camera OV 7620
Power Supply	5VDC, $\pm 5\%$
Power Requirements	<120mW Active, <10uW Standby
Array Elements:	664 x 492
Pixel Size:	7.6 x 7.6 μ m
Image Area:	4.86 x 3.64mm
Electronic Exposure	500 : 1
Scan Mode	progressive interlace
Minimum Illumination	2.5 lux @ f1.4 0.5 lux @ f1.4 (3000K)
S/N Ratio	> 48dB
Size (L x W x H):	30 x 20 x 45mm
Weight:	25 g

B.5 Communication Device

Type: Promi-SD101/102
Power Supply: 5VDC, $\pm 5\%$
Output Power: Class 2 / 2.5mW (4dBm)
Range: ~30m (Promi-SD101/102)
Baud rate: 1200~115200 bps
Features: Hardware flow control (RTS/CTS)
Bluetooth protocols: RFCOMM, L2CAP, SDP
Supported Profiles: Serial Port Profile

Current Consumption: If NOT connected to Host: 3.5 mA
 If connected to Host: 13.5 mA
 For data communications w/ Host only: 26.5 mA
 During INQUIRY mode: 62 mA
 For Master connection: 63 mA
 During SCAN (page & inquiry) mode: 27 mA
 Park mode: 13.8 mA
 Non-Park mode: 17.8 mA

Operating conditions: -10°C~70°C
Humidity: 90% Non-condensing
Dimensions: 60 x 26 x 16 (mm)
Weight:

C The Original ROV

Manufacturer: Sherwood Overseas Ltd.

This information is based on [<http://www.neiparts.net/rov/>].

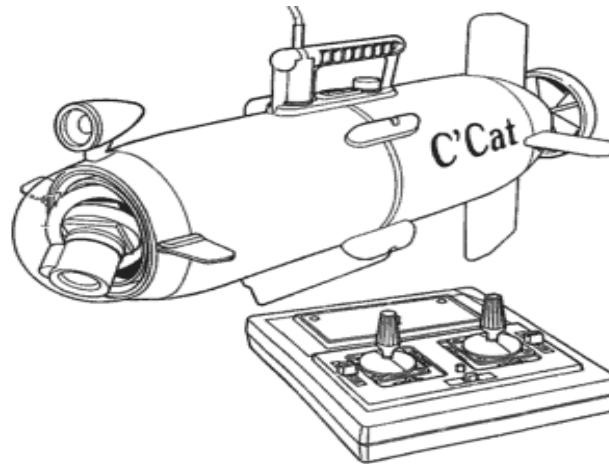


Figure C.1: The USAL C'Cat

C.1 Vehicle

Five sections: coloured injection moulded plastic.

Length: 700mm (2.29 ft)

Diameter: 150mm (6 in)

Weight: 10.5kg (23.1 lb)

Umbilical Length: 50m (165 ft)

Crush Depth: 90m (303 ft)

C.2 Body Hull

Constructed from polycarbonate-based plastic with excellent impact strength, dimensional stability and mechanical performance. Further additives ensure chemical resistance and protection from ultra-violet light degradation. Front hemispherical viewing dome moulded in clear polycarbonate. Transparent cover called the contact lens, provided for additional protection. The two fore planes are for vehicle protection and improved stability and are designed to be a snap fit. In the event of a collision the fore planes will protect the velure and may dislodge. Under no circumstances should the fore planes be glued or permanently fixed to the vehicle as this may cause damage to the nose dome assembly. Four extra fore planes are supplied in the event of loss.

C.3 Umbilical Cable

The Cable is detachable from vehicle and control module. Cable fitted with one waterproof connector.

Length 50m (165ft): Coaxial cable and incorporating strength members.

Breaking strain in excess of ten times vehicle weight. Specific Gravity/Density 1.02

Breaking Stain: 100kg (220lb)

C.4 Power Supply

On-Board Power: NiCad batteries. (SAFT VR 10) 10 x 1.2V = 12V at 10Ah Batteries removable by manufacturer only.

The batteries are rechargeable via umbilical cable connector and banana plug under vehicle handle.

Duration: Approx. 2.5hrs without lights

 Approx 1hr using lights

C.5 Charger

Recharges C'Cat 12V 10Ah NiCad batteries and the control module 9.6V 0.5Ah batteries from nominal 120V 60Hz supply or nominal 240V 50Hz supply.

Dependent upon customer selection of SAA or t.FL version.

NOTE: Overcharge prevention is incorporated in C'Cat and control box and does not form part of the charger.

Control Module

8 x 1.2V = 9.6V at 0.5Ah NiCad batteries, rechargeable through rear of module.

Duration: Approx. 3hrs.

C.6 Camera

The camera is equipped with an auto iris and a manufacturer interchangeable lens. Standard lens: 6mm wide angle F1.4.

The on-board vehicle camera is a colour sensitive Charge Coupled Device (CCD) able to withstand shock, impact and vibration.

Light sensitivity: 10 lux.

Horizontal resolution: 250 lines for NTSC system and 280 lines for PAL system.

Remote pan and tilt operation, also remote white balance correction.

Voltage input 9.9 to 14.4V dc. Refer Sherwood Overseas Co. Pty Ltd approved specifications for National Camera Model WV- CDIIIO/SP for NTSC system and Model WV-CDIIIO/SE for the PAL system.

C.7 Control Module

Lightweight, multi-function, injection moulded plastic base incorporating:

1. Joystick control for operating fins.
2. Joystick control for camera pan and proportional forward/reverse speed controller.
3. Slide control for camera tilt.
4. Light on/off and intensity controlled from surface by slide control.
5. Remote control camera white balance by rotary pre- set panel control.
6. Light on control module panel indicates control module POWER ON.
7. Light on control module panel indicates underwater light ON or OFF.
8. Fine video balance rotary control.
9. Light ON / OFF switch located on top of left hand joystick.

D The Competition

This chapter spotlights the AUV Competition for real and simulated AUVs presented by the University of Western Australia.

D.1 Restrictions

There are no restrictions at this stage.

D.2 Mission Tasks

Task 1: Wall Following

The AUV is placed close to a corner of the pool. The task is to follow the pool wall without touching it. The AUV should perform one lap around the pool, return to the starting position, then stop.

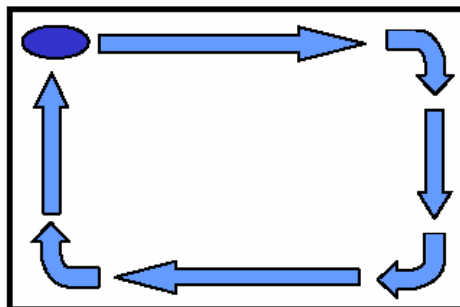


Figure E.1: Wall Following

Task 2: Pipeline Following

A plastic pipe (diameter and colour to be specified) is placed along the bottom of the pool, starting on one side of the pool and terminating on the opposite side. The pipe is made out of straight pieces and angle pieces. The AUV is placed over the beginning of the pipe close to a side-wall of the pool.

The task is to follow the pipe on the ground until the opposite wall has been reached.

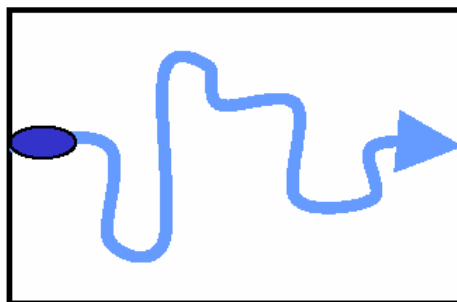


Figure E.2: Pipeline Following

Task 3: Target Finding

The AUV is placed close to a corner of the pool. A target plate with a distinctive checkerboard texture (size and color to be specified) will be placed at a random position within a 3m diameter from the center of the pool.

The task is to find the target plate in the pool, drive the AUV directly over it and drop an object on it from the AUV's payload container. (AUV's without the ability to drop a payload should just hover over the target plate).

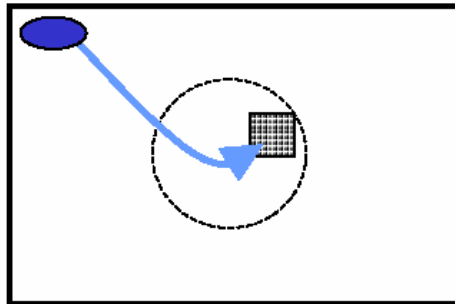


Figure E.3: Target Finding

Task 4: Object Mapping

A number of simple objects (balls and boxes, color and sizes to be specified) will be placed near the bottom of the pool, distributed over the whole pool area. The AUV starts in a corner of the pool.

The task is to survey the whole pool area, e.g. using a sweeping pattern, and record all objects found at the bottom of the pool. The AUV shall return to its start corner and stop there. In a subsequent data upload (AUV may be taken out of the pool and a cable attached to its onboard system), a map of some format should be uploaded that shows location and type (ball or box) of all objects found by the AUV.

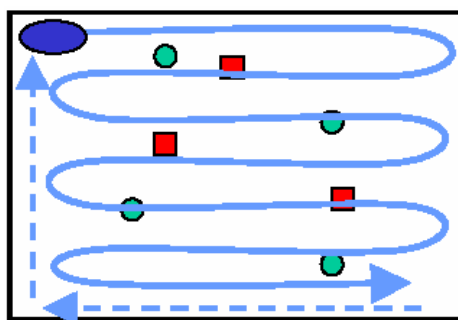


Figure E.4: Object Mapping

E User Instructions

USAL – AUV

THE YELLOW SUBMARINE

USER INSTRUCTIONS

BY
MICHAEL DRTIL
DRTIL@IEEE.COM

PLEASE READ CAREFUL ALL USER INSTRUCTIONS BEFORE USE
RISK OF LIFE!

Table of Contents

1	INTRODUCTION.....	3
2	LOCATION OVERVIEW	4
3	BASIC INFORMATION.....	6
3.1	DISASSEMBLING THE AUV	6
3.2	ASSEMBLING THE AUV	6
3.3	ACTIVATE/ DEACTIVATE/ PROGRAM THE AUV	7
4	PREPARATIONS FOR USAGE.....	8
4.1	IMPORTANT INFORMATION	8
4.2	CHECKLIST BEFORE USAGE	8
4.3	CHECKLIST AFTER USAGE	8
5	RECHARGE	9
6	COMMUNICATION.....	10
6.1	EYEBOT DISPLAY	10
6.2	INFRARED REMOTE CONTROL.....	10
6.3	BLUETOOTH.....	11
7	TROUBLESHOOTING	14
7.1	GENERAL AUV.....	14
7.2	THE EYEBOT CONTROLLER.....	15
7.3	BLUETOOTH CONNECTION	17
8	TECHNICAL DATA	18

PLEASE READ CAREFUL ALL USER INSTRUCTIONS BEFORE USE

RISK OF LIFE!

1 Introduction

The USAL-AUV is a small high transportable and high performance autonomous underwater vehicle, constructed to participate in AUV competitions and to provide a basement for future research.

For saving money purposes it is based on a former ROV (remote operated vehicle), which was given to the University for free. After modifications navigation and map building from the gain of the sensor suite as well as motion control with the help of actuators controlled by onboard controller make the vehicle able to perform mission tasks autonomous.

The yellow USAL-AUV is the second AUV constructed in the Mobile Robotics Lab. The first one is much more bigger and a massive construction. Easy transport to other locations becomes pedestrian and expensive.

The AUV is equipped with two thrusters, one for movement in x-direction and one for movement in z-direction. A rudder blade in the stern (back) provides yaw movement when the AUV is travelling. An independent small bow rudder is also integrated for providing yaw movement in small operation areas.

The AUV is controlled by a powerful embedded controller system called Eyebot. This Controller running on 35 MHz has a 2 MB Memory and is equipped with all necessary interfaces especially an interface for a colour camera.

A huge sensor suite for mission and navigation tasks was integrated into the design. It contains range measurement front, sides and downwards, a compass, a 3-axis accelerometer and a depth sensor.

An inside water sensor prevents the AUV from damage in the case of leakage. Communication is provided via Bluetooth for up- and downloading data and basic instructions can be send by Infrared Remote Control.

2 Location overview

This chapter gives an overview of the locations of different sensors, actuators and devices. All sensors are located in the bow hull; all motor drivers are located in the stern hull. The electronics are mounted on a metal rack, which can be detached from the bow hull for maintenance purposes. Figure 2.1 shows a view from the outside.

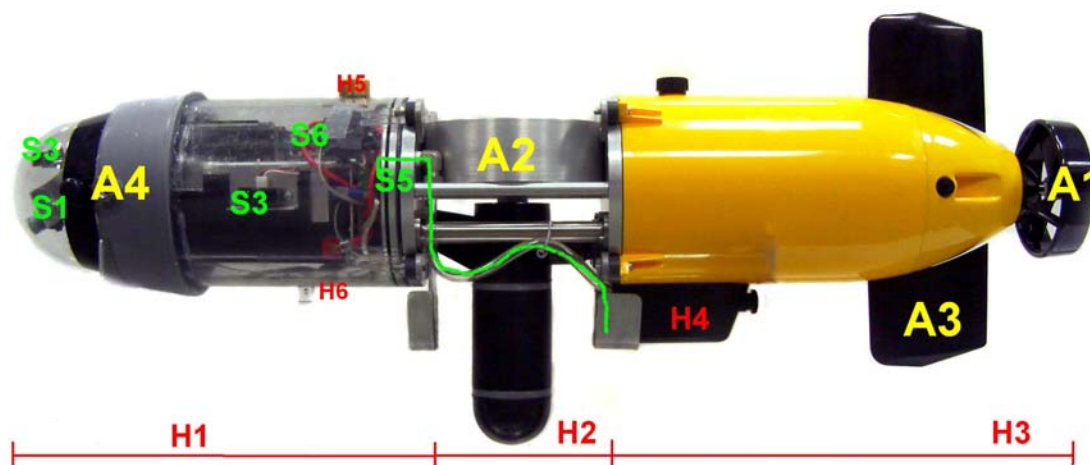


Figure 0.1: Parts located outside

Actuators

- A1) Stern Thruster
- A2) Heave Thruster
- A3) Main Yaw Rudder
- A4) Small Bow Rudder System

Sensors

- S1) Colour Camera
- S2) Compass
- S3) PSD-Sensor
- S4) Accelerometer
- S5) Pressure Sensor
- S6) Battery Gauge

Parts of the Hull

- H1) Bow Hull
- H2) Middle Thruster
- H3) Stern Hull
- H4) Lead Weight Rack
- H5) Recharge Unit
- H6) On/Off Switch

Figure 2.2 shows the electronic rack detached from the bow hull. Nearly all sensors except the depth sensor are installed together with the controller on this rack, which sits on the battery.

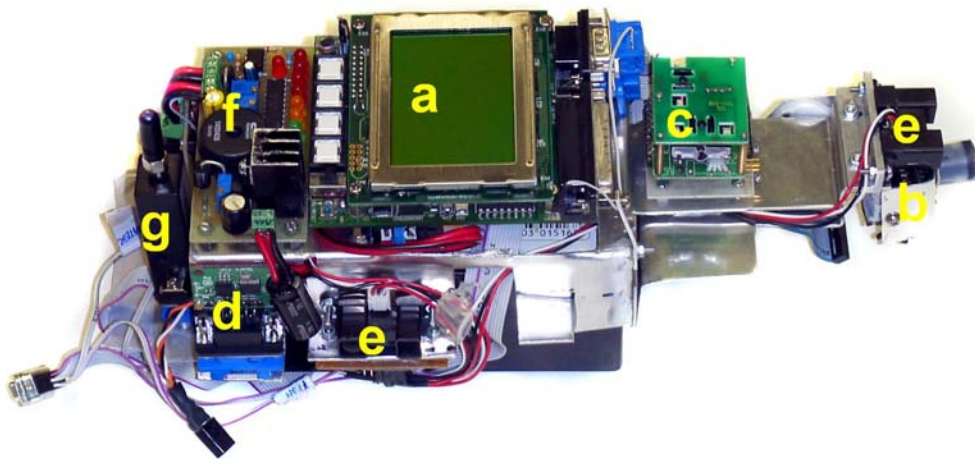


Figure 0.2: Electronic rack

- Eyebot
- Camera
- Compass
- Accelerometer
- PSD-Sensor
- Battery Gauge and DC/DC Converter
- Bluetooth

3 Basic Information

3.1 Disassembling the AUV

Make sure, that the AUV is switched off. To disassemble the AUV it has to lie down on the side. Detach the weight-rack by unscrewing the black screw and by pulling it on the screw side down.

Then start unscrewing the hull screws on the top of laying side. After that turn the AUV carefully on the other side. Then unscrew the screws on this side.

After unscrewing, detach the stern hull from the heave thruster unit. If it won't move, try turning it a bit. Make sure to disconnect the servo, stern motor and water sensor after detaching. Then unconnect the bow rudder motor from the driver board.

After this, the bow hull can be detached as well. Unconnect the stern power, data connector and finally the battery.

The rack can now be detached from the bow hull after disconnecting the water sensor from the bottom, simply by holding it down a pull it a bit.

3.2 Assembling the AUV

First insert the electronics rack careful into the bow hull. Make sure, that the bow pump power cable is routed till the back. Connect battery, motor-driver, signal-cable and get the cable from the bow pump trough the power-pipe of the heave thruster. Check proper fit of the depth sensor pressure-hose.

Attach bow hull to the heave unit and press together until the outer o-ring contact everywhere with the hull. Now tighten the four screws. The screw-threats are not designed to press the hull to the o-ring; this must be done by hand. They are only for locking.

Connect electric cables of stern-thruster, bow-pump, rudder-servo and water-sensor to the motor-board. Then attach stern hull to the heave unit and tighten the screws. Attaching the hull is the same process as the bow hull. Please do not use the screws to do the last centimetres.

Put the AUV on its rack and attach the weight rack to it.

3.3 Activate/ Deactivate/ Program the AUV

The AUV can be easily activated by removing the magnet from the switch area.

There is a short delay until the controller starts.

The Eyebot is then in the root menu and ready for downloading, loading and running of programs. Easiest way through these menus is normally the IR remote control. The four coloured keys accord to the four keys on the Eyebot. Attaching the magnet back to the switch area deactivates the system.

Note: Please never deactivate the AUV in the water.

Holding the magnet shortly to the switch area can do a short reset.

To upload a program, connect the host-computer via Bluetooth to the AUV. Refer chapter 6 for further information.

4 Preparations for usage

Important information

The AUVs thrusters are not intended for use outside water due to its design. Please do not use them outside pool. This will cause damage to the sealing.

Connecting to the AUV Bluetooth system is only possible when the AUV is on the surface or not in water.

Please consider the movement in the wrong direction of the main rudder for turning.

Avoid hitting walls or obstacles.

Always use the correct lubrication for the O-rings. Wrong lubrication can cause damage to the o-rings. Water leakage will be the result.

If the AUV gives a water leakage error, switch it off immediately and open hull to control the systems.

Checklist before usage

Check hull for damage.

Check connections between hulls and heave thruster for proper fit.

Check screws.

Check hose of depth-sensor.

Check battery.

Check controller.

Checklist after usage

Rinse the AUV well. Chlorine or salt-water causes heavy corrosion.

Dry the AUV.

Check hull for damage

Download data

Recharge battery

5 Recharge

For recharging the AUV the Battery Fighter Recharging Unit is necessary. Figure 5.1 shows the recharger.



Figure 0.1: AUV recharger

Important Notes:

Please recharge to AUV only out of water, never in water or inside the pool!!

Make sure, that the AUV is dry, when connecting cables!

Always make sure, that the mains cannot get on contact with water!!

To recharge

Put the AUV on a proper stand or holding

Switch the AUV off with the magnet.

Connect the (-) Pole of the recharger with the metal middle part.

Connect the (+) Pole of the recharger with the top metal nose.

Connect the recharger with the mains.

A red light on the recharger indicates the recharging process.

When the light is green, the battery is fully loaded and prepared for use.

Please unconnect the recharger and the pole-cables.

6 Communication

The AUV is equipped with 3 communication devices.

- Eyebot Display (one-way)
- Infrared Remote Control (one way)
- Bluetooth (two-way)

6.1 Eyebot Display

The easiest way to check the status of the controller is to look through the transparent hull on the display. The graphical 128 * 64 pixels show permanently the status of the controller or the outputs given by the programs.

Please note: Reading the display becomes impossible when AUV dived or is far away.

6.2 Infrared Remote Control

It is possible to control basic operations with a remote control. The system is setup to be used with a NOKIA Remote Control. When the programs support more keys more functions become available. The four coloured buttons on the Nokia Remote Control accord to the four buttons on the Eyebot.

There is no Setup necessary to use this Control due to its implementation in the hardware description table on the controller.

Please note: This control is only available onshore, on the surface and down to 0.5 m depth depending on water visibility.



Figure 0.1: Nokia IR Remote

6.3 Bluetooth

The USAL-AUV Communication System provides:

- Initialising the System
- Upload of Programs to the Eyebot
- Download of Data from the Eyebot
- Sending Commands for Testing
- Receiving Information for Testing

The USAL-AUV uses a Serial to Bluetooth-Stick, attached to serial port COM2 to communicate with the Host Computer when surfaced. The Intinium Promi-SD™ 102 Bluetooth System is developed for long range, easy-to-install low-cost wireless serial communications. Provided is point-to-point wireless connection without standard RS232 cables.

It is a Class 2 Device with an Output Power: 2.5mW (4dBm) provided with variable baud rate up to 115200 baud, with automatic detection of hardware flow control and DTR/DSR for loop-back & full transfer.

The AUV was tested with a Nokia Phone 6260 with software to contact the Eyebot and to represent its display.

But this is more a simple remote function. It's more interesting to connect the AUV with a computer. That gives the possibility to upload programs, download data, write own powerful control programs, see the video picture and as well do the basic Eyebot control.

If you are using your own Bluetooth device you have to install the Eyebot software package on your computer and the hardware driver for your Bluetooth device. Please refer your documentation how to connect to a Bluetooth device and how to use its services.

The following section deals with the multi serial port (MSPP) and the IVT BlueSoleil software, which is available in the Mobile Robots Lab and installed on most computers there. This section is mainly adapted from the Eyebot Bluetooth manual [Schmitz, 2004] and gives a quick step-by-step guide how to run the Eye-Net. This guide assumes, that the software is installed. Refer to the MSPP manual to see how to install it.

1. Connect the multi serial port to the USB port of your PC.
2. Run the IVT BlueSoleil software.
3. Double click on the red sun. The available Bluetooth devices will appear.
4. Double click on a HandyPort symbol. The MSPP checks the available services for this device. After a short while the serial cable symbol should turn purple.
5. Double click the purple serial cable symbol. A connection to the highlighted HandyPort should be established. A pop-up window shows you the appropriate COM port.
6. Run the RemoteUI program.
7. Tick the COM port boxes to which the HandyPort(s) is connected.
8. Press the 'Start/Refresh' button.
9. The EyeBots should authenticate by transmitting their IDs, which are displayed next to the COM tick box.
10. Run your EyeBot program that might use the RADIO functions or use the remote functions.
11. On authentication an 'EyeConsole' symbol appears. Click on the symbol to show the EyeConsole.

The Eyebot controller comes with the RemoteUI software. Figure 6.2 shows the graphical user interface of the program.

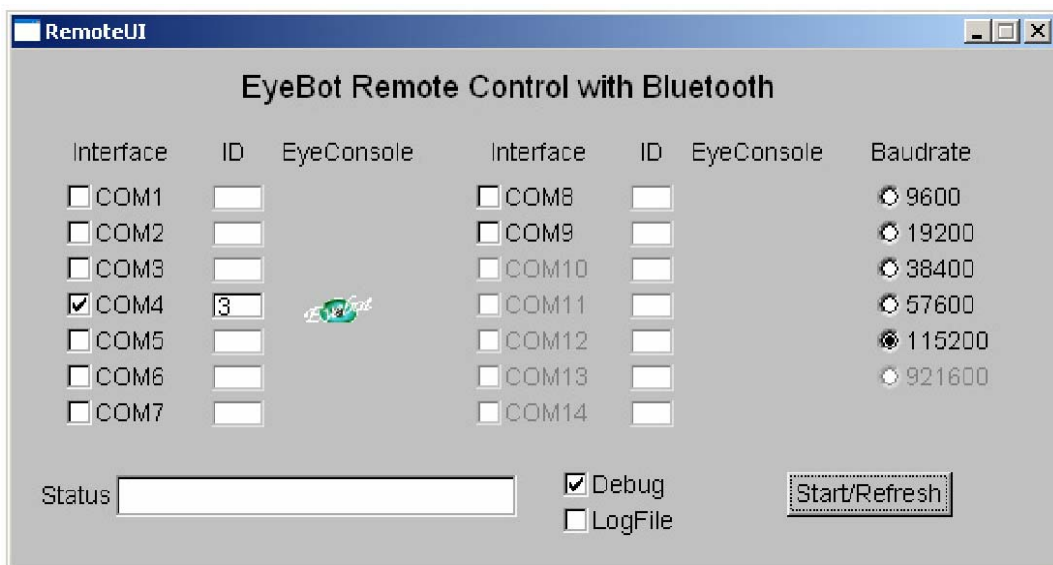


Figure 0.2: RemoteUI [Schmitz, 2004]

After the HandyPorts are connected to the MSPP, tick the right COM port boxes.

1. Press the 'Start/Refresh' button.
2. You can now either run your program on the EyeBot, that uses the RADIO functions, or enable the remote function.
3. The EyeBot will authenticate and its ID will appear beside the COM port tick box.
4. A small EyeConsole icon will also appear in the same row. Use this icon to view the EyeConsole. The EyeConsole, shown in Figure 8, shows you the current display of the real EyeBot. Through the buttons of the EyeConsole you have full control of your EyeBots.

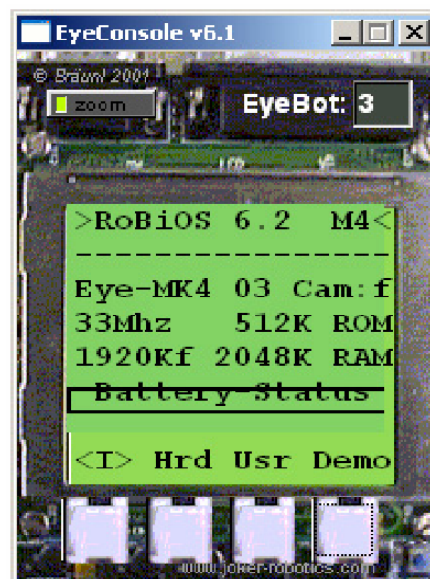


Figure 0.3: Eyebot Control Window [Schmitz, 2004]

To view the traffic through the MSPP, tick the 'Debug' tick box. All incoming messages will be displayed in a console window (NOTE: only the first 10 bytes of the whole message are displayed).

Choose the 'Logfile' box to create a file called 'logfile.txt'. All incoming messages will be listed there (NOTE: every byte will be written to the file)

7 Troubleshooting

This chapter deals with problems, which can occur when working with the AUV especially with the onboard controller and offers solutions.

7.1 General AUV

AUV shows no function reaction.

Battery empty. Recharge battery.

No light on the recharger when trying to recharge.

Recharger not connected to battery. Check recharger cables, switch AUV to recharge mode and check battery fuse.

Controller did not react on Remote Control.

Batteries of remote Control are empty or AUV too deep or out of range.

Water inside hull.

Check hull for breaches. Replace O-rings on the heave thruster unit. Make sure that lubrication is ok. Check the pressure hose of the depth sensor.

AUV is not level in the water.

Do a fine-trimming with the lead-weight in the lower rack.

7.2 The Eyebot Controller

This text is adapted from the Eyebot online documentary [Braeunl, 2005]. It provides help for the most cases of problems with the Eyebot.

Accidentally erasing the EyeBot's Flash-ROM.

The RoBiOS (Robot Basic Input/Output system) on the EyeBot is stored in flash memory and can therefore be upgraded using software. The hardware description table (HDT) is also stored in the same flash memory. RoBiOS makes it possible to download new HDTs and even new versions of RoBiOS, just like you download a user program, over a serial cable.

In the rare case that RoBiOS gets corrupt, for example if a corrupt version of RoBiOS is downloaded, the controller cannot boot, so you cannot fix it by just download a new working version of RoBiOS.

In this case, you have to use the Background Debugger Module (BDM). A socket on the Eyebot marked "BDM" needs to be connected with the supplied cable to the parallel port of a PC. Besides re-writing the Flash-ROM, this connection can be used to debug/single-step a program on the Eyebot from a PC.

Please note: the supplied cable (MK3 and later) does not contain circuitry like the "standard Motorola BDM cable". This is not needed, since the circuitry is already included on the EyeBot controller itself.

Re-installing RoBiOS using the BDM also wipes out any installed radio license code. If this happens to you, you need to email your distributor with the controller's serial number to obtain a new radio key. This can be installed by pressing <I> / REG.

EyeBot does not boot at power on or reset.

Does the display show a horizontal line when pressing reset?

If so, you probably accidentally erased the RoBios operating system from the flash-ROM. Look at section 'Debug' on how to reinstall RoBios using the background debugger. Does the display not show anything at all?

In that case, you may have blown the controller's fuse, either by connecting power with wrong polarity or by a too high current (e.g. short circuit). Use a multimeter to check whether any current is flowing when you switch on the EyeBot. If current is flowing, try to re-install RoBios via the background debugger as discussed above.

EyeBot serial connection to PC does not work.

Trance (Windows) or Terraterm does not detect the controller.

Windows: use tool transhx32.exe. In PC Bios the serial port addresses may be specified as "to be automatically assigned". Change this to stationary and standard address.

Set EyeBot CPU frequency to 33MHz, because this causes the least speed discrepancy. See baudrate-note.

Make sure serial cable is connected correctly on EyeBot and serial port COM1 on the PC (or any other port if you change the standard scripts).

Make sure the Baud rate on the EyeBot and on the PC match (EyeBot standard is 115,200 Baud - some older PC cannot go that fast).

See section Download on how to change serial settings on the EyeBot.

If problem persists, try using a different host PC.

EyeBot wireless communication demo does not work.

Make sure the optional wireless communication module is inserted. Press menu item "< | >" from the main menu on the EyeBot then press "REG".

This will display the "Register Radio" screen. You need to send (email) the serial number displayed on the LCD to your distributor, who will supply you with the security key to enter. After this procedure, the wireless communication functions are enabled.

7.3 Bluetooth Connection

What is the PIN-Code?

The PIN-code is: 0000

When do I need the PIN-Key?

The PIN-Key is necessary for the pairing process. When connecting the Bluetooth stick to a computer or other Bluetooth device the PIN-Key will be requested.

What is the range of Bluetooth in water?

The range in water is only a few centimetres.

What are the states of the USB-Stick?

The Promi-SD™ STATUS LED indicates the following:

Amber STATUS LED indicates standard mode on Promi-SD™ power-up.

Green STATUS LED indicates Promi-SD™ is connected to another Bluetooth device

Green flashing STATUS LED every second indicates Promi-SD™ INQUIRY Operation

Green flashing STATUS LED every 3 seconds indicates Promi-SD™ INQUIRY SCAN or PAGE SCAN operation

The devices are connected, but transmission not possible

The HandyPort and the serial port do not have the same settings or HandyPort and the chosen baud rate of the RemoteUI program do not match. The chosen COM port in the RemoteUI and the COM port to which the HandyPort is connected, do not match.

Message: 'Error while initialising COM'

The chosen COM port is not registered with the operation system. Make sure that the COM port is available under the operation system.

8 Technical Data

This chapter presents selected a short overview of basic technical data of the AUV. Please refer Thesis “Electronic and sensor design for an autonomous underwater vehicle” for further information.

Size	865mm length with a diameter of 150mm
Weight	14.08kg
Buoyant force	3.34N
Operation area	swimming pool (static water)
Maximum speed	0.9m/s
Maximum depth	15m
Working time	avg 1.5 hrs
Recharging duration	max 14hrs
Maximum range IR control	7m
Maximum range Bluetooth	20m

F Alternative solutions

This chapter presents an alternative solution for a buoyancy control system that would suit very well in the AUV and are recommended in future work.

The following section describes two kits for buoyancy control of model submarines. The Engel Diving Systems are based on an operational principle that has already existed since 1850. It enables model U-boats (submarines) to use the static diving method up to a depth of 10 metres. The pump mechanism and the ballast tank form a compact unit, the so-called piston tank, often also simply referred to as ballast tank.

A piston tank consists of a cylinder, a piston, a piston rod with thread, a motor with gears, levers as well as multiple end switches. By adjusting the piston in the cylinder, the water is sucked in or discharged, whereby the electric drive allows for a sensitive metering of the water quantity (filling volume).

There are several sized available. The relatively sizable volume of each piston tank causes a high level of buoyancy which, among other things, offers the advantage of a model being able to, for example, tear itself away with its own strength if it should become entangled with water plants and is subsequently able to resurface undamaged. Furthermore, the large volume also allows for the mounting of mock-ups (such as a sea monster, shark fin or similar) or other auxiliary systems (e.g. underwater camera) on the hull. In addition, diving systems with AutoTrim (tallow simple "over trimming" which makes it possible to ground the model (park mode), whereby this position is limited in relation to the capacity of the receiver battery.

A decisive advantage of this diving technology is its highly reliable performance. The discharge pressure is sufficient for a diving depth of more than 20 meters and is therefore 10 times higher than is required for the normal operating depth of approximately 2 metres.

Within this operating range, only a slight demand is placed on the system, resulting in a very minimal use of electricity and yielding a high level of operational safety. Moreover, since there are two independent piston tanks belonging to a system, a double safety factor exists.

A further considerable advantage is the system's insensitivity to pollution. Even when pure sludge is sucked in, the ballast tanks will continue to work trouble-free since everything that is sucked in is also discharged.

The entire system requires almost no maintenance. Servicing is limited to the occasional lubricating of the gears with a few drops of oil.

The operation of the system requires a hermetically sealed hull. Air displaced from the cylinder is compressed and stored within the hull so that excess pressure develops, which in turn causes increased compression strength of the hull's casing.

Since no venting and pressure equalization are required, no air exchange takes place and no water condensation can develop.

The switch unit in connection with a pressure switch form the heart of the diving system. The switch unit serves for the controlling of each ballast tank and also takes over the automatic emergency surfacing function as soon as the pressure switch determines that the model is sinking below its maximum operating depth of approx. 2 metres.

The pressure switch incorporates an additional safety function: As in the diving mode the ballast tanks are flooded (filled) the pressure within the pressure proof compartment inside the hull increases. If the pressure switch now senses a decrease of pressure within the hull resulting from a leakage, the diving mode is immediately stopped and the emerging mode is initiated.

All ballast tanks and respective diving systems are also available with the AutoTrim device. With this function, the model can be automatically brought into a state of perfect buoyancy under water and can be easily kept in this position without manual re-trimming. The AutoStop feature (automatic end position shut-off) remains a standard component of the AutoTrim device, so that this feature is completely sustained. Ballast tanks and diving systems that are ordered with the AutoTrim device come also already equipped with the necessary levers and micro switches. The switch unit LTA serves to drive and control the system. It is already included with the complete system type TA.



Figure G.1: Piston tank system [Engel, 2005]

Technical Data:

Operating Volume 825 ml

Cylinder outer diameter 75 mm (2.95")

Cylinder length 265 mm (10.4")

Length overall min./max (full/empty): 347/505 mm (13.7/19.9")

Filling time approx. 18 sek.

Burst pressure of cylinder: 7 bar

Drive Motor:

Operating voltage: 12 V
Voltage range: 6-24 V
Power input (at 2 meters depth): 0,5 A
Motor (12V) blocks at 3 bar



Figure G.2: Ballast bag system [Brueggen, 2005]

Technical Data:

Operating Volume: 100-300 ml
Operation Depth: 0-15 meter

Pump:

Operating voltage: 12 V
Voltage range: 6-12 V
Current: 220ml/min

Comes with pressure switch, electronic circuit

G Alternative Sensors

G.1 Ultrasonic Proximity Sensors

Ultrasonic proximity sensors are useful over distances out to several feet for detecting most objects. If an object enters the acoustical field, energy is reflected back to the receiver. As is the case with any reflective sensor, maximum detection range is dependent not only on emitted power levels, but also on target cross-sectional area, reflectivity and directivity. Once the received signal amplitude reaches a present threshold, the sensor output changes state, indicating detection. Due to advantages the development of low-cost micro controllers, such devices have been replaced for most situations by more versatile ultrasonic ranging systems that provide a quantitative indicator of distance to the detected object.

A variety of acoustic systems have been developed for this requirement. These range from simple, single beam echo sounders which look ahead of the vehicle to more sophisticated multi beam sonar's which can detect, track and classify an obstacle and then carry out one or more pre-programmed avoidance manoeuvres.

There are two different type of sonar: active and passive sonar. Recognizing obstacles in water requires an active sonar system.

Sonar systems working in air with ultrasonic sounds are relative cheap and widely available, but an underwater sonar system although being the first choice to AUVs are too big, complex and expensive within the limitations of this project.

Figure G.01 shows a picture of one of the transducers of the Mako-AUV. Its dimensions are 70mm and a diameter of 65mm: Much too big for use in USAL-AUV.



Figure G.01: Ultrasonic transducer of the Mako-AUV

G.2 Rate Gyroscopes

Another way to measure yaw, pitch or roll is a Rate Gyroscope. These are sensors that measure the rate of rotation about a particular axis. Four gyroscope technologies are available: mechanical, solid-state, fiber-optic (FOG), and ring-laser (RLG).

A mechanical gyroscope uses the inertia of a very fast spinning ball to detect any angular change about its axis. Despite their high reliability and accuracy, these mechanical sensors are not currently adapted for small AUVs (1–3 metres in length) because they are cumbersome, consume much power, and can generate undesired mechanical vibrations.

Solid-state gyros are operated based on the principle of the Coriolis effect: when a translating body is subject to angular rotation, the Coriolis force experienced is proportional to an applied angular rate and an analogue signal quantifying this rate of rotation is produced.

The most basic method to get pitch or roll angles is to use a potentiometer with a pole or pendulum attached to it. Feeding the wiper output from the potentiometer to an ADC and can determine position or tilt angle. This is the standard classic approach to balancing robots that balance a pole on top of them.

G.3 Paddlewheel

A paddle wheel mechanism to discern the distance is a simple way to get this information by producing a pulse per paddle wheel rotation. These pulses are then counted and multiplied by the circumference of the wheel to calculate the total distance travelled. These sensors however also suffer from errors produced by paddle wheel slippage. It also provides information about the velocity of the vehicle when pulses per time are measured.

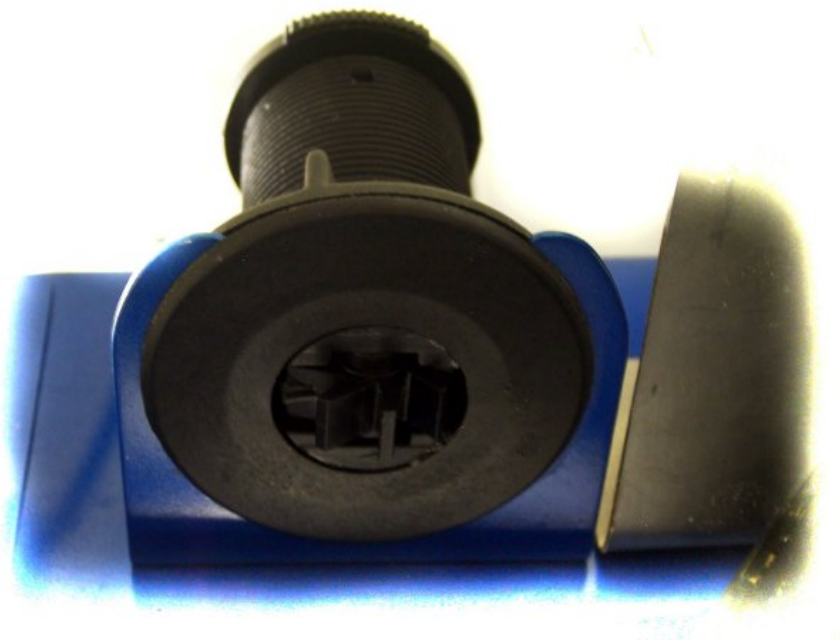


Figure G.02: Paddlewheel as used in bigger boats

G.4 Pressure Difference Measurement

Airspeed indicators work by measuring the difference between static pressure, captured through one or more static port(s) and dynamic pressure, captured through a pitot tube. The static ports are located on the exterior of the aircraft, at a location chosen to detect the prevailing atmospheric pressure as accurately as possible, that is, without any disturbance from the passage of the aircraft. Some aircraft have static ports on both sides of the fuselage or empennage, in order to more accurately measure static pressure during slips and skids.

The Pitot Static tube measures the total pressure (or impact pressure) at the nose of the Pitot tube and the static pressure of the gas stream at side ports. The difference of these pressures, i.e. the dynamic or velocity pressure (P-dynamic) varies with the square of the gas velocity. Thus the gas velocity may be expressed as:

Since the outside holes are perpendicular to the direction of travel, these tubes are pressurized by the local random component of the air velocity. The pressure in these tubes is the static pressure p_s discussed in Bernoulli's equation. The centre tube, however, is pointed in the direction of travel and is pressurized by both the random and the ordered air velocity. The pressure in this tube is the total pressure p_t discussed in Bernoulli's equation. The pressure transducer measures the difference in total and static pressure, which is the dynamic pressure q .

Measurement: $q = p_t - p_s$

With the difference in pressures measured and knowing the local value of air density r from pressure and temperature measurements, we can use Bernoulli's equation to give us the velocity. Bernoulli's equation states that the static pressure plus one half the density times the velocity V squared is equal to the total pressure.

$$p_t = p_s + 0.5 * r * V^2$$

Solving equation for V :

$$V = \sqrt{2 \frac{(p_t - p_s)}{r}}$$

There are, however, some practical limitations to this equation:

If the velocity is low, the difference in pressures is very small and hard to accurately measure with the transducer. Errors in the instrument could be greater than the measurement! So pitot-tubes don't work very well for very low velocities.

If the velocity is very high (supersonic), we've violated the assumptions of Bernoulli's equation and the measurement is wrong again. At the front of the tube, a shock wave appears that will change the total pressure. There are corrections for the shock wave that can be applied to allow us to use pitot tubes for high-speed aircraft

This Principle can be easy and cheap transferred to the AUV. The static measurement system is still available, because it is part of the depth sensor. Only a second sensor looking forward must be integrated. Figure G.03 shows a possible solution.

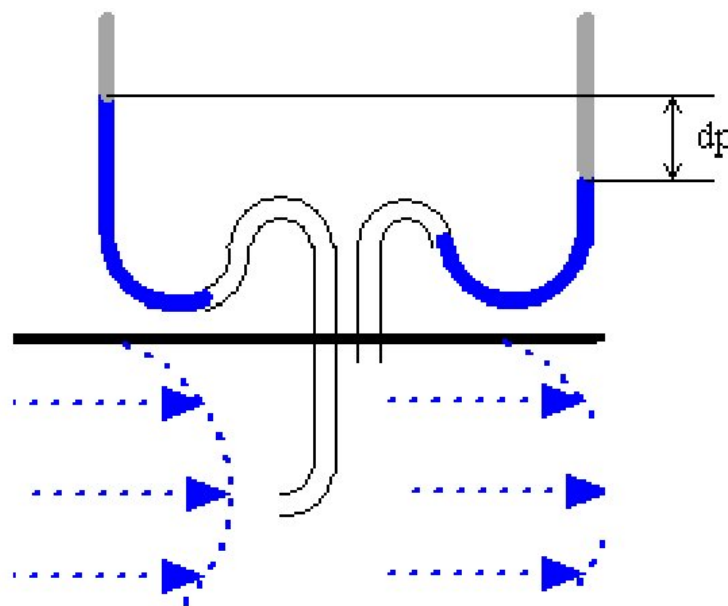


Figure G.03: Pressure Difference Measurement Principle

G.5 Doppler Velocity Measurement

Precise ground and water velocity measurements can be acquired underwater using DVL sonar. A DVL transmits an acoustic ping of a specific frequency and receives returns from the ocean bottom and particulate in the water column. Any shift in frequency (Doppler shift) in the returned signals with respect to the transmitted signal is then determined in order to calculate the vehicle's velocity (forward, starboard, and vertical) expressed in the DVL frame. The frequency of transmission determines the resolution of the measurement, the transducer size, and the range. To reduce the spreading loss, the instrument uses a narrow beam width. Typically, a DVL error is smaller than 1% of the vehicle speed.

Instruments such as the laser Doppler velocimeter (LDV), and Acoustic Doppler Velocimeter (ADV) have been developed to measure velocities in a fluid flow. The LDV and ADV emit a light or acoustic beam, and measure the doppler shift in wavelengths of reflections from particles moving with the flow. This technique allows non-intrusive flow measurements, at high precision and high frequency [Chong-moo, 2003]

There are many ways to measure the Doppler effect, each with its own advantages and drawbacks. Nortek implements a narrowband auto-covariance method because it has been established as robust, reliable and accurate.

Sound does not reflect from the water itself, but rather from particles suspended in the water. These particles are typically zooplankton, suspended sediment or small bubbles. Bubbles cause trouble at far lower acoustic frequencies, but they look like any other scatterer at the Aquadopp's frequency (2 MHz). Long experience with Doppler current sensors tells us that the small particles the Aquadopp sees move on average at the same speed as the water - the velocity it measures is the velocity of the water.

Doppler current sensors use large transducers (relative to the wavelength of the sound) to obtain narrow acoustic beams. The Aquadopp's beams have a beamwidth of 1.7° (2 MHz) or 3.4° (1 MHz) . Narrow beams are essential for obtaining good data.

The microwave radar sensor is aimed downward at a prescribed angle (typically 45) to sense o ground movement as shown in Fig. 1.4. Actual ground speed V is derived from the measured A velocity V according to the following equation [Schultz, 1993]:

$$V_A = \frac{V_D}{\cos \alpha} = \frac{cF_D}{2F_0 \cos \alpha}$$

where

V_A = actual ground velocity along path A

V_D = measured Doppler velocity D

α = angle of declination

c = speed of light

F_D = observed Doppler shift frequency D

F_0 = transmitted frequency.

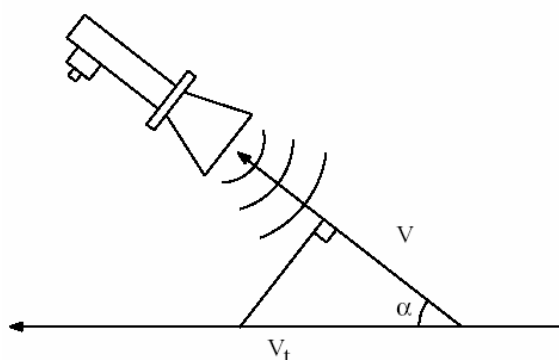


Figure G.04: A Doppler ground speed sensor inclined at an angle alpha as shown measures the velocity component V of true ground speed V (wiki[Schultz, 1993]).

Errors in detecting true ground speed arise due to side-lobe interference, vertical velocity components introduced by vehicle reaction to road surface anomalies, and uncertainties in the actual angle of incidence due to the finite width of the beam. Byrne et al. [1992] point out another interesting scenario for potentially erroneous operation, involving a stationary vehicle parked over a stream of water. The Doppler ground-speed sensor in this case would misinterpret the relative motion between the stopped vehicle and the running water as vehicle travel. Due to its price and effort to implement it, this sensor was not integrated into the AUV.

H Modelling of AUVs

This chapter presets some mathematical basics for dealing with vehicle states.

H.1 Reference Frame Transformation

Transformation between different reference frames becomes necessary when the same quantity must be expressed in different reference frames. A transformation of a vector and a rotation matrix between reference frames is described as follows.

Define ${}^W P$ as a vector P in a reference frame $\{W\}$, ${}^W P \in \mathfrak{R}^3$

Define ${}^W_B R$ as a 3×3 rotations matrix of frame $\{B\}$ relative to frame $\{W\}$, ${}^W_B R \in \mathfrak{R}^{3 \times 3}$

Translation kinematics of vector P in frame $\{W\}$ and $\{B\}$ can be written as

$${}^W P = {}^W_B R P + {}^W P_{B_{org}}$$

where ${}^W P_{B_{org}}$ is the origin of frame $\{B\}$ relative to frame $\{W\}$.

Rotation kinematics of vector P in frame $\{W\}$ and $\{B\}$ can be written as

$${}^W P = {}^W_B R P$$

A translation with rotation, for the kinematics of vector P between frame $\{W\}$ and frame $\{B\}$ can be written as

$${}^W P = {}^W_B R P + {}^W P_{B_{org}}$$

Or more compact as:

$${}^W P = {}^W_B T P$$

where ${}^W_B T$ is a 4×4 matrix

$${}^W_B T = \begin{bmatrix} {}^W_B R & {}^W P_{B_{org}} \\ 0 & 0 & 0 & 1 \end{bmatrix}$$

H.2 Attitude Representation in Euler Angles

In the previous section attitude between two frames can be represented as a 3×3 rotation matrix. In this section Euler angles, equivalent angle-axis parameters and Euler parameters are described. Most of these attitude representations can be found on robotics textbooks. [Craig, 1989; Lewis, 1993]

The Cartesian angles set of Euler angles is commonly used and probably the most popular means to represent an attitude. They are corresponding to rotation angles of yaw ψ pitch θ and roll ϕ .

$${}^W_B R = R_z(\psi)R_y(\theta)R_x(\phi)$$

where

$$R_x(\phi) = \begin{bmatrix} 1 & 0 & 0 \\ 0 & \cos \phi & -\sin \phi \\ 0 & \sin \phi & \cos \phi \end{bmatrix}$$

$$R_y(\theta) = \begin{bmatrix} \cos \theta & 0 & \sin \theta \\ 0 & 1 & 0 \\ -\sin \theta & 0 & \cos \theta \end{bmatrix}$$

$$R_z(\psi) = \begin{bmatrix} \cos \psi & -\sin \psi & 0 \\ \sin \psi & \cos \psi & 0 \\ 0 & 0 & 1 \end{bmatrix}$$

The rotation matrix can thus be expressed as:

$${}^w_B\mathfrak{R} = \begin{bmatrix} \cos \alpha \cos \beta & \cos \alpha \sin \beta \sin \gamma - \sin \alpha \cos \gamma & \cos \alpha \sin \beta \cos \gamma + \sin \alpha \sin \gamma \\ \sin \alpha \cos \beta & \sin \alpha \sin \beta \sin \gamma + \cos \alpha \cos \gamma & \sin \alpha \sin \beta \cos \gamma - \cos \alpha \sin \gamma \\ -\sin \beta & \cos \beta \sin \gamma & \cos \beta \cos \gamma \end{bmatrix}$$

Normally Euler angles must be restricted from representing a vertical orientation or mathematical singularities will result. Permitted ranges of Euler angles follow:

$$-\pi < \phi \leq \pi$$

$$-\frac{\pi}{2} < \theta < \frac{\pi}{2}$$

$$0 \leq \psi < 2\pi$$

These are the permitted ranges of Euler angles that do not result in a singular matrix for \mathfrak{R} .

H.3 Vehicle State Representation

In this section a state space representation of the AUV is given using Euler angles to represent attitude.

First, define P to be a position state vector, V to be a velocity state vector, and F to be a force and torque vector. Consistent with the definition of P , V , and F , let P_B be the position state vector of the vehicle, V_B its velocity state vector, and FK the force and torque vector.

Consider P_B in each of two frames, $\{W\}$ and $\{B\}$, wP_B is position of the vehicle in frame $\{W\}$, which has an intuitive physical meaning. Note that ${}^B P_B$ is a constant vector since the position of the vehicle in frame $\{B\}$ is fixed, by definition of frame $\{B\}$. For convenience later on, wP_B is denoted as P in writing a system model.

wV_B is the velocity of the vehicle in frame $\{W\}$, while ${}^B V_B$ is the velocity of the vehicle in frame $\{B\}$. Due to the nature of an autonomous underwater vehicle, which has actuators that move with the reference frame $\{B\}$, ${}^B V_B$ is used in deriving the dynamic model and for convenience, is denoted as V later on.

The position state vector P_K is the position in Cartesian coordinates, stacked together with the orientation given by, the Euler angles. Define the position state vector to be

$$P_B = \begin{bmatrix} x_B \\ \Theta_B \end{bmatrix}$$

where,

$$x_B = \begin{bmatrix} x \\ y \\ z \end{bmatrix},$$

and

$$\Theta_B = \begin{bmatrix} \phi \\ \theta \\ \psi \end{bmatrix}.$$

In the above x_B is the position vector and Θ_B is the set of Euler angles representing attitude.

The velocity state vector V_K is the position in Cartesian coordinates, stacked together with the orientation given by, the Euler angles. Define the position state vector to be

$$V_B = \begin{bmatrix} v_B \\ w_B \end{bmatrix},$$

where

$$v_B = \begin{bmatrix} u \\ v \\ w \end{bmatrix},$$

and

$$w_B = \begin{bmatrix} p \\ q \\ r \end{bmatrix}.$$

In the above, v_B is the linear velocity vector in the Cartesian coordinates and w_B is the angular velocity vector in the Cartesian coordinates.

The force and torque vector T_B is the force in Cartesian coordinates, stacked together with the torque vector in the Cartesian coordinates. Define the force and torque vector to be

$$T_B = \begin{bmatrix} F_B \\ Q_B \end{bmatrix},$$

where

$$F_B = \begin{bmatrix} X \\ Y \\ Z \end{bmatrix},$$

and

$$Q_B = \begin{bmatrix} K \\ M \\ N \end{bmatrix}.$$

In the above F_B is the force vector and Q_B is the torque vector in the Cartesian coordinates.

H.4 Equivalent Angle-Axis

With a set of Euler angles, a frame is rotated three times through three principle axes. The same rotation can be represented by rotation of the frame around a single axis. Any orientation can be represented by choosing a proper rotation axis and an appropriate amount of rotation. This attitude representation is called equivalent angle-axis representation.

Euler parameter is a four parameters attitude representation that is closely related to the equivalent angle-axis attitude representation. It can be seen as a scalar rotation angle plus a rotation vectors. From the definition of the equivalent angle axis Euler parameters may be defined as

$$q = \begin{bmatrix} \eta \\ \varepsilon \end{bmatrix}$$

$$\text{where, } \varepsilon = \begin{bmatrix} \varepsilon_1 \\ \varepsilon_2 \\ \varepsilon_3 \end{bmatrix}.$$

In the above is

$$\eta = \cos \frac{\theta}{2},$$

$$\varepsilon_1 = k_x \sin \frac{\theta}{2},$$

$$\varepsilon_2 = k_y \sin \frac{\theta}{2},$$

$$\varepsilon_3 = k_z \sin \frac{\theta}{2}.$$

H.5 Transformation of States Position State Vector

In modelling are two reference frames used $\{W\}$ (world) and $\{B\}$ (body). The transformation of state vectors between these two frames is described below.

The linear position part of the transformation of the position state vector between frame $\{W\}$ and $\{B\}$ can be written as

$${}^w x_K = {}^w R^B x_B + {}^w x_{B_{org}}$$

This can be reduced if the AUV is located at the origin of frame $\{W\}$

$${}^w x_B = {}^w x_{k_{org}}$$

This means that the linear position of the AUV at any time t is the same as the position of the reference frame $\{B\}$ to the world $\{W\}$

For orientation each set of Euler angles has an associated rotation matrix, ${}^w R(\Theta)_B$.

The Orientation transformation can be written as

$${}^w R(\Theta)_B = {}^w R^B R_B.$$

When the AUV is aligned relative to frame $\{B\}$ such that ${}^B R_B = I_{3 \times 3}$ equation xx is reduced to

$${}^w R(\Theta)_B = {}^w R.$$

This means that orientation of the AUV at any time t is the orientation of reference frame $\{B\}$ relative to the world $\{W\}$.

H.6 Hydrodynamic Forces and Moments

From equations 2.1 T_{RB} can be written as

$$T_{RB} = T - M_A \dot{V} - C_A(V)V - D(V)V - g(q),$$

where

T is the force and torque from the thrusters

M_A and $C_A(V)$ are the hydrodynamic added mass to the inertia and the Coriolis matrix and $D(V)$ is the hydrodynamic damping.

Hydrodynamic Added Mass

The rigid –body-like hydrodynamic added mass is defined by the SNAME (the society of Naval Architects and Marine Engineers) as

$$M_B = - \begin{bmatrix} X_{\dot{u}} & X_{\dot{v}} & X_{\dot{w}} & X_{\dot{p}} & X_{\dot{q}} & X_{\dot{r}} \\ Y_{\dot{u}} & Y_{\dot{v}} & Y_{\dot{w}} & Y_{\dot{p}} & Y_{\dot{q}} & Y_{\dot{r}} \\ Z_{\dot{u}} & Z_{\dot{v}} & Z_{\dot{w}} & Z_{\dot{p}} & Z_{\dot{q}} & Z_{\dot{r}} \\ K_{\dot{u}} & K_{\dot{v}} & K_{\dot{w}} & K_{\dot{p}} & K_{\dot{q}} & K_{\dot{r}} \\ M_{\dot{u}} & M_{\dot{v}} & M_{\dot{w}} & M_{\dot{p}} & M_{\dot{q}} & M_{\dot{r}} \\ N_{\dot{u}} & N_{\dot{v}} & N_{\dot{w}} & N_{\dot{p}} & N_{\dot{q}} & N_{\dot{r}} \end{bmatrix}$$

The parameters of the added mass matrix are dependent on the shape of the vehicle.

The hydrodynamic damping matrix represents the drag and lift forces on a moving underwater vehicle. These forces can be separated into linear and quadratic terms. That is

$$D(V) = \text{diag} \{ D_L + D_Q |V| \}$$

where

D_L linear damping terms

D_Q quadratic damping terms

The hydrodynamic damping matrix is then given

$$D(V) = \begin{bmatrix} X_u + X_{u|u}|u| & 0 & 0 & 0 & 0 & 0 \\ 0 & Y_v + Y_{v|v}|v| & 0 & 0 & 0 & 0 \\ 0 & 0 & Z_w + Z_{w|w}|w| & 0 & 0 & 0 \\ 0 & 0 & 0 & K_p + K_{p|p}|p| & 0 & 0 \\ 0 & 0 & 0 & 0 & M_q + M_{q|q}|q| & 0 \\ 0 & 0 & 0 & 0 & 0 & N_r + N_{r|r}|r| \end{bmatrix}$$

where

$$D_L = \text{diag}\{X_u \quad Y_v \quad Z_w \quad K_p \quad M_q \quad N_r\}$$

and

$$D_Q = \text{diag}\{X_{u|u} \quad Y_{v|v} \quad Z_{w|w} \quad K_{p|p} \quad M_{q|q} \quad N_{r|r}\}$$

H.7 External Forces and Moments

External forces can be grouped into those from gravitational and buoyancy forces and those from thrusters and actuators.

Gravitational and Buoyancy Forces Vector

$$G = \begin{bmatrix} f_B + f_G \\ r_B \times f_B + r_G \times f_G \end{bmatrix}$$

where the buoyant force vector f_B is defined as

$$f_B = \mathfrak{R}^{-1} \begin{bmatrix} 0 \\ 0 \\ -B \end{bmatrix}$$

and the gravitational force vector f_G as

$$f_G = \mathfrak{R}^{-1} \begin{bmatrix} W \\ 0 \\ 0 \end{bmatrix}$$

Because frame {B} is located at the center of gravity () G simplifies to

$$G = \begin{bmatrix} f_B + f_G \\ r_B \times f_B \end{bmatrix}$$

The thruster's forces and moments vector is defined as

$$T = LU$$

where

L is the mapping Index

U is the vector of the be the vehicle thrusters generated thrust.

L is normally a $6 \times n$ matrix that uses U to find the forces and moments acting on the vehicle.

H.8 Underwater Dynamics

Dynamics of underwater robotic vehicles, including hydrodynamic parameter uncertainties are highly non-linear, coupled, and time varying. Various researchers have proposed several modelling and system identification techniques for underwater robotic vehicles. Attaching one or more manipulators to a vehicle makes it a multi-body system and modelling becomes more complicated. Therefore, accurate modelling and verification by simulation are required steps in the design process [Lewis1984; Pappas, 1991]. The dynamic model of the AUV can be derived from the Newton Euler motion equation of a rigid body in fluid. [Fossen, 1995; Goheen, 1995].

In general, the motion equation can be written in a compact matrix notation in frame {B} as,

$$M\dot{V} + C(V)V + D(V)V + g(q) = T ,$$

where

M is an inertia matrix (including added mass),
C(V) is an hydrodynamic damping and lift matrix,
D(V) is the hydrodynamic damping and lift matrix,
V is the velocity state vector,
g(q) is a gravitational/buoyancy forces vector,
and T is an external force and torque input.

For the rigid body part, the dynamic compact metric equation in frame {B} can be written as

$$M_{RB}\dot{V} + C_{RB}(V)V = T_{RB}$$

where m is the mass of the vehicle

I_B is the AUVs inertia tensor with respect to {B}

$$I_K = \begin{bmatrix} I_{xx} & -I_{xy} & -I_{xz} \\ -I_{yx} & I_{yy} & -I_{yz} \\ -I_{xz} & -I_{zy} & I_{zz} \end{bmatrix}$$

$r_G = \begin{bmatrix} x_G \\ y_G \\ z_G \end{bmatrix}$ is the centre of gravity of the AUV with respect to {B}

Modelling Mass and Inertia Matrix means from equation x.xx the term

$$M_{RB}\dot{V} = \begin{bmatrix} m\dot{v} + m\dot{w} \times r_G \\ I_K \dot{w} + m r_G \times v \end{bmatrix}$$

When the origin of the reference frame {B} is accurately places at the centre if gravity thence since the AUV is quite symmetrical in all planes M_{RB} can be simplified as

$$M_{RB} = \begin{bmatrix} mI_{3 \times 3} & 0_{3 \times 3} \\ 0_{3 \times 3} & \hat{I}_K \end{bmatrix} = \begin{bmatrix} m & 0 & 0 & 0 & 0 & 0 \\ 0 & m & 0 & 0 & 0 & 0 \\ 0 & 0 & m & 0 & 0 & 0 \\ 0 & 0 & 0 & I_{xx} & 0 & 0 \\ 0 & 0 & 0 & 0 & I_{yy} & 0 \\ 0 & 0 & 0 & 0 & 0 & I_{zz} \end{bmatrix}$$

where

m is the mass of the vehicle

I inertial tensors

H.9 Mass and Inertia Matrix

Frame {B} at the centre of gravity and vehicle fairly symmetrical in all axes simplified to

Ridged Body Matrix

$$M_{RB} = \begin{bmatrix} m & 0 & 0 & 0 & 0 & 0 \\ 0 & 0 & 0 & 0 & 0 & 0 \\ 0 & 0 & m & 0 & 0 & 0 \\ 0 & 0 & 0 & 0 & 0 & 0 \\ 0 & 0 & 0 & 0 & 0 & 0 \\ 0 & 0 & 0 & 0 & 0 & I_z \end{bmatrix}$$

where

m is the mass of the AUV (14.08 kg)

I_z inertial moment about the z axis because of yaw

Roll, pitch and sway are negligible equation can be further. Added mass matrix is then

$$M_A = \begin{bmatrix} X_{\dot{u}} & 0 & 0 & 0 & 0 & 0 \\ 0 & 0 & 0 & 0 & 0 & 0 \\ 0 & 0 & Z_{\dot{w}} & 0 & 0 & 0 \\ 0 & 0 & 0 & 0 & 0 & 0 \\ 0 & 0 & 0 & 0 & 0 & 0 \\ 0 & 0 & 0 & 0 & 0 & N_{\dot{r}} \end{bmatrix}$$

I Contents of the CD-ROM

The following survey shows which data is provided on the various folders of the CD-ROM.

Thesis

- The written thesis as word and as pdf document.
- User Instructions (USAL – AUV)

Literature Research

- The literature research as word and pdf document.
- Papers of the literature research

Source Code

- This folder contains all the source code from the programs written for the Eyebot controller.

Data Sheets

- Datasheets of used micro chips

System Identification

- Excel sheets containing data of experiments.

Papers

- Refereed papers.

Programs

- Subsim, simulator for AUVs (including example files)
- SMS, simulation program for the DC/DC converter
- TeraTerm, terminal program

Media

- Pictures
- Videos